

Department of Food and Nutrition  
University of Helsinki  
EKT-series 1949

# Mass Spectrometry Methods for the Structural Analysis of Glucan- and Arabinoxylan-Derived Oligosaccharides

Minna Juvonen

ACADEMIC DISSERTATION

To be presented, with the permission of the Faculty of Agriculture and Forestry of the University of Helsinki, for public examination in Hall 1, Metsätalo, on 20 August 2020, at 12 noon.

Helsinki 2020

Custos: Professor Vieno Piironen  
Department of Food and Nutrition  
University of Helsinki, Finland

Supervisors: Professor Maija Tenkanen  
Department of Food and Nutrition  
University of Helsinki, Finland

Docent Päivi Tuomainen  
Department of Food and Nutrition  
University of Helsinki, Finland

Reviewers: Professor Kati Hanhineva  
Department of Biochemistry  
University of Turku, Finland

Associate Professor Francisco Vilaplana  
Division of Glycoscience  
KTH Royal Institute of Technology, Sweden

Opponent: Associate Professor Laura Nyström  
Department of Health Sciences and Technology  
ETH Zürich, Switzerland

ISBN 978-951-51-6383-7 (paperback)  
ISBN 978-951-51-6384-4 (PDF; <http://ethesis.helsinki.fi>)  
ISSN 0355-1180

Unigrafia  
Helsinki 2020

## ABSTRACT

Oligosaccharides potentially present in cereal matrices have attracted attention because of their health-related properties, such as prebiotic potential. In addition to those that are naturally present, oligosaccharides can be formed during processing by the hydrolysis of cereal polysaccharides, such as arabinoxylan, by endogenous or microbial enzymes. In sourdough fermentation, additional poly- and oligosaccharides may be produced by lactic acid bacteria (LAB).

In the work performed for this thesis, mass spectrometry (MS) methods were implemented in the structural analysis of various enzymatically produced oligosaccharides. The research was focused on finding solutions to separating and identifying oligosaccharide isomers. To determine the linkage positions of linear mixed-linked glucooligosaccharides (GLOS), the feasibility of the positive and negative electrospray ionisation multiple-stage MS (ESI-ITMS<sup>n</sup>) were compared. Next, the ability of ESI-ITMS<sup>n</sup> to detect the branching points and linkage positions of complex arabinoxylan-oligosaccharides (A)XOS was studied. The MS method was also coupled to hydrophilic interaction liquid chromatography (HILIC) to separate and identify the (A)XOS in mixtures. Finally, the potential of travelling wave ion mobility spectrometry (TWIMS) combined with MS to differentiate the isomeric (A)XOS was evaluated. To study the structures of the isomeric acceptor products formed by dextransucrase from LAB, <sup>13</sup>C-labelling was applied with ESI-ITMS<sup>n</sup>.

The ESI-ITMS<sup>n</sup> method provided structural information about the molecular weights, sequences and linkage positions of the linear mixed-linked GLOS and (A)XOS. Negative ionisation was found to be more informative than the positive ionisation mode in analysing the linkage positions. The stepwise C-ion fragmentation in negative mode from the reducing end towards the non-reducing end allowed to study the linkage diagnostic fragment ions from the middle and the non-reducing end in both linear and branched oligosaccharides. *O*-2 or/and *O*-3 arabinofuranosyl substituents of AXOS were determined by the presence or absence of diagnostic ions in the ESI-ITMS<sup>3</sup> analysis in the negative mode. The ESI-ITMS<sup>n</sup> method, combined with <sup>13</sup>C-isotope labelling, enabled the analysis of unique trisaccharides produced by dextransucrase as well as the further detailed analysis of the isomeric product ions. Coupling MS/MS to HILIC enabled the separation and identification of all AXOS by the combination of retention times and the MS/MS spectra. CID-TWIMS-MS/MS was shown to be a powerful tool in differentiating the isomeric AXOS when both the fragment ions and the precursor ions were analysed.

## ACKNOWLEDGEMENTS

This research work was performed in the department of Food and Nutrition in Faculty of Agriculture and Forestry, University of Helsinki. The Raisio Research Foundation, the Finnish Food Research Foundation and the Finnish Concordia Fund are gratefully acknowledged for funding the research.

I owe my deepest gratitude to my supervisors Professor Maija Tenkanen and Docent Päivi Tuomainen. Maija, thank you for giving me an opportunity to work in this project and introducing me to the fascinating world of carbohydrates. I very much appreciate the advice, support and encouragement you have given to me during these years. It has been inspiring to work with you. Päivi, your intensive laboratory course on chromatography got me initially interested in chromatography and analytical chemistry. Thank you for supporting me even after your retirement. I highly appreciate the knowledge of chromatography you have and all the advice given to me.

I am extremely grateful to Professor in Food chemistry Vieno Piironen for guiding me through this process. During these years the doctoral school has changed the instructions so many times, but you were always willing to help and find solutions how to proceed with the studies.

I wish to thank my opponent Associate Professor Laura Nyström for agreeing to evaluate my thesis. I look forward to our discussion. I want to thank also the thesis pre-examiners Professor Kati Hanhineva and Associate Professor Francisco Vilaplana for their valuable comments and suggestions.

I would like to express my gratitude to all the co-authors for giving their expertise to the articles: Edwin Bakx, Professor Rosário Domingues, Yaxi Hou, Docent Jouni Jokela, Ilkka Kajala, Markus Kotiranta, Docent Hannu Maaheimo, Docent Ndegwa Maina, Dr. Antti Nyysölä, Dr. Qiao Shi, Professor Henk Schols and Docent Liisa Virkki. Especially my gratitude goes to my former master thesis supervisors, Docent Jouni Jokela and Docent Ndegwa Maina, for introducing me to the world of mass spectrometry and for sharing your valuable knowledge, to Dr. Qiao Shi for enjoyable collaboration in a joint article, to Professor Henk Schols for opportunity to visit his research group at Wageningen University and Edwin Bakx for instructing me during the research visit. Special thanks go to master thesis workers Yaxi Hou and Markus Kotiranta for the excellent laboratory work.

I also wish to thank Miikka Olin for the technical support with the analytical instruments, Taru Rautavesi for helping in lab and ordering the reagents and Docent Velimatti Ollilainen for advice on mass spectrometry and ion mobility techniques.

I wish to acknowledge colleagues and office roommates through the years: Suvi Alakalhunmaa, Dr. Sun-Li Chong, Dr. Abdul Ghafar, Kati Hakala, Dr. Susanna Heikkinen, Dr. Satu Kirjoranta, Dr. Sanna Koutaniemi, Ida Nikkilä, Docent Kirsi Mikkonen, Docent Kirsti Parikka, Dr. Leena Pitkänen, Maijuleena Salminen, Yue Tuan, Dr. Jaana Valo, Dr. Yan Xu and Hongbo Zhao. Thank you for all your support and friendship.

I would like to thank also all colleagues in Food and Nutrition department for chats, laughs and friendly atmosphere in the coffee room.

Last but not least, I want to also thank my friends and family for the support during this project. Special thanks go to my fiancé Aki Malmstedt for always encouraging and believing in me.

Helsinki, August 2020

A handwritten signature in black ink, appearing to read 'Minna Juvonen', with a stylized, flowing script.

Minna Juvonen

## LIST OF ORIGINAL PUBLICATIONS

This thesis is based on the following publications:

I Maina, N., Juvonen, M., Domingues, R. M., Virkki, L., Jokela, J., & Tenkanen, M. 2013. Structural analysis of linear mixed-linkage glucooligosaccharides by tandem mass spectrometry. *Food Chemistry*, 136(3-4), 1496-1507.

II Shi, Q., Juvonen, M. K., Hou, Y., Kajala, I., Nyyssölä, A., Maina, H. N., Maaheimo, H., Virkki, M-L. & Tenkanen, T. M. 2016 Lactose- and cellobiose-derived branched trisaccharides and a sucrose-containing trisaccharide produced by acceptor reactions of *Weissella confusa* dextransucrase. *Food Chemistry*, 109, 226-236.

III Juvonen, M., Kotiranta M., Jokela J., Tuomainen P., & Tenkanen, M. 2019. Identification and structural analysis of cereal arabinoxylan-derived oligosaccharides by HILIC-MS/MS. *Food Chemistry*, 275, 175-186.

IV Juvonen, M., Bakx E., Schols H. & Tenkanen, M. 2020. Separation of isomeric cereal-derived arabinoxylan-oligosaccharides by collision induced dissociation and travelling wave ion mobility spectrometry–tandem mass spectrometry. Manuscript.

The publications are referred to in the text by their roman numerals. The publications 1-III are reproduced with the kind permission of the copyright holder Elsevier.

The author's contributions to the publications as follows:

I                Minna Juvonen planned the study with the other authors and performed all mass spectrometry analyses of the oligosaccharide model compounds. She participated in interpreting the results and preparing the manuscript.

II                Minna Juvonen planned the MS analysis of the study with the other authors and performed mass spectrometry analyses on isotope-labelled compounds. She had the main responsibility of interpreting the mass spectrometry results and writing the sections related to the analysis in the manuscript.

III                Minna Juvonen planned the study with the other authors. She was responsible for the experimental work and performed HILIC-MS analyses. She had the main responsibility of interpreting the results, and she was the corresponding author of the paper.

IV                Minna Juvonen planned the study with the other authors. She performed all the experimental work. She had the main responsibility of interpreting the results, and she is the corresponding author of the paper.

## ABBREVIATIONS

AX	arabinoxylan
(A)XOS	arabinoxylan-derived oligosaccharides
AXOS	arabinoxyloligosaccharides
CCS	collision cross-section
CID	collision-induced dissociation
Da	dalton
DP	degree of polymerisation
dt	drift time
ESI	electrospray ionisation
HILIC	hydrophilic interaction liquid chromatography
HPAEC	high-performance anion extraction chromatography
GC	gas chromatography
GH	glycoside hydrolase
GLOS	glucooligosaccharides
GOS	galactooligosaccharides
IM	ion mobility
IMS	ion mobility spectrometry
IT	ion trap
LAB	lactic acid bacteria
LC	liquid chromatography
LWS	low-molecular weight sugars
MALDI	matrix-assisted laser desorption ionisation
MS	mass spectrometry
MS/MS	tandem mass spectrometry
MS <sup>n</sup>	multiple-stage mass spectrometry
<i>m/z</i>	mass-to-charge ratio
NMR	nuclear magnetic resonance spectroscopy
PSD	post-source decay
qTOF	quadrupole time-of-flight analyser
RP	reverse phase
TWIMS	travelling wave ion mobility spectrometry
XOS	xylooligosaccharides



# CONTENTS

ABSTRACT

ACKNOWLEDGEMENTS

LIST OF ORIGINAL PUBLICATIONS

ABBREVIATIONS

1	INTRODUCTION.....	11
2	REVIEW OF THE LITERATURE.....	13
2.1	Carbohydrates in cereal grains .....	13
2.2	Enzymatically produced carbohydrates in cereal matrix .....	14
2.2.1	Endogenous enzymes in cereal grains .....	14
2.2.2	Exopolysaccharides produced by lactic acid bacteria enzymes ...	15
2.2.3	Oligosaccharides produced by glucansucrases.....	16
2.3	Arabinoxylan and arabinoxylan oligosaccharides.....	16
2.4	Structural analysis of oligosaccharides by tandem mass spectrometry	18
2.4.1	Domon and Costello's nomenclature of MS/MS fragment ions ..	19
2.4.2	Fragmentation mechanisms of underivatized oligosaccharides....	21
2.4.3	Linkage position determination by MS/MS .....	28
2.4.4	Oligosaccharide analyses by MS/MS and MS <sup>n</sup> .....	32
2.4.5	Combining MS and liquid chromatography .....	35
2.4.6	Combining MS and ion mobility spectrometry .....	41
3	OBJECTIVES OF THE STUDY .....	43
4	MATERIALS AND METHODS .....	44
4.1	Materials.....	44
4.1.1	Commercial disaccharide and oligosaccharide standards (I–IV)	44
4.1.2	GLOS from <i>W. confusa</i> and <i>L. citreum</i> produced dextrans (I)....	45
4.1.3	Trisaccharides produced by <i>W. confusa</i> dextransucrase (II) .....	45
4.1.4	(A)XOS from cereal arabinoxylan (III and IV).....	46

4.2	Analytical methods .....	48
4.2.1	Structural analysis by using direct infusion ESI-MS <sup>n</sup> (I–III) .....	48
4.2.2	HILIC-MS/MS analysis (III).....	48
4.2.3	Ion mobility MS (IV) .....	50
4.2.4	Data analysis (I-IV).....	51
5	RESULTS .....	53
5.1	Structural analysis of GLOS by ESI-MS <sup>n</sup> (I).....	53
5.2	ESI-MS <sup>n</sup> of trisaccharide acceptor products of <i>W. confusa</i> (II) .....	59
5.3	Linkage analysis of linear (A)XOS by ESI-MS <sup>n</sup> (III) .....	63
5.4	Identification of branches from (A)XOS by ESI-MS <sup>3</sup> (III) .....	65
5.5	Implementation of HILIC-MS/MS for identification of AXOS (III) .	67
5.6	Identifying AXOS isomers by IMS-MS/MS method (IV) .....	69
5.6.1	Separation of precursors by ESI-TWIMS-MS .....	69
5.6.2	Separation of fragment ions ESI-CID-TWIMS-MS/MS .....	70
5.6.3	Base peak mobilogram (BPM) as a fingerprinting tool .....	72
6	DISCUSSION.....	73
6.1	Remarks on labelling the fragments according to a nomenclature ....	73
6.2	Feasibility of MS in the structural analysis of neutral oligosaccharides .....	74
6.2.1	Determination of glycosidic linkage positions by MS <sup>n</sup> (I, III).....	74
6.2.2	Influence of branch on fragmentation of oligosaccharides in MS/MS (II,III) .....	76
6.2.3	Differentiation of oligosaccharide isomers (I-IV).....	78
6.2.4	Advantages and limitations of MS methods in structural analysis of oligosaccharides.....	80
7	CONCLUSIONS .....	81
8	REFERENCES .....	84

## 1 INTRODUCTION

Cereal grains have been an important part of human nutrition for over 9,000 years. Nowadays, high-yield cereal crops are predominant in agriculture worldwide. In 2018, 3,000 million tonnes of cereal grains were produced globally (FAO 2018). Cereal grains consist of a high amount of carbohydrates, mainly in the form of energy rich starch. Cereal grains are also good source of protein, vitamins and minerals (MacEvilly 2003). Besides starch, cereal grains contain other carbohydrates: cell wall polysaccharides and small amounts of mono-, di- and oligosaccharides (Knudsen 1997).

In addition to oligosaccharides which are naturally present in grains, plant cell wall polysaccharides can also be hydrolysed to oligosaccharides during processing by either endogenous or microbial enzymes. For example, oligosaccharides hydrolysed from cereal cell wall arabinoxylan have been found in beer (Broekaert et al. 2011). In sourdough fermentation, additional oligo- and polysaccharides are produced by lactic acid bacteria (LAB) (Gänzle 2014). Because of their prebiotic potential and other health-related effects, there has been increased interest in studying their structures (Broekaert et al. 2011). However, because the structures of these oligosaccharides and polysaccharides are complex, they can be challenging to analyse.

Mass spectrometry (MS) is an analytical method used to measure mass-to-charge ratios of gas-phase ions (El-Aneed 2009). The advantages of MS are that only a small amount of sample is required, and the analysis is performed quickly. Gas chromatography MS (GC-MS) has been a popular technique for the structural analysis of oligosaccharides (Björndal 1967). Prior to GC-MS, oligosaccharides needed to be hydrolysed and derivatised, such as by per-*O*-methylation. Previously, the use of liquid chromatography (LC) was limited to reverse-phase LC (RP-LC) because MS unsuitable solvents were used in normal-phase LC. However, the recently invented hydrophilic interaction liquid chromatography (HILIC) uses MS compatible solvents and therefore can be easily coupled to MS. A benefit of the HILIC-MS is that oligosaccharides can be analysed in mixtures without derivatisation (Brokl et al. 2011; Hernández-Hernández et al. 2012).

Tandem mass spectrometry (MS/MS) has been shown to be a useful tool in studying the structures of oligosaccharides (Asam & Glish 1997; Garozzo et al. 1990; Pasanen et al. 2007; Pfenninger et al. 2002a; Usui et al. 2009). The

limitation of MS/MS is the inability to differentiate the isomeric structures of oligosaccharides built of the same mass monosaccharides. Recently, ion mobility spectroscopy (IMS) coupled to MS has been reported as a promising technique for the differentiation of isomeric oligosaccharides and their structures (Both et al. 2014; Zhu et al. 2009; Yamagaki & Sato 2009). These new techniques have raised interest in studying the feasibility of MS/MS methods to identify and analyse the structures of oligosaccharides that are potentially present in foods.

In this thesis, the literature review presents an overview of carbohydrates, especially oligosaccharides, that are potentially present in cereal matrices and the structural analyses of oligosaccharides by MS/MS. First, carbohydrates in cereal grains and matrices are briefly presented. Then the nomenclature of carbohydrate fragmentations occurring in MS/MS are provided in the following section. Next the fragmentation reaction mechanisms are reviewed in detail and the common fragments formed from different di- and oligosaccharide structures are presented. Finally, the diverse applications of MS/MS methods used to analyse isomeric oligosaccharides are presented.

In the experimental part of this thesis, the data in the four publications (I–IV) are summarised. In the research, MS and LC-MS methods were developed for the structural analysis of isomeric oligosaccharides in cereal matrices. The main aim was to find solutions to the analysis of isomeric structures in glucan- and arabinoxylan-derived oligosaccharides (GLOS and (A)XOS) by MS/MS. The studies began by performing structural and linkage analyses of linear mixed-linked GLOS and (A)XOS using electrospray ionisation multiple-stage mass spectrometry (ESI-MS<sup>n</sup>). Next, hydrophilic interaction chromatography (HILIC) coupled to the MS/MS method was implemented for the fast separation and identification of (A)XOS isomers in mixtures. Finally, the ability of travelling wave ion mobility spectrometry (TWIMS) coupled to MS to differentiate isomeric structures was studied. The ESI-MS<sup>n</sup> with <sup>13</sup>C<sub>6</sub>-isotopic labelling was also applied to analyse trisaccharides produced by LAB dextransucrase.

## 2 REVIEW OF THE LITERATURE

### 2.1 Carbohydrates in cereal grains

Dietary carbohydrates are classified to three main groups based on their degree of polymerisation (DP). The degree of polymerisation indicates the number of monomer residues/units in a molecule. The three carbohydrate groups are sugars (DP 1-2), oligosaccharides (DP 3-9) and polysaccharides (DP  $\geq$  10). Polysaccharides are divided to two subgroups: starch ( $\alpha$ -glucans) and non-starch polysaccharides (NSP). NSPs consist of all polysaccharides except starch (FAO 1998).

Cereal grains consist mainly of the following carbohydrates: mono-, di- and oligosaccharides, starch, and cell wall polysaccharides. The total content of carbohydrates is 70–80% of dry matter in cereal grain. Table 1 presents the carbohydrate composition of barley, oat, rye and wheat, which are the most cultivated cereals in Finland.

Table 1. Carbohydrate composition of cereal grain (g/100 g of dry matter) (Knudsen 1997).

Carbohydrates	Barley		Oat		Rye	Wheat
	Hulled	Hulless	Hulled	Hulless		
Monosaccharides	0.4	n.m.	0.2	n.m.	0.6	0.3
Maltose		n.m.		n.m.	n.m.	n.m.
Sucrose	1.2	n.m.	1.1	n.m.	1.9	1.1
Raffinose	0.5	n.m.	0.3	n.m.	0.4	0.4
Stachyose	0.1	n.m.	0.2	n.m.	0.2	0.2
Total LWS	2.1	n.m.	1.7	n.m.	3.2	1.9
Starch	58.7	64.5	46.8	55.7	61.3	65.1
Arabinoxylan	8.4	4.8	9.8	3.6	9.7	7.6
$\beta$ -glucan	4.2	4.2	2.8	4.1	1.6	0.8
Cellulose	4.3	1	8.2	1.4	1.6	2
Fructan	0.4	n.m.	0.3	n.m.	3.1	1.5
total NSP	18.6	12.4	23.2	11.6	15.2	11.9
Total	79.4	76.9	71.7	67.3	79.7	78.9

LWS = low weight sugars, NSP = non-starch polysaccharides, n.m. = not measured, hulled = variety which grain has hull (lemma and palea), hulless = variety which hull naturally falls off.

Mono-, di- and oligosaccharides are often called low-molecular weight sugars (LWS). The LWS content in cereal grains is about 2–3 g/100 g (dry matter) (Knudsen 1997). Sucrose is the main LWS in maize, wheat, rye, barley and oat grains (Knudsen 1997). Their monosaccharide content is 0.2–0.6 g/100 g. The main monosaccharides are glucose, galactose and fructose.

Cereal grains naturally consist of small amounts of oligosaccharides built from fructose, galactose or/and glucose, such as raffinose, stachyose and fructooligosaccharides (Liu & Rochfort 2015; Verspreet et al. 2015). The raffinose content in cereal grain is 0.3–0.5 g/100 g (Knudsen 1997). Recent studies have shown that 6G-kestose, 1-kestose and raffinose are the major trisaccharides in wheat flour (Liu & Rochfort 2015).

Starch is the most abundant polysaccharide in cereal grains; 47–65% of the dry weight of cereal grains is starch (Knudsen 1997). Starch is formed of amylose and amylopectin polymer chains. The NSP content in common cereal grains is 11–23% of dry weight (Knudsen 1997). NSPs in cereal grains consist of cellulose, AX, mixed-linked  $\beta$ -glucan, fructans, glucomannans, xyloglucans, pectic polysaccharides, callose and arabinogalactan proteins (AGP). All NSPs except fructan and AGP are key components of cereal cell walls (Fincher 2016).

## **2.2 Enzymatically produced carbohydrates in cereal matrix**

### **2.2.1 Endogenous enzymes in cereal grains**

Most endogenous enzymes in cereal grains are hydrolytic enzymes, hydrolases. Their biological purpose is to degrade polysaccharides and proteins for the germination of plants. Hydrolytic enzymes can be divided by their target substrate into amylolytic enzymes, cellulases and hemicellulases, proteases, lipases and esterases. Amylolytic enzymes (e.g.  $\alpha$ -amylases,  $\beta$ -amylases, glucoamylases and pullulanases) hydrolyse starch. Cellulases and hemicellulases target cell wall components, such as cellulose,  $\beta$ -glucan and pentosans (arabinoxylan). This group includes endoglucanases (EC 3.2.1.4), endoxylanases (EC 3.2.1.8) and  $\alpha$ -L-arabinofuranosidases (EC 3.2.1.55) (Poutanen 1997).

### 2.2.2 Exopolysaccharides produced by lactic acid bacteria enzymes

LAB fermentation is utilised in the production of food, such as yoghurt and sourdough bread. In addition to acidity, aroma and flavour, many LAB genera, such as *Lactobacillus*, *Leuconostoc*, *Streptococcus* and *Weissella*, produce extracellular polysaccharides (i.e. exopolysaccharides [EPS]) in fermented products. EPS protect LAB from environmental stress (Leemhuis et al. 2013).

The rheological and textural properties of fermented food can be improved by EPS produced *in situ* (Welman 2009). In sourdough bread, EPS produced by *Leuconostoc* and *Weissella* strains have been shown to be highly potential hydrocolloids (Korakli et al 2001; Tieking et al. 2003; Katina et al. 2009), which can improve the volume, softness, crumb texture and shelf life of sourdough bread (Vandamme et al. 1997).

EPS can be homopolysaccharides (HOPS) synthesised from sucrose by extracellular glucansucrases or fructansucrases. EPS can also be heteropolysaccharides (HEPS) that are synthesised by glycosyltransferases from sugar nucleotide precursors (Tieking & Gänzle 2005). In sourdough, EPS are a HOPS-type of EPS in which glucans or fructans are produced by extracellular glucan- or fructansucrases.

Glucansucrases belong to the glycoside hydrolase family 70 (GH 70). Most enzymes classified as GH70 use sucrose as the D-glucopyranosyl donor to synthesise  $\alpha$ -D-glucans. D-fructofuranose is released to the matrix. Glucansucrases can catalyse the synthesis of various types of glycosidic linkages:  $\alpha$ -(1 $\rightarrow$ 2);  $\alpha$ -(1 $\rightarrow$ 3);  $\alpha$ -(1 $\rightarrow$ 4); and  $\alpha$ -(1 $\rightarrow$ 6). The polysaccharide chain thus formed can be linear or branched (Remaud-Simeon 2015).

Glucansucrases (GH70) are classified by Nomenclature Committee of the International Union of Biochemistry and Molecular Biology based on the reaction catalysed and the specificity as follows: dextransucrases (E.C 2.4.1.5); mutansucrases (E.C 2.4.1.125); reuteransucrases (E.C 2.4.1.-); and alternansucrases (E.C 2.4.1.140) (Remaud-Simeon 2015). Dextransucrases synthesise mainly  $\alpha$ -(1 $\rightarrow$ 6)-linkages, mutansucrases synthesise  $\alpha$ -(1 $\rightarrow$ 3)-linked main chain, reuteransucrases mainly  $\alpha$ -(1 $\rightarrow$ 4)-linkages and alternansucrases alternating  $\alpha$ -(1 $\rightarrow$ 6)- and  $\alpha$ -(1 $\rightarrow$ 3)-linkages (Leemhuis et al. 2013).

### 2.2.3 Oligosaccharides produced by glucansucrases

In addition to the production of polymeric glucans, glucansucrases are known to produce oligosaccharides (Leemhuis et al. 2013). In these reactions, maltose and other di- and oligosaccharides that are present in cereal matrices act as acceptors, and they synthesise oligosaccharides instead of dextrans (Leemhuis et al. 2013). Previous studies on acceptor reactions were mainly focused on maltose as an acceptor. Maltose is known to form initially trisaccharide panose, which elongates to larger isomalto-oligosaccharides (IMOs). Moreover, oligosaccharides having linkages other than the (1→6)-linkage can be formed. *Leuconostoc mesenteroides* was found to synthesise (1→2)-branches to IMOs. (1→2)-linked trisaccharides were found when acceptors such as lactose, lactulose and cellobiose were used (García-Cayuela et al. 2014; Ruiz-Matute et al. 2011). Recently, oligosaccharide acceptor products have attracted interest because their possible prebiotic properties (García-Cayuela et al. 2014; Ruiz-Matute et al. 2011). They have also been suggested to have antistaling properties in sourdough bread (Katina et al. 2009).

### 2.3 Arabinoxylan and arabinoxylan oligosaccharides

In addition to  $\beta$ -glucan, AX is a major polysaccharide in the cell walls of cereal grain endosperm (Fincher 2016). AX is the main cell wall polysaccharide in wheat, rye, maize and sorghum. Oat and barley contain high proportions of  $\beta$ -D-glucan. (Saulnier et al. 2007). The arabinoxylan content of whole grains is 3.6–9.8 g/100 g (Knudsen 1997).

AX is a complex heteroxylan (Fincher 2016). In cereal grain, AX is formed by  $\beta$ (1→4)-linked xylopyranosyl residue backbone attached to  $\alpha$ (1→2) and/or  $\alpha$ (1→3)-linked arabinose furanosyl (Araf) substituents (Saulnier et al. 2007).  $\beta$ -D-Xylp-(1→2)- $\alpha$ -L-Araf-(1→3) disaccharide substituents have been found in oat spelt and barley husks (Höjje et al. 2006; Pastell et al. 2009). Some ferulic acid substituents are also O-5-linked to arabinose residues (Mathew & Abraham 2004; Wende & Fry 1997). The outer tissues of cereal grains consist of acidic glucuronoxylan and methylated glucuronoxylan (Saulnier et al. 2007). They are formed by  $\alpha$ (1→2)-linked glucopyranosyluronic acid or 4-O-methyl-glucopyranosyluronic acid substituents attached to the xylan backbone.

The structural features of AXs are known to vary in different cereals, tissues and even in tissue layers (Barron et al. 2007; Biliaderis & Izydorczyk 2007). For example, the AX in wheat endosperm is less substituted (Ara/Xyl 0.50-



0.71) than in the bran layer (Ara/Xyl 0.82-1.07) (Biliaderis & Izydorczyk 2007). Its structural features are related to physicochemical properties, such as water solubility, viscosity and gelation (Saulnier et al. 2007b). For example, in bread making, the addition of water-soluble AXs was found to improve crumb structure and loaf volume (Biliaderis et al. 1995), but the opposite outcome was observed when water-insoluble AXs were added (Courtin & Delcour 2002). Both AX and  $\beta$ -glucan content have been found to be related to the viscosity of beer (Schwartz & Han 1995).

Intestinal microbiota in the human colon degrade AX to arabinoxylan oligosaccharides ((A)XOS) by enzymatic hydrolysis. Enzymatic hydrolysis can occur also during food processing, such as in brewing beer or baking bread (Broekaert et al. 2011). In this thesis, the abbreviation (A)XOS refers to both xylooligosaccharides (XOS) and arabinoxylooligosaccharides (AXOS).

Most microbial xylanases belong to GH family 10 or 11. However, all known plant xylanases belong to GH family 10 (Simpson et al. 2003). Both GH10 and GH11 include most endo-1,4- $\beta$ -xylanases that hydrolyse the xylan backbone and release oligosaccharides (Pollet et al. 2010). GH10 endo-1,4- $\beta$ -xylanases can cleave the AX backbone next to the branching residues, while GH11 endoxylanases cleave one unit further from the branched residue, which leads to differently structured (A)XOS.

AX and (A)XOS are both considered dietary fibre (Mendis & Simsek 2014). Recently, evidence of the prebiotic effects of (A)XOS was presented in vitro in human and animal studies (Broekaert et al. 2011). A rat trial study showed that the prebiotic potential of cereal AX “depends strongly on their structural properties and joint presence” (Damen et al. 2011).

AX and (A)XOS have also been associated with many health benefits, including the attenuation of type II diabetes, immunomodulatory activity, serum cholesterol and glucose levels (Broekaert et al. 2011; Mendis & Simsek 2014).

## 2.4 Structural analysis of oligosaccharides by tandem mass spectrometry

MS has become a popular technique used in the structural analysis of carbohydrates. This analytical technique is used to measure mass-to-charge-ratios ( $m/z$ ) of gas-phase ions. Currently, the most commonly used mass analysers are quadrupole (q), ion trap (IT), time-of-flight (TOF) and Fourier-transform ion cyclotron resonance analysers (FT-ICR) (El-Aneed et al. 2009). At present, mass spectrometers are often hybrid instruments that combine two or more MS measurement techniques. For example, the Synapt mass spectrometer, which is manufactured by the Waters Corporation, is a quadrupole time-of-flight (qTOF) instrument that includes three other cells: an ion mobility cell and two collision-induced dissociation (CID) cells.

In MS analysis, the compounds in samples have to be ionised in an ion source before entering into the mass spectrometer. Different techniques have been invented for ionisation. Ionisation techniques are both soft and hard, depending on the ionisation conditions and the degree to which precursors fragment during ionisation. Electron impact ionisation (EI) is a hard ionisation technique in which samples are ionised by electron bombardment. Soft ionisation techniques include electrospray ionisation (ESI), matrix-assisted laser desorption ionisation (MALDI) and chemical ionisation (CI) (El-Aneed 2009). All soft ionisation techniques function under atmospheric pressure.

Tandem mass spectrometry (MS/MS) is an analytical technique in which targeted ions, as precursors, are first isolated from the ion stream to IT cells. Then the precursor ions are fragmented to product/fragment ions by CID. In CID, the ions are collided with an inert collision gas, such as argon or helium, which induces the ions to dissociate. The  $m/z$  of the formed fragment ions are then measured using MS and presented as MS/MS spectra. The fragment ion patterns in MS/MS spectra provide information about the structure of the precursor. IT instruments can be used to measure multiple stages of MS/MS, which is called multiple-stage mass spectrometry ( $MS^n$ ). Other fragmentation techniques have also been used. For example, MALDI ion source can produce fragment ions by high-energy laser beam, which causes the post-source decay (PSD) of precursor ions.

### 2.4.1 Domon and Costello's nomenclature of MS/MS fragment ions

Domon and Costello (1988) developed a nomenclature of carbohydrate fragment ions. Carbohydrate fragment ions are formed by the cleavage of glycosidic bond or by cross-ring fragmentation. The reactions that cause this fragmentation are presented in section 2.4.2. Domon and Costello's (1988) nomenclature was developed for glycoconjugates with aglycone or carbohydrates with the reducing sugar unit. An example of the fragmentation nomenclature is presented in Figure 1. In this nomenclature, fragment ions that contain aglycone or the reducing end are marked A-, B-, and C- ions. Fragment ions that contain the other end are called X-, Y- and Z-ions. For A-, B- and C-ions subscripts are used to indicate the number of cleaved glycosidic bonds counted from the non-reducing end. For X-, Y-, and Z-ions, the subscript represents the glycosidic bond counted from the aglycone (or reducing end). The superscript in cross-ring fragment ions indicates the cleaved bonds in the ring.

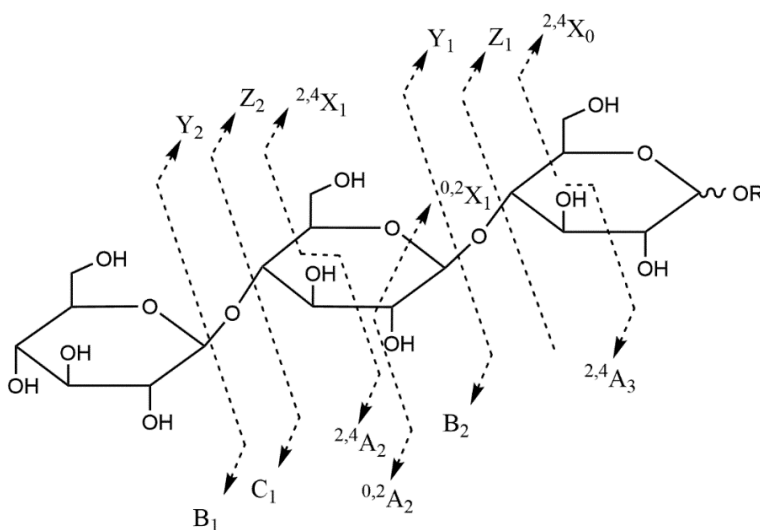


Figure 1. Nomenclature of carbohydrate fragmentations. Dotted line illustrates the fragmented bond and arrow the ionized side of the molecule. A and X = ions formed by cross-ring cleavages. B, C, Y and Z = ions formed by glycosidic bond fragmentation. Subscript = number indicates the position of cleaved glycosidic bond. Superscript = numbers indicate the positions of cleaved bonds in ring (Domon & Costello 1988)

More symbols are assigned to branched carbohydrate structures. As shown in Figure 2, the fragmentation nomenclature of branched oligosaccharides is presented. Greek letters are used as symbols to differentiate each branch or antennae from the core unit. The largest branch has the letter  $\alpha$ , and the second-largest has the letter  $\beta$ . The core unit is presented without Greek letters. If the mass spectra have isomeric fragment ions that originate from both antennae,  $\alpha$  and  $\beta$  are combined and indicated by the symbol  $x$  (e.g.  $Y_{2x}$ ).

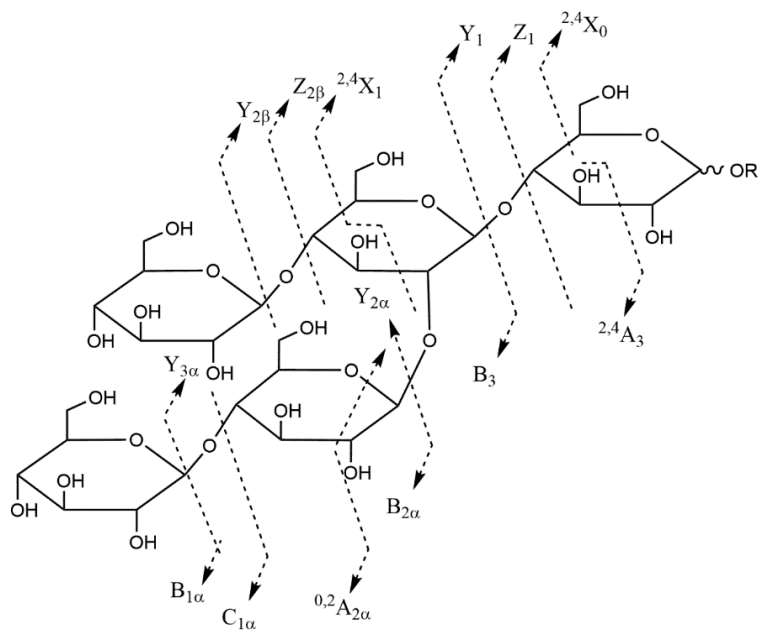


Figure 2. Nomenclature of fragment ions of branched oligosaccharide Dotted line illustrates the fragmented bond and arrow the ionized side of the molecule. A and X = ions formed by cross-ring cleavages. B, C, Y and Z = ions formed by glycosidic bond fragmentation. Subscript = number indicates the position of cleaved glycosidic bond. Superscript = numbers indicate the positions of cleaved bonds in ring. Greek letters differentiate the branches (Domon & Costello 1988)

## 2.4.2 Fragmentation mechanisms of underivatised oligosaccharides

Several previous studies presented the fragmentation reaction mechanisms in neutral di- and oligosaccharides (Carroll et al. 1995; Dallinga & Heerma 1991; Domon & Costello 1988; Garozzo et al. 1990; Hofmeister et al. 1991; Spengler et al. 1990; Spina et al. 2004). The fragmentation of neutral oligosaccharide can occur by the loss of water, cleavage of glycosidic bond, cross-ring cleavage or six-atom rearrangement.

### *Loss of water*

Based on their study on  $^{18}\text{O}$ -labelled gentiobiose by FAB-MS/MS, Hofmeister et al. (1991) suggested that the loss of water reaction in disaccharides occurs by the mechanism demonstrated in Figure 3. Their proposal is supported by the observations that (1 $\rightarrow$ 1) or (1 $\rightarrow$ 2)-linked disaccharides do not lose water. This loss of water reaction needs to have free hydroxyl groups in C-1 and C-2 to form an epoxide structure.

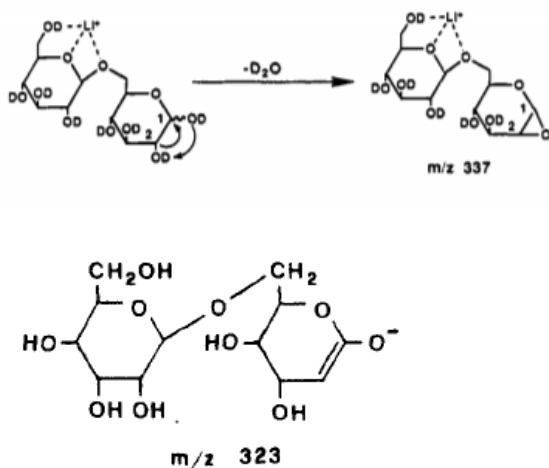


Figure 3. Loss of a water molecule in positive ionisation FAB-MS/MS (left). Adapted from Hofmeister et al. (1991). Loss of water molecule in negative ionisation FAB-MS/MS (right). Adapted from Garozzo et al. (1990)

In a study on negatively charged disaccharides Garozzo et al. (1990) proposed a different type of product ion (Figure 3, right) in the water loss molecule. In this mechanism, the loss of water leads to the double-bond structure of the deprotonated molecule.

### Glycosidic bond cleavage (B-, C-, Z- and Y-ions)

The glycosidic bond cleavage forms B- and C-ions or Z- and Y-ions, depending on which side the charge is located. In their original oligosaccharide nomenclature paper, Domon and Costello (1988) proposed structures for positively charged B- and Y-ions formed from aglycone. B-ion was suggested to have a double-bond structure. However, in a study on reducing lithium cationised and deuterated disaccharides, Hofmeister et al. (1991) suggested that the B-ion may have an epoxide structure similar to the water loss molecule (Figure 4). The reaction starts by the abstraction of the hydroxyl proton.

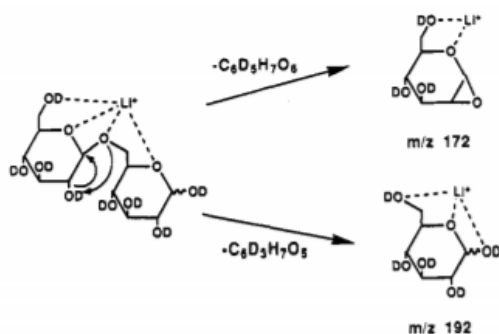


Figure 4. Proposed mechanism of glycosidic bond cleavage in FAB-MS/MS and the formation of B- and Y-ions.  $m/z$  172 = B-ion.  $m/z$  192 = Y-ion. Adapted from Hofmeister et al. (1991)

Dallinga and Heerma (1991) demonstrated the mechanism in the glycosidic bond cleavage of deprotonated disaccharide using FAB-MS and deuterated disaccharides (Figure 5). In this reaction, B- and Z-ions were formed. In their study on LSIMS/FTMS, Carroll et al. (1995) suggested that in addition to the mechanism presented above, competitive dissociation (i.e. competition for the proton) may occur, and therefore deprotonated anomeric oxygen is allowed to form (Figure 6), which leads to the formation of C- and Z-ions.

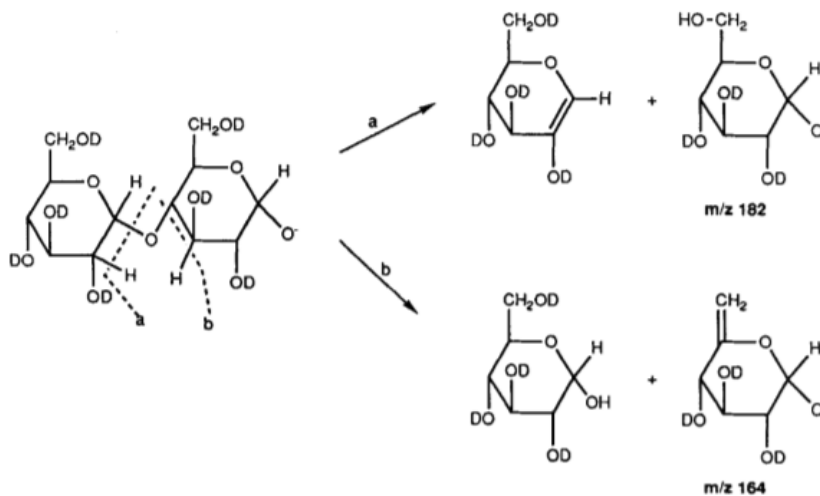


Figure 5. Proposed deprotonated B- and Y-type glycosidic bond fragment ions.  $m/z$  182 = Y-ion.  $m/z$  164 = Z-ion. Adapted from Dallinga and Heerma (1991)

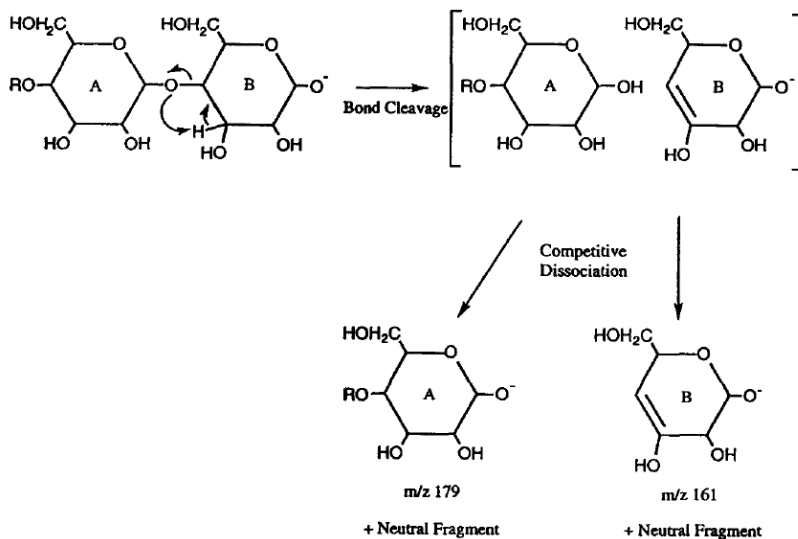


Figure 6. Proposed reaction mechanism in deprotonated C- and Z-type glycosidic bond fragment ions.  $m/z$  179 = C-ion.  $m/z$  161 = Z-ion. Adapted from Carroll et al. (1995)

### *Cross-ring cleavages (A- and X-ions)*

Both Spengler et al. (1990) and Hofmeister et al. (1991) proposed fragmentation mechanisms in the cross-ring cleavages (A- and X-ions) of disaccharides. Spengler et al. (1990) studied the mechanisms of sodiated disaccharides using infrared laser desorption mass spectrometry (IR-LDMS) and Hofmeister et al. (1991) lithiated disaccharides using FAB-MS/MS. Both speculated about the possible pathways (e.g. retro-aldol and retro-ene reactions). Hofmeister et al. (1991) suggested that based on the isotope labelling experiments, the cross-ring reaction of two-carbon fragment (60 Da) was a retro-aldol-reaction. They also proposed that for loss of three carbon fragment (90 Da loss) to occur, carbonyl migration was needed prior to bond cleavage. Because the C-4 oxygen is protected in (1→4)-linked disaccharides, such as lactose, this type of fragmentation does not occur. The loss of a four-carbon fragment from gentiobiose was found to occur directly from the precursor, not through two-carbon fragmentation. This finding suggested that the loss of the four-carbon fragment reaction was initiated by carbonyl migration to C-3 through keto-enol tautomerism. However, because Spengler et al. (1990) and other studies (section 2.4.3) also observed the loss of the four-carbon fragment from the (1→4)-linked disaccharides, it seems likely that the other retro-aldol reaction could occur after the loss of the two-carbon fragment in some conditions. Figure 7 and Figure 8 present the fragmentation mechanisms of (1→6)-linked gentiobiose and the formation of  $^{0,2}A$ ,  $^{0,3}A$  and  $^{0,4}A$  ions proposed by Hofmeister et al. (1991). The reactions are initiated by the opening of the reducing sugar hemiacetal ring and the formation of hydroxide aldehyde, which is followed by the fragmentation reaction.



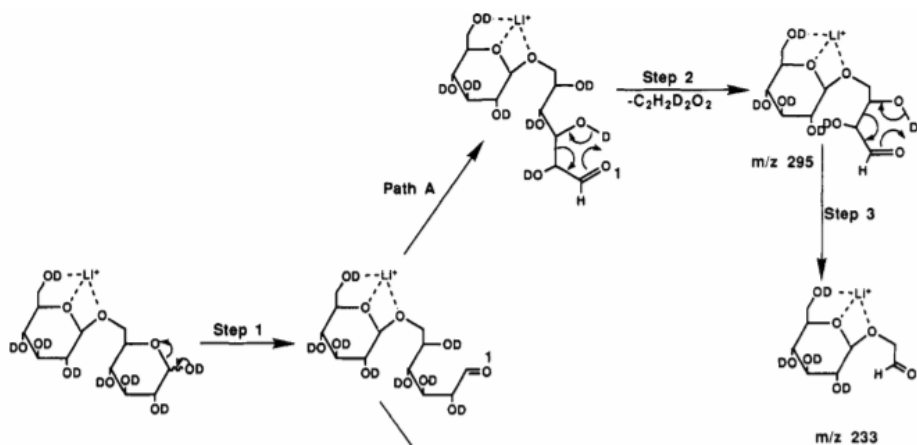


Figure 7. Proposed mechanism in the cross-ring cleavage of deuterated (1→6)-linked gentiobiose in positive ionisation FAB-MS/MS: retro-aldol reaction and the loss of two (step 2) and four carbon (step 3) fragments.  $m/z$  295 =  $^{0,2}$ A-ion.  $m/z$  233 =  $^{0,4}$ A-ion. Adapted from Hofmeister et al. (1991)

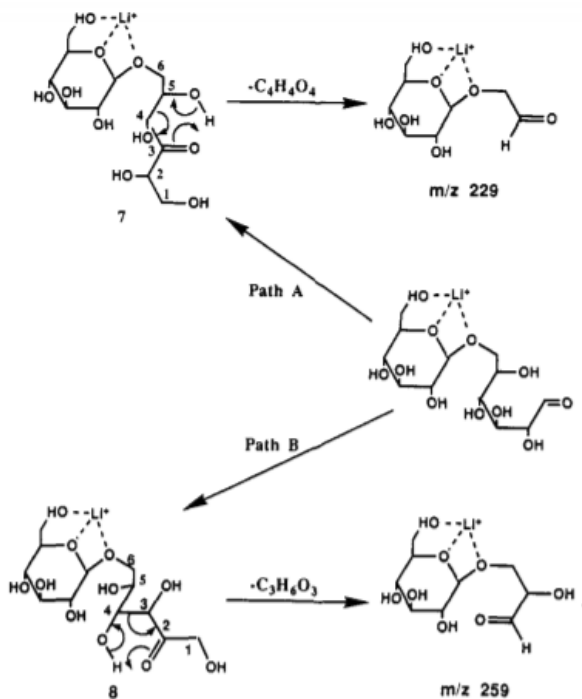


Figure 8. Proposed mechanism in the cross-ring cleavage of (1→6)-linked gentiobiose: keto-enol tautomerisation and fragmentation reaction of three (path B) and four carbon (path A) fragments.  $m/z$  229 =  $^{0,4}$ A-ion.  $m/z$  259 =  $^{0,3}$ A-ion. Adapted from Hofmeister et al. (1991)

### *Double glycosidic bond cleavages (D-ions)*

In their study on human urine oligosaccharides, Chai et al. (2001) observed double glycosidic bond fragmentation (both C- and Z- types), which was analysed by negative ionisation ESI-MS. The ions were assigned as D-ions. The reaction mechanism (Figure 9) in D-ion fragmentation was proposed by Harvey (2005). The fragmentation occurs in O-3-branched oligosaccharides. D-ions were also observed in positive mode MALDI-QIT-TOF MS/MS spectra (Harvey 2004). In contrast to the negative mode, the D-ions in positive mode were suggested to be formed by B and Y rather than C and Z fragmentation pathways.

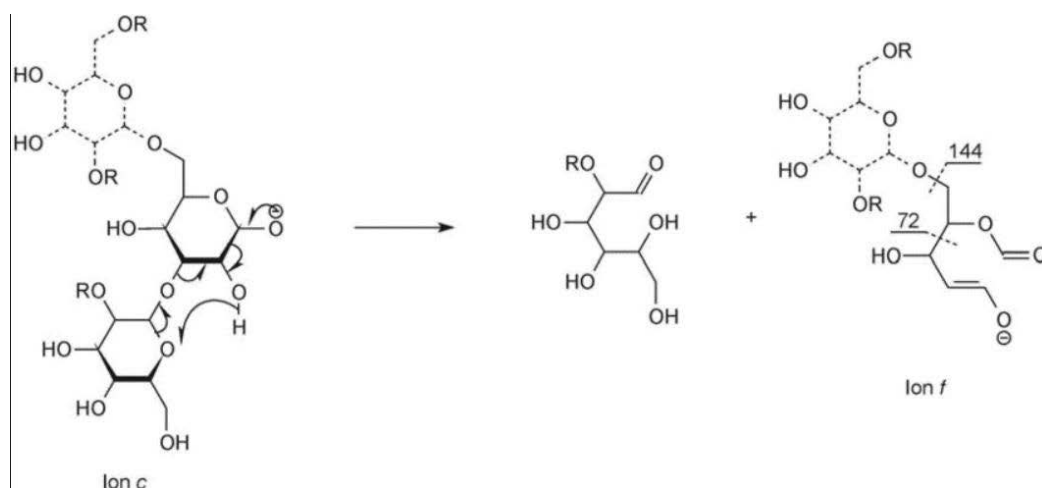
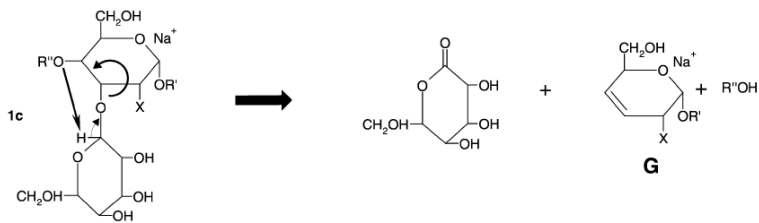
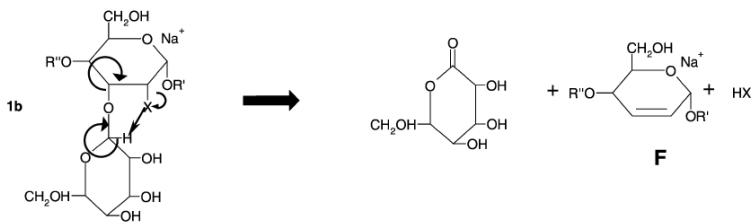
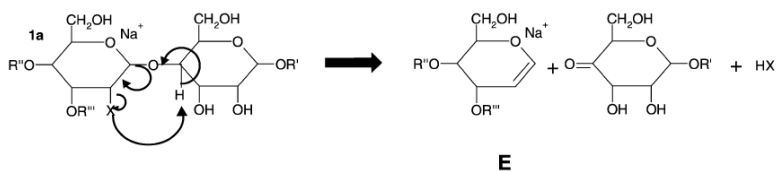


Figure 9. Proposed mechanism in D-ion formation in negative ionisation ESI-MS/MS. Adapted from Harvey (2005)

### *Six-atom rearrangement (E-, F- and G-ions)*

The proposed six-atom rearrangement fragmentation mechanism was observed when human milk oligosaccharides were analysed by a novel MALDI-TOF/TOF MS system (Spina et al. 2004). These fragmentations could also be described as double fragmentations, in which, in addition to glycosidic bond cleavage Z- or B-type, the neighbouring hydroxyl group is cleaved (Figure 10). These types of fragmentations have not been reported as occurring in the application of other MS techniques.



X = OH or NHCOCH<sub>3</sub>

Figure 10. Formation of E-, F- and G-ion by six-atom rearrangement in positive ionisation MALDI-TOF/TOF-MS. Adapted from Spina et al. (2004)

### 2.4.3 Linkage position determination by MS/MS

Several previous studies established that the cross-ring fragmentations of disaccharides in MS/MS are diagnostic of linkage position determination in both positive (Table 2) (Asam & Glish 1997; Čmelík & Chmelík 2010; Hernández-Hernández et al.2012; Hofmeister et al 1991; Lee et al. 2012; Spengler et al.1990; Zhang et al. 2008) and negative ionisation modes (Table 3) (Čmelík & Chmelík 2010; Garozzo et al.1990; Guan & Cole 2008; Jiang & Cole 2005, Zhu & Cole, 2001). Although some fragmentation conditions may vary and influence the abundance of cross-ring fragments, the main cross-ring fragmentation pathways remain the same. These fragmentation conditions include the collision gas (e.g. helium or argon), collision energy (low or high; low energy if quadrupole or IT is used), adducts and MS instruments used in the process.

Previous studies clearly showed that in the positive mode, (1→2)-linked reducing hexopyranosyl disaccharides, such as manno- and sophorose, fragmented from the reducing end mainly by 120 Dalton (Da) cross-ring fragment and form  $^{0,2}X_0$ -ion (Table 2, lines 2, 12, 13 and 14). (1→3)-linked reducing disaccharides, nigerose and laminaribiose were found to fragment by the loss of 90 Da cross-ring fragment from the reducing end and form  $^{0,3}X_0$  ions (Table 2, lines 3, 4, 15). In the positive mode, (1→4)-linked disaccharides, such as maltose, cellobiose and lactose, fragment from the reducing end mainly by 60 Da cross-ring fragment ( $^{0,2}A_2$ -ion), and they do not lose 90 Da cross-ring fragment (Table 2, lines 5–7, 17–19). (1→6)-linked disaccharides fragment from the reducing end by the loss of three types of fragments—60 Da, 90 Da and 120 Da—and they form  $^{0,2}A_2$ ,  $^{0,3}A_2$  and  $^{0,4}A_2$  – ions. However, non-reducing disaccharides, such as trehalose, do not form cross-ring fragments (Table 2, lines 1 and 11).

In addition, fructose-containing disaccharides have diagnostic fragmentation patterns in the positive ionisation mode. (1→2)-linked sucrose is a non-reducing disaccharide, and it does not form cross-ring fragment ions (Table 2, line 24). (1→3)-linked turanose ( $\alpha$ -D-Glcp-(1→3)-D-Fru) fragments by the loss of 60 Da and 90 Da neutrals (Table 2, line 25). (1→4)-linked lactulose has been found to fragment by the loss of 48 Da, 60 Da and 90 Da cross-ring fragments (Table 2, line 26). Palatinose/isomaltulose ( $\alpha$ -D-Glcp-(1→6)-D-

Fru), which has (1→6)-linkage, produces fragments by 30 Da, 60 Da, 90 Da and 120 Da neutral loss (Table 2, line 28).

Table 2. Main cross-ring fragment ions produced from neutral disaccharides in positive ionisation MS/MS.  $[M+Li]^+$  and  $[M+Na]^+$  precursor ions.

Line	Precursor <i>m/z</i>	Trivial name	Structure	Neutral loss, X					Reference
				18 Da	60 Da	90 Da	120 Da	others	
$[M-X+Li]^+$				331	289	259	229		
1	349	Trehalose	$\alpha$ -D-Glcp-(1→1)- $\alpha$ -D-Glcp						1),3)
2	349	Sophorose	$\beta$ -D-Glcp-(1→2)-D-Glc				1)		1)
3	349	Nigerose	$\alpha$ -D-Glcp-(1→3)-Glc	1)		1)			1)
4	349	Laminaribiose	$\beta$ -D-Glcp-(1→3)-D-Glc	3)		3)			3)
5	349	Maltose	$\alpha$ -D-Glcp-(1→4)-D-Glc	1)	<u>1</u> )		1)		1)
6	349	Cellobiose	$\beta$ -D-Glcp-(1→4)-D-Glc	1)	<u>1</u> )		1)		1)
7	349	Lactose	$\beta$ -D-Galp-(1→4)-D-Glc	1),3)	<u>1</u> ),3)		1)		1),3)
8	349	Melibiose	$\alpha$ -D-Galp-(1→6)-D-Glc	3)	3)	3)	3)		3)
9	349	Isomaltose	$\alpha$ -D-Glcp-(1→6)-Glc	1)	<u>1</u> )	1)	1)		1)
10	349	Gentiobiose	$\beta$ -D-Glcp-(1→6)-Glc	1),3)	<u>1</u> ),3)	1),3)	1),3)		1),3)
$[M-X+Na]^+$				347	305	275	245		
11	365	Trehalose	$\alpha$ -D-Glcp-(1→1)- $\alpha$ -D-Glcp						1),2),4),5),6)
12	365	Mannobiose	$\alpha$ -D-Manp-(1→2)-D-Man	6)	6)	6)	<u>6</u> )		6)
13	365	Koijbiose	$\alpha$ -D-Glcp-(1→2)-D-Glc				5)		5)
14	365	Sophorose	$\beta$ -D-Glcp-(1→2)-D-Glc				1)		1)
15	365	Nigerose	$\alpha$ -D-Glcp-(1→3)-D-Glc	1),5)		1),(2),5)			1),2),5)
16	365	Laminaribiose	$\beta$ -D-Glcp-(1→3)-D-Glc						
17	365	Maltose	$\alpha$ -D-Glcp-(1→4)-D-Glc	1),2),6),7)	<u>1</u> ),2),6),7)		1),2)		1),2),6),7)
18	365	Cellobiose	$\beta$ -D-Glcp-(1→4)-D-Glc	1),(2),4)	<u>1</u> ),2), <u>4</u> )	4)	1),2)		1),2)
19	365	Lactose	$\beta$ -D-Galp-(1→4)-Glc	1),5)	<u>1</u> ), <u>5</u> )		1),(5)		1)
21	365	Melibiose	$\alpha$ -D-Galp-(1→6)-D-Glc	4),7)	<u>4</u> ), <u>5</u> ),7)	4),(5),7)	4),(5),7)		4),(5),7)
22	365	Isomaltose	$\alpha$ -D-Glcp-(1→6)-D-Glc	1),6)	<u>1</u> ),2), <u>6</u> ),7)	1),(2),6),7)	1),(2),6),7)		1),(2),6),7)
23	365	Gentiobiose	$\beta$ -D-Glcp-(1→6)-D-Glc	1),(2),4)	<u>1</u> ),2), <u>4</u> )	1),(2),4)	1),(2),4)		1),(2),4)
24	365	Sucrose	$\alpha$ -D-Glcp-(1→2)- $\beta$ -D-Fruf						2),4),7)
25	365	Turanose	$\alpha$ -D-Glcp-(1→3)-D-Fru	7)	7)	7)			7)
26	365	Lactulose	$\beta$ -D-Galp-(1→4)-D-Fru	5)	5)	(5)		<u>5</u> ) 317	5)
27	365	Leucrose Palatinose/	$\alpha$ -D-Glcp-(1→5)-D-Frup	4)	4)	<u>4</u> )			4)
28	365	isomaltulose	$\alpha$ -D-Glcp-(1→6)-D-Fru	4),7)	4),7)	2), <u>4</u> ),7)	4),7)	7) 335	2),7)

1) Asam & Glish 1997 (ESI-MS<sup>n</sup>, CID gas helium), 2) Spengler et al.1990 (IR-LDMS) 3) Hofmeister et al. 1991 (FAB-MS/MS, CID gas argon), 4) Lee et al. 2012 (IMS-CID-MS), 5) Hernández-Hernández et al. 2012 (LC-ESI-MS<sup>n</sup>, CID gas helium), 6) Zhang et al. 2008 (MALDI-ITMS/MS), 7) Čmelík & Chmelík 2010 (ESI-MS<sup>n</sup>). Main peak of cross-ring fragments underlined, if presented. Low intensity peak in parenthesis (if mentioned or under 3%).

Table 3 presents the main cross-ring fragments produced from neutral hexose disaccharides as  $[M-H]^-$  and  $[M+Cl]^-$  precursors in negative ionisation MS/MS. The fragment ion patterns of negatively charged disaccharides differ partially from positively charged disaccharides. In addition to fragmentation by the loss of 60 Da, 90 Da and 120 Da cross-ring fragments, the negatively charged disaccharides were found to produce the loss of 78 Da cross-ring fragments (Garozzo et al. 1990). This is 60 Da cross-ring fragment combined with a loss of water molecule. The loss of the 78 Da fragment is formed from (1→2) and (1→4)-linked disaccharides (Table 3, lines 2–4, 7–9, 15, 17, 20–23). The fragment ions are always in deprotonated form even if the precursor ion is an anion adduct, such as  $[M+Cl]^-$ . Similar to the positive mode, the non-reducing disaccharides trehalose and sucrose do not form cross-ring fragments (Table 3, lines 1 and 13).

Table 3. Summary of main cross-ring fragment ions produced from neutral disaccharides in negative ionisation MS/MS.  $[M+Cl]^-$  and  $[M-H]^-$  precursor ions.

Line	Precursor <i>m/z</i>	Trivial name	Structure	Neutral loss, X					Reference
				30 Da	60 Da	78 Da	90 Da	120 Da	
<b><math>[M+Cl-X-HCl]^-</math></b>				311	281	263	251	221	others
1	377	Trehalose	$\alpha$ -D-Glcp-(1→1)- $\alpha$ -D-Glcp						2),4)
2	377	Mannobiose	$\alpha$ -D-Manp-(1→2)-D-Man			4)		<u>4</u> )	4)
3	377	Koijbiose	$\alpha$ -D-Glcp-(1→2)-D-Glc			<u>4</u> )		4)	4)
4	377	Sophorose	$\beta$ -D-Glcp-(1→2)-D-Glc			<u>4</u> )		4)	4)
5	377	Nigerose	$\alpha$ -D-Glcp-(1→3)-D-Glc					(4)	4)
6	377	Laminaribiose	$\beta$ -D-Glcp-(1→3)-D-Glc					(4)	2),4)
7	377	Maltose	$\alpha$ -D-Glcp-(1→4)-D-Glc		<u>4</u> ),5)	4),5)		5)	4),5)
8	377	Cellobiose	$\beta$ -D-Glcp-(1→4)-D-Glc		2),3),4)	2), <u>3</u> ), <u>4</u> )		3)	2),3),4)
9	377	Lactose	$\beta$ -D-Galp-(1→4)-D-Glc		4)	<u>4</u> )			4)
10	377	Melibiose	$\alpha$ -D-Galp-(1→6)-D-Glc	5)	4),5)		4),5)	<u>4</u> ), <u>5</u> )	4)
11	377	Isomaltose	$\alpha$ -D-Glcp-(1→6)-D-Glc		4),5)		4),5)	<u>4</u> ), <u>5</u> )	4), 5)
12	377	Gentiobiose	$\beta$ -D-Glcp-(1→6)-D-Glc		2),4)		2),4)	<u>2</u> ), <u>4</u> )	4)
13	377	Sucrose	$\alpha$ -D-Glcp-(1→2)- $\beta$ -D-Fruf						2),4) 197,215
14	377	Turanose	$\alpha$ -D-Glcp-(1→3)-D-Fru				2),4),5)		2),4),5)
15	377	Lactulose	$\beta$ -D-Galp-(1→4)-D-Fru		4)	<u>4</u> )		4)	4),2)
16	377	Palatinose/ isomaltulose	$\alpha$ -D-Glcp-(1→6)-D-Fru	5)	2),4),5)		<u>2</u> ), <u>4</u> ), <u>5</u> )	2),4),5)	2),4),5)
<b><math>[M-X-H]^-</math></b>				311	281	263	251	221	
17	341	Sophorose	$\alpha$ -D-Glcp-(1→2)-D-Glc		1)	<u>1</u> )		1)	1)
18	341	Nigerose	$\alpha$ -D-Glcp-(1→3)-D-Glc		1)		<u>1</u> )		1)
19	341	Laminaribiose	$\beta$ -D-Glcp-(1→3)-D-Glc		<u>1</u> )		1)		1)
20	341	Maltose	$\alpha$ -D-Glcp-(1→4)-D-Glc		<u>1</u> )	1)			1)
21	341	Cellobiose	$\beta$ -D-Glcp-(1→4)-D-Glc		<u>1</u> ),3)	1), <u>3</u> )		3)	1), 3) small peaks
22	341	Lactose	$\beta$ -D-Galp-(1→4)-D-Glc		<u>1</u> )	1)			1)
23	341	Epilactose	$\beta$ -D-Galp-(1→4)-D-Man		<u>1</u> )	1)			1)
24	341	Melibiose	$\alpha$ -D-Galp-(1→6)-D-Glc	1)	1)		<u>1</u> )	1)	1)
25	341	Isomaltose	$\alpha$ -D-Glcp-(1→6)-D-Glc	1)	<u>1</u> )		1)	1)	1)
26	341	Gentiobiose	$\beta$ -D-Glcp-(1→6)-D-Glc	1)	1)		<u>1</u> )	1)	1)

1) Garozzo et al. 1990 (FAB-MS/MS, CID gas helium) 2) Zhu & Cole 2001 (ESI-MS/MS, CID gas argon) 3) Jiang & Cole 2005 (ESI-MS/MS, CID gas argon) 4) Guan & Cole 2008 (MALDI-TOF-PSD) 5) Čmelík & Chmelík 2010 (ESI-ITMS<sup>n</sup> CID). Main peak of cross-ring fragments underlined, if presented. Low intensity peak in parenthesis (if mentioned or under 3%).

#### 2.4.4 Oligosaccharide analyses by MS/MS and MS<sup>n</sup>

As discussed in section 2.4.3, several studies analysed the structure of disaccharides in MS/MS or MS<sup>n</sup> in both positive and negative ionisation. Most previous analyses of oligosaccharides were focused on N-linked glycans or glycopeptides (Black et al. 2012; Chai et al. 2001; Chai et al. 2002; Harvey 2005; Pfenninger et al. 2002a; Pfenninger et al. 2002b). However, there are previous studies on oligosaccharides hydrolysed from plant polysaccharides, such as starch (Asam & Glish 1997; Čmelík & Chmelík 2010; Garozzo et al. 1990; Yamagaki & Sato 2009), cellulose (Asam & Glish 1997), xylan (Pu et al. 2017; Reis et al. 2005), arabinoxylan (Bowman et al. 2012b; Matamoros-Fernández et al. 2003b; Maslen et al. 2007; Plancot et al. 2014, Quemener et al. 2006; Wang et al. 2009), glucuronoxylans (Chong et al. 2011; Reis et al. 2004a; Reis et al. 2004b),  $\beta$ -glucan (Boulos & Nyström 2016), xyloglucans (Liu et al. 2016; Vinueza et al. 2013) and fructans (Liu & Rochfort 2015; Verspreet et al. 2015) or produced by LAB, such as dextrans (Čmelík et al. 2004, Yi et al. 2015).

Oligosaccharides have been analysed by MS using the soft ionisation techniques MALDI and ESI. Previous studies on oligosaccharides showed that MS/MS can be used to determine the sequences, linkages, branches and fragmentation patterns of oligosaccharides. MS/MS is also excellent tool for the identification and characterisation of oligosaccharide isomers. MS analysis can be enhanced by combining it with separation techniques, such as gas chromatography (GC), LC and IM. Previous MS studies on oligosaccharides are introduced in this section.

##### *Native oligosaccharides*

Positively charged native oligosaccharides have been analysed by MS mainly as lithium or sodium adduct ions (Asam & Glish 1997; Čmelík & Chmelík 2010), but other metal adduct ions, such as cobalt (König & Leary 1998), have been tested. The samples in positive ionisation MS are often derivatised, but some studies have examined oligosaccharides in their native form. For example, positive MALDI-MS or AP-MALDI-MS methods have successfully been used to determine the molecular weight distribution of oligosaccharides mixtures and extracts, such as starch GLOS (Broberg et al. 2000) and acetylated (A)XOS (Chong et al. 2011). In MALDI-MS it is possible also to



determine the molecular weights of fractionated polysaccharides, such as dextrans (Garrozzo et al. 1995).

The identification of commercial GLOS by different cross-ring fragmentation patterns and linkage information was performed by ESI-qIT-MS<sup>n</sup> (Asam & Glish 1997) and FTICR-MS (Pasanen et al. 2007). The characterisation of acetylated patterns of underivatised acetylated neutral and acidic XOS was determined by ESI-MS and ESI-MS/MS (Reis et al. 2005).

Most recent MS/MS studies were focused on the negative ionisation mode. Garozzo et al. (1990) reported that the negative charge was localised on anomeric hydroxyl at the reducing end because of its acidity, which allowed for the identification of linkage at the reducing end and oligosaccharide sequencing. The linkage position and sequencing were determined by fragmentation patterns from deprotonated commercial oligosaccharides using FAB-MS/MS (Garozzo et al. 1990), ESI-MS<sup>n</sup> (Cmelik & Chmelík 2010; Usui et al. 2009) and LC-MS/MS (Yi et al. 2015). Studies on oligosaccharides were also performed using anion adducts such as chlorine (Guan & Cole 2007; Usui et al. 2009).

#### *MS compatible derivatisation techniques for carbohydrates*

Because MS can differentiate only the precursor and product ions by  $m/z$ , it might be challenging or even impossible to identify isobaric fragment ions if the oligosaccharides are built by the same mass monosaccharides. Therefore, in most MS studies on oligosaccharides, the samples were derivatised prior to the analysis. Derivatisation is also needed in RP chromatography to separate the (isomeric) oligosaccharides in mixtures. Some common derivatisation techniques are presented in the following paragraphs.

#### *Per-O-methylation*

The per-*O*-methylation of carbohydrates is an old derivatisation technique in which all hydroxyl groups of carbohydrates are derivatised to methyl ethers. This method was developed by Ciucanu and Kerek (1984) and Ciucanu (2006) for use in complex carbohydrates. In the past, the technique was usually combined with GC in the Björndal method, in which the oligosaccharides samples are hydrolysed and analysed by GC-MS as partially methylated alditol acetates (Björndal 1967).

Recently, the per-*O*-methylation technique was used with direct infusion positive ionisation ESI-MS/MS to characterise the linkages, sequence, composition and structure of oligosaccharides (Ashline et al. 2009; Bowman et al. 2012b; Lemoine et al. 1993, Matamoros-Fernández et al. 2003; Mazumder et al. 2010). Per-*O*-methylated oligosaccharides can also be reduced to alditols before per-*O*-methylation. Reduction helps to differentiate the reducing end fragments from the non-reducing end fragments (Morelle et al. 2004).

### *Reduction*

Reduction to alditols has also been used without per-*O*-methylation to differentiate reducing-end and non-reducing-end fragment ions (Everest-Dass et al. 2013a; Karlsson et al. 2004; Reis et al. 2004b). Reduction is usually performed using sodium borohydride or sodium borodeuteride. Reduced oligosaccharides produce fewer cross-ring fragments because the alditol does not have a carbonyl group with which to initiate the retro-aldol reaction. However, the original reducing end residue can be differentiated after reduction from the other end using a different mass in the sequencing of monomers (Reis et al. 2004b).

### *Isotope labelling*

Because isotope labelling does not change the chemistry of molecules, it is an excellent technique for use in studies on example fragmentation mechanisms. The common isotope labelling techniques used for oligosaccharides include hydroxyl group labelling. For example, all protons in hydroxyl groups can be changed to deuteriums (Dallinga & Heerma 1991; Hofmeister et al. 1991). Oxygen at the reducing end in the hydroxyl group can be changed to the <sup>18</sup>O-isotope (Hofmeister et al. 1991). This technique enables the separation of reducing end fragments from non-reducing end fragments.

Commercial standard manufacturers offer a variety of <sup>13</sup>C-labelled sugars. In a structural study on the oligosaccharides produced by fructosyl transferase, Harrison et al. (2012) demonstrated the use of sucrose with <sup>13</sup>C-labelled fructose residue to differentiate fructose residue from isomeric glucose residues.

### *Reducing end labelling*

Another common reducing end labelling technique is reductive amination. MS studies in positive mode have used 2-aminobenzoic acid (2-AA) labelled and 2-aminobenzamide (2-AB) labelled (A)XOS (Maslen et al. 2007). In negative mode, such as 2-AA (Jonathan et al. 2017) and 2-AB (Harvey 2005b), labels were used to analyse glucuronoxyloligosaccharides (UXOS), xyloglucooligosaccharides (XGLOS) and N-linked glycans. These labels were detectable by fluorescence or a UV-detector. The labelling reaction starts with the condensation of the amine group from the label molecule with the aldehyde group from the reducing oligosaccharide (Ruhaak et al. 2010). The end product, imine or Schiff base is then reduced to secondary amine (Ruhaak et al. 2010). Instead of reductive amination, another type of the reducing end label can also be used. For example, 1-phenyl-3-methyl-5-pyrazolone (PMP) was used as a reducing end label that was added by nucleophilic addition reaction (Ruhaak et al. 2010). Pu et al. (2016) used PMP labelling in an analysis of an XOS mixture.

### **2.4.5 Combining MS and liquid chromatography**

Chromatographic methods are techniques used to separate mixtures. Many chromatographic methods, (e.g. GC, capillary electrophoresis and LC) combined with MS have been developed for the analysis of oligosaccharides. The most common high-performance liquid chromatography (HPLC) methods are introduced in the following paragraphs.

In LC-MS, both monosaccharides and oligosaccharides can be analysed. Reverse phase liquid chromatography (RP-LC) can be coupled to MS because it uses MS compatible solvents, such as acetonitrile, methanol and water. The column stationary phase is usually C18. Because oligosaccharides, like all carbohydrates, are polar compounds, they can be analysed using RP-LC only after derivatisation. Reverse phase liquid chromatography (RP-LC) combined with MS or/and MS<sup>n</sup> was used to analyse reduced and per-*O*-methylated oligosaccharides (Bowman et al. 2012b) and 2-AA labelled oligosaccharides released from corn stover (Jonathan et al. 2017). Pu et al. (2016) used PMP labelling to analyse XOS by RP-LC-MS. The advantage of 2-AA and PMP labelling is that oligosaccharides are also detectable by spectrophotometer.

Guignard et al. (2005) identified underivatized oligosaccharides in poplar leaf extract using high-performance anion exchange chromatography (HPAEC) as well as MS and MS/MS. HPAEC uses a high alkali solvent eluent, which is not suitable in MS. Therefore, prior to MS, HPAEC-MS requires a desalting instrument to remove extra alkali salts.

Porous graphitized carbon LC (PGC-LC) coupled to MS/MS has been demonstrated to be an excellent tool for the analysis of complex isomeric mixtures of N- and O-glycans (Everest-Dass et al. 2013; Everest-Dass 2013b; Karlsson et al. 2004). Harrison et al. (2012) also used PGC-LC-MS to analyse a mixture of isomeric fructooligosaccharides (FOS). MS compatible solvents are used in PGC.

A new era in the LC-MS analysis of oligosaccharides began when hydrophilic interaction liquid chromatography (HILIC) was invented. HILIC techniques use MS compatible solvents, such as acetonitrile, methanol and water. As the name implies, the columns have a hydrophilic stationary phase formed of amide or other polar compounds, such as zwitterionic phase. Oligosaccharides are separated by their hydrophilic interaction with the stationary phase, and retention increases with the hydrophilicity of analytes (Alpert 1990).

Examples of HILIC methods for oligosaccharides and their chromatographic conditions are presented in Table 7. Samples of oligosaccharides have been analysed mainly by HILIC-MS in their native underivatized form in either negative (Black et al. 2012; Boulos & Nyström 2016; Bowman et al. 2012a; Leijdekkers et al. 2011; Leijdekkers et al. 2015; Verspreet et al. 2015; Yi et al. 2015) or positive ionisation mode (Black et al. 2012; Hernández-Hernández et al. 2012; Leijdekkers et al. 2015; Liu et al. 2016; Maslen et al. 2007; Pu et al. 2017; Tryfona et al. 2019; Vismeh et al. 2013). Reducing end labelling, such as 2-AA, 2-AB and 3-AQ, were also used (Bowman et al. 2012a; Maslen et al. 2007). The usual mobile phases are organic solvent, such as acetonitrile and water/aqueous solvent. In the mobile phases, some MS compatible buffers and pH modifiers were used, such as ammonium formate, formic acid and ammonia. In general, in oligosaccharide analysis, the elution profile begins at the high organic solvent content of 95–80%, which decreases in gradients to about 50%.

Table 4. Analyses of oligosaccharides by HILIC-MS/MS

Oligo-saccharides	Sample origin	LC column	Mobile phases	Chromatographic conditions	Derivatisation	Analysis	Ionisation, adducts	Reference
(A)XOS	commercial XOS, (A)XOS from switch grass AX	HILIC amide-80 2.0 x 150 mm (Tosoh Biosciences, King of Prussia, PA)	A: 50 mM ammonium formate (pH 3.5) B: ACN	0.2 ml/min, 30 °C, 0-45 min A 20%-50%	2-AA labelling	LC-ESI-MS/MS	-, [M-H] <sup>-</sup>	Bowman et al. 2012a
(A)XOS	wheat AX	NP-HPLC, Amide-80 column 300 µm x 15 cm (Dionex, Sunnyvale, CA)	A: 50 mM ammonium formate (pH 4.4) B: 20% A in ACN	3 µl/min isocratic 0-5 min A 5%, 5-131 min A 5%-52%	2-AB and 2-AA labelling	HPLC-MALDI-TOF/TOF-MS/MS	+, [M+Na] <sup>+</sup>	Maslen et al. 2007
(A)XOS and GLOS	corn stover, (A)XOS from oat spelt xylan and birch wood xylan	Prevail Carbohydrate ES 2x150 mm, 5 µm (Alltech Associates Inc, Deerfield, IL, USA)	A: ACN B: 0.15% HCOOH	0.25 ml/min, 1 min A 95%, 1-8 min A 95-70%, 9-18 min 70-50%, 18-25 min isocratic	-	HPLC-TOFMS, HPLC-TOFMS/MS	+/- -, various, [M+Cl] <sup>-</sup>	Vismeh et al. 2013
AXOS and UXOS	Grass GAX	Amide-80, 300 µm x 25 cm, 3 µm (Dionex)	A: 50mm ammonium formate pH 4.4 B: ACN	ambient T, 3 µl/min, 0-6 min B 95%-75%, 6-86 min B 75%-55%	2-AA labelling	HILIC-MALDI-TOF-MS/(MS)	+, [M+Na] <sup>+</sup>	Tryfona et al. 2019
FOS	wheat grains	two Acquity UPLC HSS T3 C18 alkyl 2.1x100, 1.8µm (Waters) in series	0.1% formic acid	0.35 ml/min	-	UPLC-HESI-MS/MS	-, [M-H] <sup>-</sup>	Verspreet et al. 2015

Oligo-saccharides	Sample origin	LC column	Mobile phases	Chromatographic conditions	Derivatisation	Analysis	Ionisation, adducts	Reference
GLOS	$\beta$ -glucan	Acquity UPLC BEH amide column 2.1 x 150 mm, 1.7 $\mu$ m (Waters, Milford, MA, USA)	A: ACN B: water 0.1% NH <sub>4</sub> OH	0.17 ml/min, 35 °C a) 0-3 min 35%-45% B, 3-7 min isocratic b) 0-16 min 20%-38% B	Fenton degradation	UPLC-ESI-MS/(MS)	<sup>-</sup> , [M-H] <sup>-</sup>	Boulos & Nyström 2016
GLOS	dextran, commercial GLOS	Acquity UPLC BEH Glycan column 2.1-150 mm, 1.7 $\mu$ m (Waters, Milford, MA, USA)	A: 95% ACN B: water, in both 10 mM CH <sub>3</sub> COONH <sub>4</sub> , pH 7.5, pH 5.0 and pH 10	0.2 ml/min, 20°C 0-15 min B 85%-25%.	-	UHPLC-ESI-MS, UHPLC-ESI-MS/MS	<sup>-</sup> , [M-H] <sup>-</sup>	Yi et al. 2015
GLOS and FOS	commercial oligosaccharides, wheat trisaccharides (1-kestose, Raffinose, 6G-kestose)	Prevail Carbohydrate ES column 250 x 4.6 mm, 5 $\mu$ m (Grace Davison Discovery Sciences)	A: ACN B: water, 0.1% formic acid in both	0.6 ml/min, 30 °C, 0-30min 20-50% B.	-	1) LC-ESI-QTOFMS 2) LC-IT-MS/MS	<sup>-</sup> , 1) [M+HCOO] <sup>-</sup> 2) [M-H] <sup>-</sup>	Liu & Rochfort 2015
GLOS, FOS etc.	commercial mono-, di- and oligosaccharides juice extracts	Luna 3 $\mu$ m NH <sub>2</sub> 100A (2.0 x 150 mm, 3 $\mu$ m), guard NH <sub>2</sub> (2.0 x 4.0) (Phenomenex, Bologna, Italy)	ACN/water 80:20 (v/v) post-column 0.1% HCOOH 0.3 mL/min 1:20 split	0.2 ml/min, 30°C, isocratic	-	LC-ESI-MS and LC-ESI-MS <sup>n</sup>	<sup>-</sup> , [M+HCOO] <sup>-</sup>	Verardo et al. 2009

Oligo-saccharides	Sample origin	LC column	Mobile phases	Chromatographic conditions	Derivatisation	Analysis	Ionisation, adducts	Reference
GLOS, GOS raffinose series	commercial di-oligosaccharides and mixture of GOS	a) ZIC-HILIC 2.1 x 150 mm, 3.5 µm (SeQuant, Umea, Sweden) b) PolyHydroxyethyl-A 2.1 x 100 mm, 3 µm (NestGroup, Inc., Southborough, MA, USA) c) BEH amide Xbridge 4.6 x 150 mm, 3.5 µm (Waters, Hertfordshire, UK)	A: ACN B:water modifiers various, optimised cond. 0.1% NH <sub>4</sub> OH	a) 0.2 ml/min b) 0.4 ml/min c) 0.4 ml/min 35°C, 0-31 min A 80%-50%, 5 min isocratic,	-	1) HPLC-ESI-MS, 2) HPLC-ESI-MS <sup>n</sup>	+ , [M+Na] <sup>+</sup>	Hernández et al. 2012
GOS	oligosaccharides produced by LAB	Supelcosil LC-NH <sub>2</sub> 4.6 mm x 250 mm, 5 µm (Sigma, Aldrich, Oakville, Canada)	ACN/water 80:20 (v/v) post-column CH <sub>3</sub> COONH <sub>4</sub> (40 mM in MeOH) 0.02 mL/min	1 ml/min, 25 °C, isocratic	-	HPLC-ESI-MS/MS, HPLC-ESI-MS <sup>n</sup> (in-source fragmentation)	+/- , [M-H] <sup>-</sup> , [M+Na] <sup>+</sup>	Black et al.2012
pectic oligosaccharides	plant cell wall oligosaccharides from lemon and sugar beet pectin	Acquity UPLC BEH amide 2.1 x 150 mm, 1.7 µm, VanGuard precolumn 2.1-5 mm, 1.7 µm (Waters, Milford, MA, USA)	A: 20:80 (v/v) ACN/water B:80:20 (v/v) water/ACN. C) 200 mM ammonium formate	0.6 ml/min, 35 °C, 0-30 min gradient A 15-45%, B 80-50%, C isocratic 5% . 34-40 min isocratic A45% and B 50 %.	3-AQ labelling (for fluorescence detection)	UPLC-ESI-TOFMS, UPLC-ESI-IM-TOFMS, UPLC-ESI-IM-TOFMS/MS	+/-	Leijdekkers et al.2015

Oligo-saccharides	Sample origin	LC column	Mobile phases	Chromatographic conditions	Derivatisation	Analysis	Ionisation, adducts	Reference
pectic oligosaccharides (+ GLOS, GOS, XOS, etc.)	commercial oligosaccharides, plant cell wall oligosaccharides from sugar beet pectin	Acquity UPLC BEH amide column 2.1 x 150 mm, 1.7 µm, VanGuard precolumn 2.1-5 mm, 1.7 µm (Waters, Milford, MA, USA)	A: 20:80 (v/v) ACN/water B: 80:20 (v/v) ACN/water. pH3: 10 mM ammonium acetate and 0.2% formic acid, pH 10 6.8 10 mM ammonium acetate, pH 10 0.1% NH <sub>4</sub> OH	0.6 ml/min, 35 °C, 0-1 isocratic B 100%, 1-31 min linear 70%-20% B	part of samples were partially methyl esterified or methyl esterified and acetylated	UPLC-ESI-MS <sup>n</sup>	-, [M-H] <sup>-</sup>	Leijdekkers et al. 2011
XGLOS	tamarind galactosylated xyloglucan	Xbridge Amide 1.0 mm x 50 mm, 3.5 µm, (Waters Corporation, USA)	A: ACN 5% B: ACN 95% both 0.1% formic acid	20 µl/min, various conditions e.g. 0-20 min B 100% - 60% 20-30 min B 60-100%	chemoenzymatic modification (anionic, cationic and benzyl amination)	HPLC-ESI-MS(/MS)	+, [M+Na] <sup>+</sup> , [M] <sup>+</sup> , [M+H] <sup>+</sup>	Liu et al. 2016
XOS	XOS	Zwitterionic Click Xion 4.6 x 250 mm, 5 µm (ACCHRIM Technology, Beijing, China)	A: ACN B: water, gradient 0-30 min A 75%-50%	1 ml/min, 35 °C	-	LC-ESI-ITMS	+/- [M+Na] <sup>+</sup> , [M+NH <sub>4</sub> ] <sup>+</sup>	Pu et al. 2017

ACN = acetonitrile, HCOOH = formic acid, BEH = ethylene bridged hybrid, chromatographic conditions include: flow rate, column temperature, gradient/isocratic profile



#### 2.4.6 Combining MS and ion mobility spectrometry

Ion mobility spectrometry coupled to MS (IMS-MS) is a promising analytical technique for the differentiation of isomeric oligosaccharides. IMS separates ions by their shape and size. In combination with MS, it brings a third dimension to mass and charge separation (Gabelica et al. 2019). Using the Waters hybrid instrument, IM separation can be performed before or after CID cell. IM analysis occurs in a cell that has an electric field and is filled with inert gas (e.g. nitrogen or helium). The ions are attracted through the gas, and the drift time in milliseconds is measured (Gabelica & Marklund 2018). The collision cross-section (CCS) values are calculated based on drift times and the kinetic theory of gases (Fenn & McLean 2010). The drift times are instrument- and method-dependent, but the CCS values are comparable if the ion structure, the nature of the bath gas, the temperature and the electric field/number of gas molecules per unit volume ( $E/N$ ) are known (Gabelica et al. 2019). Recommendations involving IMS data were published by a group of IMS experts (Gabelica et al. 2019).

Several previous studies analysed isomeric sugars or oligosaccharides. Even the first-generation ion mobility instruments, which were constructed in drift tubes, were reported to differentiate linkage and position isomers from disaccharides (Gabryelski & Froese 2002), trisaccharides (Clowers et al. 2005) and glycosides and simple sugars (Dwivedi et al. 2007). Zhu et al (2009) showed that the isomeric precursor ions of oligosaccharides and oligosaccharide alditols could be analysed by  $MS^n$  after separation using an ambient pressure ion mobility spectrometer.

The first commercial IM instrument was the TWIMS manufactured by the Waters Corporation. In TWIMS, because the electric field is not static, and the drift times cannot be directly converted to CCS values, some external calibrants are needed. Since CCS values depend on the nature of the calibrant, it is recommended that the latter should be similar in size, charge, and chemical class to the analytes (Gabelica & Marklund 2018). Pagel and Harvey (2013) presented the calibration protocol for TWIMS by using complex sodiated glycans and CCS values measured by drift tube IMS. Their study also showed improved resolution between the first-generation and second-generation TWIMS instruments. Fenn and McLean (2011) reported that pre- or post-IM

fragmentation prior to MS could be beneficial in the analysis of positional and structural isomers by TWIMS.

Recent studies showed that negatively charged precursor ions could be better separated in IM than positively charged precursor ions could. Negative ESI-IMS-MS/MS was demonstrated to separate isomeric oligosaccharides (Yamagaki & Sato, 2008). Harvey et al. (2013) showed that isomeric N-glycans could be separated by negative TWIMS-MS/MS. Hofmann et al. (2014) collected and analysed hundreds CCS values of N-glycans and their fragment ions. The adduct ion affects the three-dimensional shape of molecules. In comparison with negatively and positively charged oligosaccharides, glycan isomers were found to be separated in MS as  $[M-H]^-$  ions, but not as  $[M+H]^+$  or  $[M+Na]^+$  ions (Struwe et al. 2016). Hofmann et al. (2015) demonstrated that, with TWIMS-MS, connectivity and configurational isomers can be separated efficiently, especially as deprotonated ions. Their samples were trisaccharides derivatized with aminoalkyl linker.

Recent studies showed that isomeric fragment ions could be separated using new-generation IMS instruments. Both et al. (2014) showed that using the second-generation TWIMS following fragmentation, it was possible to discriminate epimeric glycans and glycopeptides. Gaye et al. (2015) built an IMS-CID-IMS-MS instrument that could distinguish between underivatized carbohydrate isomers according to the ion mobility distribution of lithiated fragment ions. Hoffman et al. (2017) presented by IM-MS/MS fingerprinting tool to differentiate Lewis and blood group isomers that had identical fragmentation spectra.

### 3 OBJECTIVES OF THE STUDY

The main aim of the thesis was to develop MS and LC-MS methods for the structural analysis of isomeric oligosaccharides in cereal matrices. The hypothesis was that MS methods can be used to identify the structures of oligosaccharides.

The main objectives were as follows:

- To determine the studied oligosaccharide samples using MS methods (I–IV)
- To study the influence of glycosidic linkage position and branch on fragmentation patterns of underivatized oligosaccharides in MS/MS (I–IV)
- To develop solutions for the separation and identification of oligosaccharide isomers (I–IV)
- To develop an LC-MS method for the quick profiling of oligosaccharide mixtures (III)

The specific objectives of the individual studies were as follows:

- To study the ability of an ESI-MS/MS method to analyse the structures of mixed-linked glucooligosaccharides (I)
- To characterise the isomeric branched oligosaccharides produced by lactic acid bacteria using isotopic labelling and ESI-MS<sup>n</sup> (II)
- To implement a method for separating and identifying linear and branched cereal arabinoxylan-derived oligosaccharides by combining the HILIC separation with MS (III)
- To study the potential of ion mobility-assisted MS for the identification of isomeric fragment ions produced from arabinoxylan oligosaccharides (IV)

## 4 MATERIALS AND METHODS

### 4.1 Materials

#### 4.1.1 Commercial disaccharide and oligosaccharide standards (I–IV)

Several commercial mono-, di- and oligosaccharides were used as model compounds in the MS studies. They are listed in Table 5.

Table 5. Commercial disaccharide standards

Saccharides	Structure	Manufacturer	Study
<u>Monosaccharides</u>			
1 Xylose (X <sub>1</sub> )	D-Xyl	Megazyme, Wicklow,Ireland	III
<u>Disaccharides</u>			
2 Mannobiose	$\alpha$ -D-Manp -(1→2)-D-Man	Dextra Laboratories,Reading,England	I
3 Nigerose	$\alpha$ -D-Glcp -(1→3)-D-Glc	Sigma-Aldrich Chemie, Steinheim, Germany	I
4 Laminaribiose	$\beta$ -D-Glcp -(1→3)-D-Glc	Megazyme, Wicklow,Ireland	I
5 Maltose	$\alpha$ -D-Glcp -(1→4)-D-Glc	Merck, Darmstadt,Germany	I
6 Cellobiose	$\beta$ -D-Glcp -(1→4)-D-Glc	Merck, Darmstadt,Germany	I
7 Isomaltose	$\alpha$ -D-Glcp -(1→6)-D-Glc	TCI Europe, Zwijdrecht,Belgium	I
8 Lactose	$\beta$ -D-Galp -(1→4)-D-Glc	Merck, Darmstadt,Germany	I,IV
9 Xylobiose (X <sub>2</sub> )	$\beta$ -D-Xylp -(1→4)-D-Xyl	Megazyme, Wicklow,Ireland	III
<u>Trisaccharides</u>			
10 Maltotriose	$\alpha$ -D-Glcp -(1→4)- $\alpha$ -D-Glcp -(1→4)-D-Glc	Sigma-Aldrich Chemie, Steinheim, Germany	I
11 Isomaltotriose	$\alpha$ -D-Glcp -(1→6)- $\alpha$ -D-Glcp -(1→6)-D-Glc	TCI Europe, Zwijdrecht,Belgium	I
12 Panose	$\alpha$ -D-Glcp -(1→6)- $\alpha$ -D-Glcp -(1→4)-D-Glc	TCI Europe, Zwijdrecht,Belgium	I
13 Galactotriose	$\alpha$ -D-Galp -(1→3)- $\beta$ -D-Galp -(1→4)-D-Gal	Dextra Laboratories,Reading,England	I
14 Glucotriose	$\beta$ -D-Glcp -(1→4)- $\beta$ -D-Glcp -(1→3)-D-Glc	Megazyme, Wicklow,Ireland	I
15 Xylotriose (X <sub>3</sub> )	$\beta$ -D-Xylp -(1→4)- $\beta$ -D-Xylp -(1→4)-D-Xyl	Megazyme, Wicklow,Ireland	III,IV
<u>Tetrasaccharides</u>			
16 Galactotetraose	$\alpha$ -D-Galp -(1→3)- $\beta$ -D-Galp -(1→4)- $\alpha$ -D-Galp -(1→3)-D-Gal	Dextra Laboratories,Reading,England	I
17 Glucotetraose 1	$\beta$ -D-Glcp -(1→4)- $\beta$ -D-Glcp -(1→3)- $\beta$ -D-Glcp -(1→4)-D-Glc	Megazyme, Wicklow,Ireland	I
18 Glucotetraose 2	$\beta$ -D-Glcp -(1→4)- $\beta$ -D-Glcp -(1→4)- $\beta$ -D-Glcp -(1→3)-D-Glc	Megazyme, Wicklow,Ireland	I
19 Maltotetraose	$\alpha$ -D-Glcp -(1→4)- $\alpha$ -D-Glcp -(1→4)- $\alpha$ -D-Glcp -(1→4)-D-Glc	Sigma-Aldrich Chemie, Steinheim, Germany	I
20 Cellotetraose	$\beta$ -D-Glcp -(1→4)- $\beta$ -D-Glcp -(1→4)- $\beta$ -D-Glcp -(1→4)-D-Glc	Sigma-Aldrich Chemie, Steinheim, Germany	I
21 Xylotetraose (X <sub>4</sub> )	$\beta$ -D-Xylp -(1→4)- $\beta$ -D-Xylp -(1→4)- $\beta$ -D-Xylp -(1→4)-D-Xyl	Megazyme, Wicklow,Ireland	III,IV
<u>Pentasaccharides</u>			
22 Xylopentaose (X <sub>5</sub> )	$\beta$ -D-Xylp -(1→4)- $\beta$ -D-Xylp -(1→4)- $\beta$ -D-Xylp -(1→4)- $\beta$ -D-Xylp -(1→4)-D-Xyl	Megazyme, Wicklow,Ireland	III,IV
23 XA <sup>2</sup> XX (+ XA <sup>3</sup> XX)	$\beta$ -D-Xylp -(1→4)-[ $\alpha$ -L-Araf-(1→2)]- $\beta$ -D-Xylp -(1→4)- $\beta$ -D-Xylp -(1→4)-D-Xyl	Megazyme, Wicklow,Ireland	III,IV
24 XA <sup>3</sup> XX	$\beta$ -D-Xylp -(1→4)-[ $\alpha$ -L-Araf-(1→3)]- $\beta$ -D-Xylp -(1→4)- $\beta$ -D-Xylp -(1→4)-D-Xyl	Megazyme, Wicklow,Ireland	III,IV
<u>Hexasaccharides</u>			
25 XA <sup>2+3</sup> XX	$\beta$ -D-Xylp -(1→4)-[ $\alpha$ -L-Araf-(1→2)]( $\alpha$ -L-Araf-(1→3))- $\beta$ -D-Xylp -(1→4)- $\beta$ -D-Xylp -(1→4)-D-Xyl	Megazyme, Wicklow,Ireland	III

#### 4.1.2 GLOS from *W. confusa* and *L. citreum* produced dextrans (I)

In study I, the structures of two tetrasaccharides, WCBIM4 ( $\alpha$ -D-Glc-(1 $\rightarrow$ 3)- $\alpha$ -D-Glcp(1 $\rightarrow$ 6)- $\alpha$ -D-Glcp-(1 $\rightarrow$ 6)-D-Glc) obtained by the enzymatic hydrolysis of *Weissella confusa* VTT E-90392 (=DSM 20194, NCDO 1975) dextran and LCBIM4 ( $\alpha$ -D-Glc-(1 $\rightarrow$ 2)- $\alpha$ -D-Glcp(1 $\rightarrow$ 6)- $\alpha$ -D-Glcp-(1 $\rightarrow$ 6)-D-Glc) of *Leuconostoc citreum* VTT E-93497 dextran, were analysed by direct infusion ESI-MS<sup>n</sup>. First, the tetrasaccharides were isolated after the enzymatic hydrolysis of the dextrans, as previously reported (Maina et al. 2011), and then identified by nuclear magnetic resonance spectroscopy (NMR) (described in study I). Sixteen model compounds were used to study the influence of the linkage position on fragmentation in ESI-MS<sup>n</sup>. The tetrasaccharides were then analysed by ESI-MS<sup>n</sup>, and the spectra were evaluated. The analysis was performed in both positive and negative ionisation modes of [M+Li]<sup>+</sup> and [M+Cl]<sup>-</sup> adducts. The studied model compounds were mannobiose, nigerose, laminaribiose, maltose, cellobiose, isomaltose, maltotriose, isomaltotriose, panose, galactotriose,  $\beta$ -glucotriose, galactotetraose,  $\beta$ -glucotetraose1,  $\beta$ -glucotetraose 2, maltotetraose and cellotetraose.

#### 4.1.3 Trisaccharides produced by *W. confusa* dextransucrase (II)

In study II, three *W. confusa* VTT E-90392 dextransucrase acceptor reaction products were studied. The acceptor reaction tests were focused on lactose and cellobiose. Prior to the ESI-MS<sup>n</sup> analysis, the samples were fractionated by gel permeation chromatography using a Biogel P2 column, identified NMR spectroscopy and enzymatic hydrolysis combined with an HPAEC-PAD analysis. Next, the identified products, 2<sup>Glc</sup>-a-Glcp-lactose, isomelezitose (6<sup>Fru</sup>-a-Glcp-sucrose or  $\alpha$ -D-Glcp-(1 $\rightarrow$ 6)- $\beta$ -d-Fruf-(2 $\rightarrow$ 1)- $\alpha$ -D-Glcp) and 2<sup>1</sup>-a-Glcp-cellobiose, were characterised by the ESI-MS<sup>n</sup> method, and their fragmentation pathways in positive and negative modes (as [M+Li]<sup>+</sup> and [M+Cl]<sup>-</sup> adduct ions) were determined. The lactose reaction mixture was also produced using <sup>13</sup>C<sub>6</sub><sup>Glc</sup>-sucrose to enable the complete characterisation of the fragmentation pattern of 2<sup>Glc</sup>-a-Glcp-lactose and isomelezitose (6<sup>Fru</sup>-a-Glcp-sucrose). The acceptor reactions and analytical methods are described in detail in the original paper (study II). The structures of the samples are presented in Figure 11.

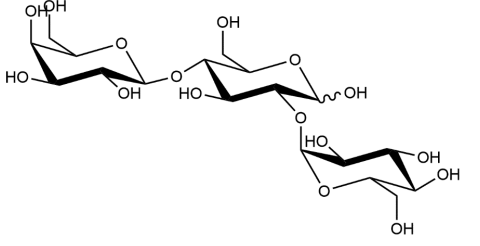
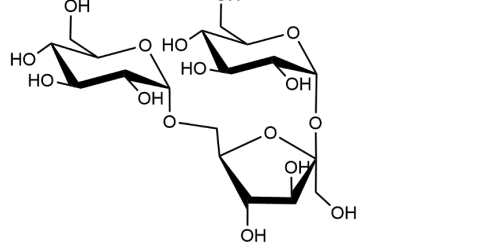
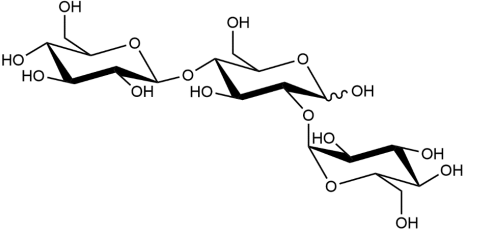
Nomenclature	Structure
2 <sup>Glc</sup> - $\alpha$ -Glc <sub>p</sub> -lactose	 $\beta$ -D-Galp-(1 $\rightarrow$ 4)-[ $\alpha$ -D-Glcp-(1 $\rightarrow$ 2)]-D-Glc
Isomelezitose/6 <sup>Fru</sup> - $\alpha$ -Glc <sub>p</sub> -sucrose	 $\alpha$ -D-Glcp-(1 $\rightarrow$ 6)- $\beta$ -D-Fruf-(2 $\leftrightarrow$ 1)- $\alpha$ -D-Glc
2 <sup>Glc</sup> - $\alpha$ -Glc <sub>p</sub> -cellobiose	 $\beta$ -D-Glcp-(1 $\rightarrow$ 4)-[ $\alpha$ -D-Glcp-(1 $\rightarrow$ 2)]-D-Glc

Figure 11. Nomenclature and structures of trisaccharide acceptor products (based on Table 1 in study II)

#### 4.1.4 (A)XOS from cereal arabinoxylan (III and IV)

In studies III and IV, the (A)XOS oligosaccharides hydrolysed from cereal arabinoxylan were analysed. (A)XOS included five linear commercial XOS (X<sub>1</sub>, X<sub>2</sub>, X<sub>3</sub>, X<sub>4</sub>, and X<sub>5</sub>), three branched commercial AXOS (XA<sup>3</sup>XX, XA<sup>2</sup>XX+XA<sup>3</sup>XX, and XA<sup>2+3</sup>XX, named GH11 AXOS) (Figure 12) and six AXOS prepared by our group (A<sup>2</sup>X, A<sup>3</sup>X, A<sup>2+3</sup>X, A<sup>2+3</sup>XX, A<sup>2</sup>XX, and D<sup>2,3</sup>X, named GH10 AXOS) (Figure 12). The abbreviations were adopted from Fauré et al. (2009). The A<sup>3</sup>X, A<sup>2+3</sup>X, A<sup>2+3</sup>XX, A<sup>2</sup>X, and A<sup>2</sup>XX were hydrolysates of wheat arabinoxylan (Megazyme International, Bray, Ireland) and the D<sup>2,3</sup>X

was hydrolysed from oat spelt arabinoxylan (Sigma Aldrich Chemie, Steinheim, Germany). The arabinoxylans were enzymatically modified by GH family 10 endo-1,4- $\beta$ -D-xylanase (Shearzyme; Novozymes, Bagsvaerd, Denmark), GH family 51  $\alpha$ -L-arabinofuranosidase (Megazyme International, Bray, Ireland), and GH family 43  $\alpha$ -L-arabinofuranosidase (Megazyme International, Bray, Ireland). The hydrolysates were fractionated by gel permeation chromatography and identified by HPAEC-PAD and NMR spectroscopy. The detailed descriptions of the enzyme treatments and NMR and HPAEC-PAD analyses were published elsewhere (Pastell et al. 2008; Pastell et al. 2009; Rantanen et al. 2007).

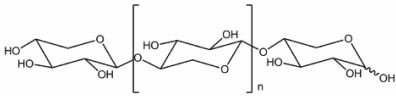
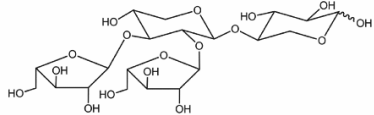
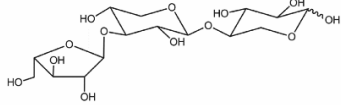
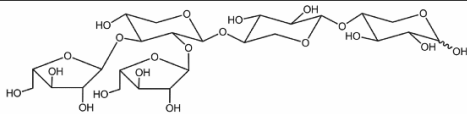
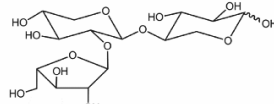
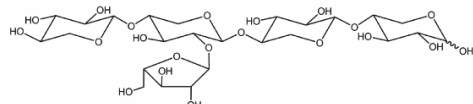
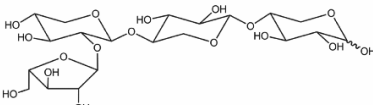
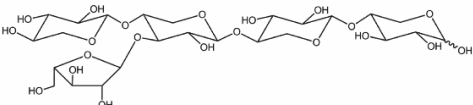
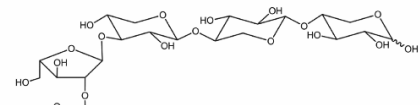
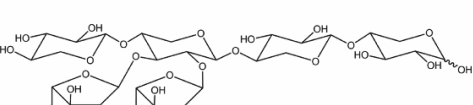
Abbr.	Linear oligosaccharides	Abbr.	Branched oligosaccharides
X <sub>3</sub> -X <sub>5</sub>	 <p><math>\beta</math>-D-Xylp [(1<math>\rightarrow</math>4)-<math>\beta</math>-D-Xylp]<sub>n</sub>-(1<math>\rightarrow</math>4)-D-Xyl</p> <p>X<sub>1</sub>, n=1; X<sub>4</sub>, n=2; X<sub>5</sub>, n=3</p>	A <sup>2+3</sup> X	 <p><math>\alpha</math>-L-Araf-(1<math>\rightarrow</math>2)-[<math>\alpha</math>-L-Araf-(1<math>\rightarrow</math>3)]-<math>\beta</math>-D-Xylp-(1<math>\rightarrow</math>4)-D-Xyl</p>
A <sup>3</sup> X	 <p><math>\alpha</math>-L-Araf-(1<math>\rightarrow</math>3)-<math>\beta</math>-D-Xylp-(1<math>\rightarrow</math>4)-D-Xyl</p>	A <sup>2+3</sup> XX	 <p><math>\alpha</math>-L-Araf-(1<math>\rightarrow</math>2)-[<math>\alpha</math>-L-Araf-(1<math>\rightarrow</math>3)]-<math>\beta</math>-D-Xylp-(1<math>\rightarrow</math>4)-<math>\beta</math>-D-Xylp-(1<math>\rightarrow</math>4)-D-Xyl</p>
A <sup>2</sup> X	 <p><math>\alpha</math>-L-Araf-(1<math>\rightarrow</math>2)-<math>\beta</math>-D-Xylp-(1<math>\rightarrow</math>4)-D-Xyl</p>	XA <sup>2</sup> XX	 <p><math>\beta</math>-D-Xylp-(1<math>\rightarrow</math>4)-[<math>\alpha</math>-L-Araf-(1<math>\rightarrow</math>2)]-<math>\beta</math>-D-Xylp-(1<math>\rightarrow</math>4)-<math>\beta</math>-D-Xylp-(1<math>\rightarrow</math>4)-D-Xyl</p>
A <sup>2</sup> XX	 <p><math>\alpha</math>-L-Araf-(1<math>\rightarrow</math>2)-<math>\beta</math>-D-Xylp-(1<math>\rightarrow</math>4)-<math>\beta</math>-D-Xylp-(1<math>\rightarrow</math>4)-D-Xyl</p>	XA <sup>3</sup> XX	 <p><math>\beta</math>-D-Xylp-(1<math>\rightarrow</math>4)-[<math>\alpha</math>-L-Araf-(1<math>\rightarrow</math>3)]-<math>\beta</math>-D-Xylp-(1<math>\rightarrow</math>4)-<math>\beta</math>-D-Xylp-(1<math>\rightarrow</math>4)-D-Xyl</p>
D <sup>2,3</sup> X	 <p><math>\beta</math>-D-Xylp-(1<math>\rightarrow</math>2)-<math>\alpha</math>-L-Araf-(1<math>\rightarrow</math>3)-<math>\beta</math>-D-Xylp-(1<math>\rightarrow</math>4)-D-Xyl</p>	XA <sup>2+3</sup> XX	 <p><math>\beta</math>-D-Xylp-(1<math>\rightarrow</math>4)-[<math>\alpha</math>-L-Araf-(1<math>\rightarrow</math>2)]-[<math>\alpha</math>-L-Araf-(1<math>\rightarrow</math>3)]-<math>\beta</math>-D-Xylp-(1<math>\rightarrow</math>4)-<math>\beta</math>-D-Xylp-(1<math>\rightarrow</math>4)-D-Xyl</p>

Figure 12. Structures and abbreviations of studied (A)XOS. Abbreviations were adopted from Fauré et al. (2009). (Adapted from study II, Fig.1)

## 4.2 Analytical methods

### 4.2.1 Structural analysis by using direct infusion ESI-MS<sup>n</sup> (I–III)

The disaccharide and oligosaccharide samples were analysed by ESI-MS<sup>n</sup> (studies I–III). The fragmentation patterns of the samples were studied in both negative and positive modes using an Agilent XCT Plus Ion Trap mass spectrometer with an ESI source (Agilent Technology, Palo Alto, CA) and direct infusion. A 1–10  $\mu\text{l}$  sample was diluted in 400  $\mu\text{l}$  of methanol and water (50:49:1, v:v:v), and 0.5–3  $\mu\text{l}$  of 10 mg/ml ammonium chloride and lithium acetate were added for the adduct ion formation ( $[\text{M}+\text{Li}]^+$  and  $[\text{M}+\text{Cl}]^-$ , respectively).  $\text{Na}^+$  cations were present naturally. The ion trap parameters are presented in Table 6. The parameters were automatically adjusted according to the mass of the analyte. The spectrum was recorded for 0.5–1 min. In the MS<sup>n</sup> analysis, the fragmentation amplitude ranges in the positive mode were 0.18–0.55 V (DP2), 0.50–0.66 V (DP3) and 0.88–0.98 V (DP4). In the negative mode, the fragmentation amplitudes were 0.25–0.50 V (DP), 0.53–0.55 V (DP3) and 0.25–0.37 V (DP4).

Table 6. Agilent XCT Ion trap parameters in ESI-MS<sup>n</sup>.

Ion trap parameters in ESI-MS <sup>n</sup>	
Flowrate	5 $\mu\text{l}/\text{min}$ or 10 $\mu\text{l}/\text{min}$
Nebulizer gas	nitrogen
Drying gas	nitrogen
Nebulizer gas pressure	15.0 psi
Drying gas flow rate	4 l/min
Drying gas temperature	325 $^{\circ}\text{C}$
Capillary voltage	3164 V (study I) / 3200 V (studies II–III)
Capillary offset	500 V
Skimmer potential	40.0 V
Trap drive	67.9

### 4.2.2 HILIC-MS/MS analysis (III)

In study III, the negative ionisation MS/MS method combined with HILIC separation was developed on a Bruker Esquire quadrupole ion trap (Bruker, Bremen, Germany) equipped with an ESI source equipped with HPLC (Agilent 1100 Series HPLC, Agilent Technologies, Santa Clara, CA, USA).

First, the MS/MS parameters were optimised by analysing the XOS standards ( $\text{X}_1$ – $\text{X}_5$ ) using direct infusion (5  $\mu\text{l}/\text{min}$ ). The optimisation is described in



detail in study III. The chromatographic separation was performed on a 3.5  $\mu\text{m}$ , 2.1x150 mm Xbridge BEH amide column (Waters, Milford, MA, USA). The mobile phase A was 80% ACN with 0.1% ammonium hydroxide ( $\text{NH}_4\text{OH}$ ) and B 20% ACN with 0.1%  $\text{NH}_4\text{OH}$ . The chromatographic conditions and elution profile are presented in Table 7.

Table 7. HILIC-MS(/MS) Chromatographic conditions and elution profile

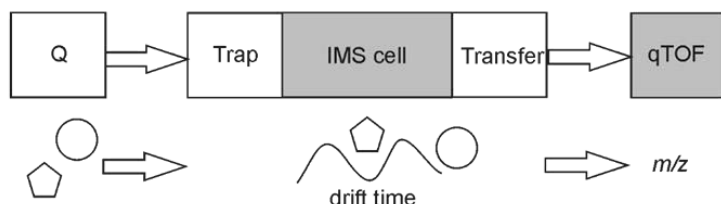
Chromatographic conditions	
Injection volume	10 $\mu\text{l}$
Flow rate	200 $\mu\text{l}/\text{min}$
Oven temperature	35 $^\circ\text{C}$
Solvent A	80% ACN
Solvent B	20% ACN
Modifier	0.1% $\text{NH}_4\text{OH}$
Elution profile	
Initial condition	100% A
0-31 min (gradient)	50% A
31-36 min (gradient)	100% A
36-51 min (wash)	100% A

The MS and MS/MS spectra were produced from all samples. The HILIC-MS was performed in segments: 0–7 min with  $X_2$  parameters, 7–12 min with  $X_3$  parameters, 12–17 min with  $X_4$  parameters, 17–23 min with  $X_5$  parameters, and 23–31 min with  $X_5$  parameters. The HILIC-MS/MS methods were set for the tri-, tetra-, penta- and hexa-saccharides by optimising the ion trap parameters and fragmentation amplitudes (described in detail in study III). The chloride adduct ions were formed by adding  $\text{NH}_4\text{Cl}$  post-column at an optimised concentration and flow rate (10  $\mu\text{g}/\text{ml}$  in 80% ACN with 0.1%  $\text{NH}_4\text{OH}$ , 200  $\mu\text{l}/\text{min}$ ) with and LC pump (Waters 501 HPL; Millipore, Milford, MA). To determine the lowest concentration of  $\text{NH}_4\text{Cl}$  to produce the maximal  $[\text{M} + \text{Cl}]^-$  adduct ion signal, the post-column addition of  $\text{NH}_4\text{Cl}$  was performed at flow rates 100  $\mu\text{l}/\text{min}$  and 200  $\mu\text{l}/\text{min}$  and at five  $\text{NH}_4\text{Cl}$  concentrations (1  $\mu\text{g}/\text{ml}$ , 2.5  $\mu\text{g}/\text{ml}$ , 5  $\mu\text{g}/\text{ml}$ , 7.5  $\mu\text{g}/\text{ml}$  and 10  $\mu\text{g}/\text{ml}$ ). Testing under different conditions was performed using 5  $\mu\text{g}/\text{ml}$  and 10  $\mu\text{g}/\text{ml}$  XOS ( $X_2$ – $X_5$ ) mixture solutions.

### 4.2.3 Ion mobility MS (IV)

The potential of TWIMS-MS to separate and identify isomeric fragment ions produced from AXOS was studied. The TWIMS-MS and CID-TWIMS-MS/MS experiments were performed using the Synapt G2-Si HDMS qTOF mass spectrometer (Waters Corp, Manchester, UK) in both positive and negative ionisation modes with ESI source and direct infusion. In the TWIMS-MS experiment, the  $[M+Na]^+$ ,  $[M-H]^-$ , and  $[M+Cl]^-$  precursor ions were first separated in an ion mobility cell and then analysed using a qTOF mass analyser. In CID-TWIMS-MS/MS, the  $[M+Na]^+$  and  $[M+Cl]^-$  precursor ions were first fragmented in a trap cell using CID and then separated in an IM cell. Finally, the  $m/z$  values of the product ions were analysed by qTOF. Schematic diagrams of both analyses are presented in Figure 13.

#### TWIMS-MS



#### CID-TWIMS-MS/MS

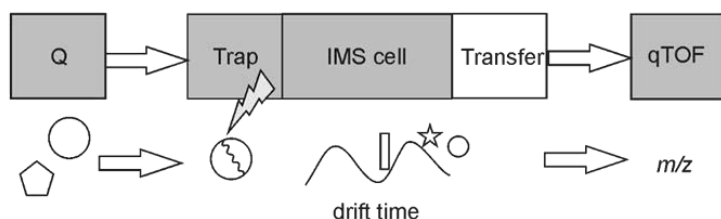


Figure 13. Schematic diagrams of TWIMS-MS and CID-TWIMS-MS/MS (Supplementary Figure S1 in study IV)

The ESI ion source parameters are presented in Table 8. The MS instrument was calibrated using sodium formate (Waters Corp, Manchester, UK) in positive and negative ionisation modes. The IM cell was calibrated using a polyalanine mixture (Waters Corp, Manchester, UK) with default parameters obtained from the manufacturer. Leucine enkephalin (Leu-Enk, Waters) was

used in both the detector check and the CCS lock spray solution. The samples were analysed in  $m/z$  50–1,200 mass ranges using the resolution mode. The ion mobility calibration was conducted at IMS wave velocity 300–1,000 m/s in a mass range of  $m/z$  50–1,200. In CID-TWIMS-MS/MS, the IMS wave velocity parameter was set at 800 m/s to separate the small product ions. Lactose and maltose were used as ion mobility testing standards. The standards and samples were diluted in an acetonitrile–water solution (4:1) with 0.1% of ammonium hydroxide (NH<sub>4</sub>OH) to obtain the final concentration of 10 µg/ml and then directly infused in the ESI ion source. NH<sub>4</sub>Cl was added to the samples for the formation of the [M+Cl]<sup>-</sup> adduct ion.

Table 8. TWIMS-MS and CID-TWIMS-MS/MS parameters (study IV)

Synapt G2 Si TWIMS-MS parameters	
<u>ESI source</u>	
Capillary voltage	3.00 kV/2.5 kV (pos.mode/neg.mode)
Sampling cone voltage	40 V
Source offset	80 V
Source temperature	110 °C
Desolvation temperature	150 °C
Cone gas flow	50 l/h
Desolvation gas flow	600 l/h
Nebulizer gas flow	6.0 bar
<u>Triwave parameters</u>	
T-Wave velocity (CID-TWIMS-MS/MS)	315 m/s
IMS wave velocity (CID-TWIMS-MS/MS)	800 m/s
IMS wave height	40 V
Trim drift time	enabled (default)/ disabled (CID-TWIMS-MS/MS)
IM gas	nitrogen
CID gas	helium
Gas controls	default
Other parameters	default

#### 4.2.4 Data analysis (I-IV)

In studies I–III, the MS and MS/MS data were collected and processed using Data analysis software (Bruker Daltonics, Bremen). In study IV, the IMS and MS/MS data were collected using MassLynx software and analysed using Unifi software (Waters). In study IV, the drift time peaks were integrated from an extracted ion mobilogram, and the MS/MS spectra and base peak

mobilograms were drawn. The fragment ions were named according to Domon and Costello's (1988) nomenclature (see section 2.4.1).

## 5 RESULTS

### 5.1 Structural analysis of GLOS by ESI-MS<sup>n</sup> (I)

The potential of positive and negative ionisation ESI-MS<sup>n</sup> methods to determine the structures of mixed-linked GLOS was studied. Specifically, the objective was to find solution to identify the positions of glycosidic linkages solely by the MS<sup>n</sup> method so that the NMR method would not be required. First, 17 linear commercial disaccharide and oligosaccharide model compounds were analysed as  $[M+Li]^+$  and  $[M+Cl]^-$  adducts. Then the two tetrasaccharides WCBIM4 ( $\alpha$ -D-Glc-(1 $\rightarrow$ 3)- $\alpha$ -D-Glcp(1 $\rightarrow$ 6)- $\alpha$ -D-Glcp-(1 $\rightarrow$ 6)-D-Glc and LCBIM4 ( $\alpha$ -D-Glc-(1 $\rightarrow$ 2)- $\alpha$ -D-Glcp-(1 $\rightarrow$ 6)- $\alpha$ -D-Glcp.(1 $\rightarrow$ 6)-D-Glc), which were obtained by the enzymatic hydrolysis of *W. confusa* VTT E-90392 and *L. citreum* VTT E-93497 dextrans, were evaluated.

#### *Commercial disaccharides*

First, the fragment ions of commercial disaccharides were studied by ESI-MS<sup>n</sup>. The (1 $\rightarrow$ 2)-linked disaccharide mannobiose had a major cross-ring fragment peak at  $m/z$  259 (M-120Da) and a minor loss of the 90 Da peak in positive mode (Table 9, line 1), a major cross-ring fragment peak at  $m/z$  229 (M-120Da) and a minor peak at  $m/z$  259 (M-78 Da) in negative mode (Table 10, line 1). The studied (1 $\rightarrow$ 3)-linked disaccharides, laminaribiose and nigerose, both had a M-90 Da cross-ring fragment ion ( $m/z$  259) in positive mode (Table 9, lines 2 and 3), and no cross-ring ions were formed from the  $[M+Cl]^-$  precursors in negative mode (Table 10, lines 2 and 3). The (1 $\rightarrow$ 4)-linked disaccharides, maltose and cellobiose, had major cross-ring peaks at  $m/z$  289 (M-60 Da), and maltose had a minor peak at 120 Da in positive mode (Table 9, lines 4 and 5). In the negative mode, anionised  $[M+Cl]^-$  maltose and cellobiose had a  $m/z$  263 (M-78 Da) cross-ring ion peak (Table 10, lines 4 and 5). In the negative mode, the maltose produced also  $m/z$  281 (M-60 Da) and  $m/z$  221 (M-120 Da) cross-ring ion peaks. The (1 $\rightarrow$ 6)-linked disaccharide isomaltose was observed to have diagnostic cross-ring ions at  $m/z$  289 (M-60 Da),  $m/z$  259 (M-90 Da) and  $m/z$  229 (M-120 Da) (Table 10, line 6).

Table 9. Main cross-ring fragment ions of model oligosaccharides from positive ESI-MS/MS and ESI-MS<sup>3</sup>. Summarised from study I.

Line	DP	MS <sup>n</sup> , n=	Precursor, m/z	Sample	Neutral loss, X=			Ion,		Reference	
					60 Da	90 Da	120 Da	linkage	at reducing end		
<b>[M-X+Li]<sup>+</sup></b>											
					289	259	229	Precursor			
1	2	2	349	Mannobiose		x	<u>x</u>	α(1→2)		Table 2 in Study I	
2	2	2	349	Nigerose		<u>x</u>		α(1→3)		Table 2 in Study I	
3	2	2	349	Laminaribiose			<u>x</u>	β(1→3)		Table 2 in Study I	
4	2	2	349	Maltose	<u>x</u>			α(1→4)		Table 2 in Study I	
5	2	2	349	Cellobiose	<u>x</u>			β(1→4)		Table 2 in Study I	
6	2	2	349	Isomaltose	<u>x</u>	x	x	α(1→6)		Table 2 in Study I	
<b>[M-Glu-X+Li]<sup>+</sup></b>											
					289	259	229	C <sub>2</sub> -ion	Y <sub>2</sub> -ion		
7	3	2	511	Maltotriose				α(1→4)	α(1→4)	Fig. 2c in Study I	
8	3	3	511→349	Maltotriose	<u>x</u>		x	α(1→4)	α(1→4)	Fig. 2d in Study I	
9	3	2	511	Isomaltotriose	<u>x</u>	x	x	α(1→6)	α(1→6)	Fig. 2a in Study I	
10	3	3	511→349	Isomaltotriose	<u>x</u>	x	x	α(1→6)	α(1→6)	Fig. 2b in Study I	
11	3	2	511	Panose	<u>x</u>		x	α(1→6)	α(1→4)	Fig. 2e in Study I	
12	3	3	511→349	Panose	<u>x</u>	x	x	α(1→6)	α(1→4)	Fig. 2e in Study I	
13	3	2	511	Galactotriose				α(1→3)	β(1→4)	Fig. 3c in Study I	
14	3	3	511→349	Galactotriose	<u>x</u>	x	x	α(1→3)	β(1→4)	Fig. 3d in Study I	
15	3	2	511	Glucotriose				β(1→4)	β(1→3)	Fig. 3a in Study I	
16	3	3	511→349	Glucotriose	x	<u>x</u>	x	β(1→4)	β(1→3)	Fig. 3b in Study I	
<b>[M-Glu-X+Li]<sup>+</sup></b>											
					289	259	229	C <sub>2</sub> -ion	C <sub>3</sub> /Y <sub>3</sub> -ion	Y <sub>2</sub> -ion	
17	4	2	673	Galactotetraose				α(1→3)	β(1→4)	α(1→3)	Fig. 5f in Study I
18	4	3	673→511	Galactotetraose	(x)		(x)	α(1→3)	β(1→4)	α(1→3)	Fig. 5g in Study I
19	4	2	673	Glucotetraose 1	x			β(1→4)	β(1→4)	β(1→3)	Fig. 5a in Study I
20	4	3	673→511	Glucotetraose 1				β(1→4)	β(1→4)	β(1→3)	Fig. 5b in Study I
21	4	2	673	Glucotetraose 2	x			β(1→4)	β(1→3)	β(1→4)	Fig. 5c in Study I
22	4	3	673→511	Glucotetraose 2	x			β(1→4)	β(1→3)	β(1→4)	Fig. 5d in Study I
23	4	4	673→655→511	Glucotetraose 2				β(1→4)	β(1→3)	β(1→4)	Fig. 5e in Study I
24	4	3	673→349	Glucotetraose 2	<u>x</u>	x	x	β(1→4)	β(1→3)	β(1→4)	suppl.data
25	4	2	673	Maltotetraose				α(1→4)	α(1→4)	α(1→4)	Study I (data not shown)
26	4	3	673→511	Maltotetraose				α(1→4)	α(1→4)	α(1→4)	Study I (data not shown)
27	4	3	673→349	Maltotetraose	x			α(1→4)	α(1→4)	α(1→4)	Study I (data not shown)
28	4	2	673	Cellotetraose				β(1→4)	β(1→4)	β(1→4)	Study I (data not shown)
29	4	3	673→349	Cellotetraose	x			β(1→4)	β(1→4)	β(1→4)	Study I (data not shown)
<b>[M-X+Li]<sup>+</sup></b>											
					451	421	391	Precursor			
30	3	2	511	Maltotriose	x			α(1→4)		Fig. 2c in Study I	
31	3	2	511	Isomaltotriose	<u>x</u>	x	x	α(1→6)		Fig. 2a in Study I	
32	3	2	511	Panose	<u>x</u>		x	α(1→4)		Fig. 2e in Study I	
33	3	2	511	Galactotriose	x			β(1→4)		Fig. 3c in Study I	
34	3	2	511	Glucotriose			x	β(1→3)		Fig. 3a in Study I	
<b>[M-Glu-X+Li]<sup>+</sup></b>											
					451	421	391	C <sub>3</sub> -ion	Y <sub>3</sub> -ion		
35	4	2	673	Galactotetraose				β(1→4)	α(1→3)		Fig. 5f in Study I
36	4	3	673→511	Galactotetraose		x		β(1→4)	α(1→3)		Fig. 5g in Study I
37	4	2	673	Glucotetraose 1				β(1→4)	β(1→3)		Fig. 5a in Study I
38	4	3	673→511	Glucotetraose 1	x	<u>x</u>		β(1→4)	β(1→3)		Fig. 5b in Study I
39	4	2	673	Glucotetraose 2	x			β(1→3)	β(1→4)		Fig. 5c in Study I
40	4	3	673→511	Glucotetraose 2	<u>x</u>	x	x	β(1→3)	β(1→4)		Fig. 5d in Study I
41	4	4	3→655→5	Glucotetraose 2		x		β(1→3)	β(1→4)		Fig. 5e in Study I
42	4	2	673	Maltotetraose	x			α(1→4)	α(1→4)		Study I (data not shown)
43	4	3	673→511	Maltotetraose	x			α(1→4)	α(1→4)		Study I (data not shown)
44	4	2	673	Cellotetraose				β(1→4)	β(1→4)		Study I (data not shown)
45	4	3	673→511	Cellotetraose	<u>x</u>		x	β(1→4)	β(1→4)		Study I (data not shown)
<b>[M-X+Li]<sup>+</sup></b>											
					613	583	553	Precursor			
46	4	2	673	Galactotetraose		x		α(1→3)		Fig. 5f in Study I	
47	4	2	673	Glucotetraose 1			x	β(1→3)		Fig. 5a in Study I	
48	4	2	673	Glucotetraose 2	<u>x</u>		x	β(1→4)		Fig. 5c in Study I	
49	4	2	673	Maltotetraose	x			α(1→4)		Study I (data not shown)	
50	4	2	673	Cellotetraose	x			β(1→4)		Study I (data not shown)	

DP = degree of polymerisation, m/z = mass-to-charge ratio, X = neutral fragment, parentheses = low abundance, underline = main peak of cross-ring fragments.

Table 10. Main cross-ring fragment ions of model oligosaccharides from negative ESI-MS/MS and ESI-MS<sup>3</sup>. Summarised from study I.

Line	DP	MS <sup>n</sup> , n=	Precursor, m/z	Sample	Neutral loss, X =				Ion, linkage at reducing end	Reference
					60 Da	78 Da	90 Da	120 Da		
<b>[M+Cl-X-HCl]<sup>-</sup></b>					281	263	251	221	Precursor	
1	2	2	377	Mannobiose		<u>x</u>		x	α(1→2)	Table 3 in Study I
2	2	2	377	Nigerose					α(1→3)	Table 3 in Study I
3	2	2	377	Laminaribiose					β(1→3)	Table 3 in Study I
4	2	2	377	Maltose	<u>x</u>	x		x	α(1→4)	Table 3 in Study I
5	2	2	377	Cellobiose		x			β(1→4)	Table 3 in Study I
6	2	2	377	Isomaltose	x		x	<u>x</u>	α(1→6)	Table 3 in Study I
<b>[M-X-H]<sup>-</sup></b>					281	263	251	221	Precursor	
7	2	2	341	Mannobiose		<u>x</u>		x	α(1→2)	suppl. data
8	2	2	341	Nigerose			x		α(1→3)	suppl. data
9	2	2	341	Maltose	x				α(1→4)	suppl. data
10	2	2	341	Cellobiose					β(1→4)	suppl. data
11	2	2	341	Isomaltose	x		x	<u>x</u>	α(1→6)	suppl. data
<b>[M+Cl-Glu-X-HCl]<sup>-</sup></b>					281	263	251	221	C <sub>2</sub> -ion	
12	3	2	539	Maltotriose	<u>x</u>	x		x	α(1→4)	Fig. 4e in Study I
13	3	3	539→341	Maltotriose	x				α(1→4)	Fig. 4g in Study I
14	3	2	539	Isomaltotriose					α(1→6)	suppl. Fig in study I
15	3	3	539→341	Isomaltotriose	x		x	<u>x</u>	α(1→6)	suppl. Fig in study I
16	3	2	539	Panose	x			<u>x</u>	α(1→6)	suppl. Fig in study I
17	3	3	539→341	Panose	x		x	<u>x</u>	α(1→6)	suppl. Fig in study I
18	3	2	539	Galactotriose					α(1→3)	Fig. 4c in Study I
19	3	3	539→341	Galactotriose					α(1→3)	Fig. 4d in Study I
20	3	2	539	Glucotriose		x			β(1→4)	Fig. 4a in Study I
21	3	3	539→341	Glucotriose	( <u>x</u> )	(x)			β(1→4)	Fig. 4b in Study I
<b>[M+Cl-Glu-X-HCl]<sup>-</sup></b>					281	263	251	221	C <sub>2</sub> -ion	
22	4	2	701	Galactotetraose					α(1→3)	Fig. 6c in Study I
23	4	2	701	Glucotetraose 1		(x)			β(1→4)	Fig. 6a in Study I
24	4	2	701	Glucotetraose 2	(x)	( <u>x</u> )			β(1→4)	Fig. 6b in Study I
25	4	2	701	Maltotetraose	x				α(1→4)	Study I (data not shown)
26	4	2	701	Cellotetraose		x			β(1→4)	Study I (data not shown)
<b>[M+Cl-X-HCl]<sup>-</sup></b>					443	425	413	383	Precursor	
27	3	2	539	Maltotriose	x	<u>x</u>		x	α(1→4)	Fig. 4e in Study I
28	3	3	539→503	Maltotriose	<u>x</u>	x			α(1→4)	Fig. 4f in Study I
29	3	2	539	Isomaltotriose	x		x	<u>x</u>	α(1→6)	suppl. Fig in study I
30	3	2	539	Panose		x		<u>x</u>	α(1→4)	suppl. Fig in study I
31	3	3	539→503	Panose		x			α(1→4)	suppl. data
32	3	2	539	Galactotriose	( <u>x</u> )	(x)			β(1→4)	Fig. 4c in Study I
33	3	2	539	Glucotriose					β(1→3)	Fig. 4a in Study I
<b>[M+Cl-Glu-X-HCl]<sup>-</sup></b>					443	425	413	383	C <sub>3</sub> -ion	
34	4	2	701	Galactotetraose	<u>x</u>	x			β(1→4)	Fig. 6c in Study I
35	4	2	701	Glucotetraose 1	x	<u>x</u>			β(1→4)	Fig. 6a in Study I
36	4	2	701	Glucotetraose 2					β(1→3)	Fig. 6b in Study I
37	4	2	701	Maltotetraose	x	x		x	α(1→4)	Study I (data not shown)
38	4	2	701	Cellotetraose	x	x			β(1→4)	Study I (data not shown)
<b>[M+Cl-X-HCl]<sup>-</sup></b>					605	587	575	545	Precursor	
39	4	2	701	Galactotetraose			(x)		α(1→3)	Fig. 6c in Study I
40	4	2	701	Glucotetraose 1					β(1→3)	Fig. 6a in Study I
41	4	2	701	Glucotetraose 2	<u>x</u>	x			β(1→4)	Fig. 6b in Study I
42	4	2	701	Maltotetraose	x	x		x	α(1→4)	Study I (data not shown)
43	4	2	701	Cellotetraose	x	x		x	β(1→4)	Study I (data not shown)

DP = degree of polymerisation, m/z = mass-to-charge ratio, X= neutral fragment, parentheses = low abundance, underline = main peak of cross-ring fragments.

Because all chloride anionised  $[M+Cl]^-$  oligosaccharides form mainly deprotonated fragment ions, the  $MS^3$  fragmentation step in larger oligosaccharides is performed from the deprotonated C or Y ion. Therefore, it was deemed important to perform the linkage position analysis from deprotonated disaccharide precursors so that the fragmentation patterns of the chloride anionised and deprotonated precursors could be evaluated. The negative  $MS^n$  spectra used in this thesis were unpublished deprotonated  $[M-H]^-$  MS/MS spectra (Table 10, lines 7-11). The (1→2)-linked and (1→6)-linked deprotonated disaccharides formed the same fragmentation patterns as  $[M+Cl]^-$  the disaccharide precursors did (Table 10, lines 1,6,7 and 11). However, the (1→4)-linked disaccharides, maltose and cellobiose, lacked most of the cross-ring fragments. Only the loss of the 60 Da cross-ring fragment ion peak from the maltose spectra was observed (Table 10, line 9). (1→3)-linked nigerose was found to produce a small loss of the 90 Da peak at  $m/z$  251 in contrast to the  $[M+Cl]^-$  precursor, which did not form any cross-ring fragments.

#### *Commercial trisaccharides*

The trisaccharide analysis was performed in two steps. First, the MS/MS fragment ion spectra of the precursor was collected. Then the  $C_2$  and/or  $Y_2$  ions were fragmented in the  $MS^3$  step. When trisaccharide contained only one type of linkage, it was observed to fragment to the same diagnostic ions as the disaccharides did. For example, isomaltotriose, which had two (1→6)-linkages, produced cross-ring fragment ions at  $m/z$  289 (M-Glu-60 Da),  $m/z$  259 (M-Glu-90 Da),  $m/z$  229 (M-Glu-120 Da), and  $m/z$  451 (M-60 Da),  $m/z$  421 (M-90Da) and  $m/z$  391 (M-120 Da) (Table 9, lines 9, 10 and 31). The maltotriose, which had only (1→4)-linkages, had major cross-ring fragments at  $m/z$  451 (M-60 Da) and at  $m/z$  289 (M-Glu-60 Da) and minor fragments at  $m/z$  229 (M-Glu-120 Da) (Table 9, lines 7, 8, 30). The same result was observed in the negative mode.

However, when the trisaccharide contained two different linkages, the positive mode ESI- $MS^n$  revealed that the fragmentation occurred in both the reducing and non-reducing ends and the  $MS^3$  analysis was performed using the isomeric mixture of  $C_2$  and  $Y_2$  ions. For example, glucotriose, which contained (1→4)- and (1→3)-linkages, produced an abundant  $m/z$  259 peak, and smaller  $m/z$  229 and  $m/z$  289 peaks from  $m/z$  349 in  $MS^3$ . This result indicates that most of the



ions in MS<sup>3</sup> step were Y<sub>2</sub> ions rather than C<sub>2</sub> ions. In contrast, the negative ionisation mode did not have this disadvantage. For example, glucotriose, which consisted of (1→4) and (1→3)-linkages, showed cross-ring fragmentation patterns as expected; it did not form a cross-ring from (1→3)-linked unit ( $m/z$  341 – 503) in the negative mode, but it had cross-ring fragment ions at  $m/z$  263 (M-Glc-78 Da), which were formed from the (1→4)-linked unit.

#### *Commercial tetrasaccharides*

The tetrasaccharides were analysed in three steps. First, the fragment ion spectra produced from the precursor ions in MS/MS were analysed. Then the C<sub>3</sub> (or Y<sub>3</sub>) ions were isolated and fragmented in MS<sup>3</sup>. In the last step, the C<sub>2</sub>, Y<sub>2</sub> and C<sub>3</sub>/Y<sub>3</sub> ions were analysed in MS<sup>3</sup>.

As expected, in the positive mode, maltotetraose and cellotetraose, which contain only (1→4)-linkages, produced dominant  $m/z$  613 (M-60 Da) cross-ring fragment ions in MS/MS and  $m/z$  349 (M-Glc-60 Da) cross-ring fragments in MS<sup>3</sup> of the  $m/z$  511 ion (Table 9). In the mixed-linked samples, glucotetraose 1 and 2, the reducing end linkages were easily confirmed to be (1→3)- and (1→4)-linkages by the  $m/z$  583 (M-90 Da) cross-ring ions of glucotetraose 1 and  $m/z$  613 (M- 60 Da) cross-ring ions in the spectrum of glucotetraose 2. However, the interpretation of other linkages in the spectra was not straightforward because of the abundant cross-ring ions from Y-type ions, which led to the mixture of cross-ring ions from two linkages.

In the negative ion mode, all the linkages in the mixed linked tetrasaccharide could be identified based on their cross-ring cleavages. E.g., the glucotetraose 1 did not form any cross-ring ions from (1→3)-linked in the reducing end but formed cross-ring ions at  $m/z$  425 and  $m/z$  443 at the middle (1→4)-linkage unit and at  $m/z$  263 in the non-reducing end (1→4)-linkage (Table 10). Glucotetraose 2, which contained the (1→4)-linkage in the reducing end had abundant  $m/z$  605 and  $m/z$  587 cross-ring ions (Table 10), but as observed in the disaccharides and trisaccharides, the middle (1→3)-linked monosaccharide did not form any cross-ring fragments. The (1→4)-linked non-reducing end again produced  $m/z$  263 and  $m/z$  281 (Table 10).

*Tetrasaccharides from W. confusa and L. citreum dextrans*

The ability of the method to determine the linkages of underivatized GLOS was tested by analysing two linear mixed-linked tetrasaccharides, WCBIM4 ( $\alpha$ -D-Glc-(1 $\rightarrow$ 3)- $\alpha$ -D-Glcp(1 $\rightarrow$ 6)- $\alpha$ -D-Glcp(1 $\rightarrow$ 6)-D-Glc) and LCBIM4 ( $\alpha$ -D-Glc-(1 $\rightarrow$ 2)- $\alpha$ -D-Glcp(1 $\rightarrow$ 6)- $\alpha$ -D-Glcp(1 $\rightarrow$ 6)-D-Glc), which were obtained by the hydrolysis of *W. confusa* and *L. citreum* dextrans. Both positive and negative modes confirmed that both *W. confusa* and *L. citreum* dextrans had (1 $\rightarrow$ 6)-linkages in the reducing end by the neutral losses of 60 Da, 90 Da and 120 Da fragments in MS/MS (Table 11). The cross-ring fragments in positive MS/MS and MS<sup>3</sup> indicated (incorrectly) that two other linkages were also (1 $\rightarrow$ 6). The negative MS<sup>3</sup> confirmed that the middle linkages were (1 $\rightarrow$ 6) in MS<sup>3</sup>, but contrary to misleading spectra in the positive mode, the negative mode spectra determined the (1 $\rightarrow$ 3)-linkage in the non-reducing end of WCBIM4 by the absence of cross-ring ions and (1 $\rightarrow$ 2)-linkage in LCBIM4 by the loss of 78 Da neutral fragments ( $m/z$  263) (Table 12).

Table 11. Positive ESI-MS<sup>n</sup> spectra of [M+Li]<sup>+</sup> cationised tetrasaccharides of *W. confusa* and *L. citreum* dextrans. WCBIM4 from *W. confusa*, LCBIM4 from *L. citreum*

DP	MS <sup>n</sup> n=	$m/z$	Sample	Neutral loss, X=			Ion,			Reference
				60 Da	90 Da	120 Da	Linkage	at reducing end		
<u>[M-Glu<sub>2</sub>-X+Li]<sup>+</sup></u>				289	259	229	C <sub>2</sub> -ion	C <sub>3</sub> /Y <sub>3</sub> -ion	Y <sub>2</sub> -ion	
4	2	673	LCBIM4				$\alpha$ (1 $\rightarrow$ 2)	$\alpha$ (1 $\rightarrow$ 6)	$\alpha$ (1 $\rightarrow$ 6)	Fig. 7b in Study I
4	3	673 $\rightarrow$ 511	LCBIM4	<u>x</u>	x	x	$\alpha$ (1 $\rightarrow$ 2)	$\alpha$ (1 $\rightarrow$ 6)	$\alpha$ (1 $\rightarrow$ 6)	Study I (data not shown)
4	2	673	WCBIM4				$\beta$ (1 $\rightarrow$ 3)	$\alpha$ (1 $\rightarrow$ 6)	$\alpha$ (1 $\rightarrow$ 6)	Fig. 7a in Study I
4	3	673 $\rightarrow$ 511	WCBIM4	<u>x</u>	x	x	$\beta$ (1 $\rightarrow$ 3)	$\alpha$ (1 $\rightarrow$ 6)	$\alpha$ (1 $\rightarrow$ 6)	Study I (data not shown)
<u>[M-Glu-X+Li]<sup>+</sup></u>				451	421	391	C <sub>3</sub> -ion	Y <sub>3</sub> -ion		
4	2	673	LCBIM4	<u>x</u>	x	x	$\alpha$ (1 $\rightarrow$ 6)	$\alpha$ (1 $\rightarrow$ 6)		Fig. 7b in Study I
4	3	673 $\rightarrow$ 511	LCBIM4	x	x	x	$\alpha$ (1 $\rightarrow$ 6)	$\alpha$ (1 $\rightarrow$ 6)		Study I (data not shown)
4	2	673	WCBIM4	(x)	(x)		$\alpha$ (1 $\rightarrow$ 6)	$\alpha$ (1 $\rightarrow$ 6)		Fig. 7a in Study I
4	3	673 $\rightarrow$ 511	WCBIM4	x	x	x	$\alpha$ (1 $\rightarrow$ 6)	$\alpha$ (1 $\rightarrow$ 6)		Study I (data not shown)
<u>[M-X+Li]<sup>+</sup></u>				613	583	553	Precursor			
4	2	673	LCBIM4	<u>x</u>	x	x	$\alpha$ (1 $\rightarrow$ 6)			Fig. 7b in Study I
4	2	673	WCBIM4	<u>x</u>	x	x	$\alpha$ (1 $\rightarrow$ 6)			Fig. 7a in Study I

Table 12. Negative ESI-MS<sup>n</sup> spectra of [M+Li]<sup>+</sup> cationised tetrasaccharides of *W. confusa* and *L. citreum* dextrans. WCBIM4 from *W. confusa*, LCBIM4 from *L. citreum*

DP	MS <sup>n</sup>		Sample	Neutral loss, X=				Ion/ Linkage at reducing end	Reference
	n=	m/z		60 Da	78 Da	90 Da	120 Da		
<u>[M+Cl-Glu<sub>2</sub>-X-HCl]<sup>-</sup></u>				281	263	251	221	C <sub>2</sub> -ion	
4	2	701	LCBIM4		x			α(1→2)	Fig. 8c in Study I
4	3	701→503	LCBIM4		x			α(1→2)	Fig. 8d in Study I
4	2	701	WCBIM4					α(1→3)	Fig. 8a in Study I
4	3	701→503	WCBIM4					α(1→3)	Fig. 8b in Study I
<u>[M+Cl-Glu-X-HCl]<sup>-</sup></u>				443	425	413	383	C <sub>3</sub> -ion	
4	2	701	LCBIM4	x			<u>x</u>	α(1→6)	Fig. 8c in Study I
4	3	701→503	LCBIM4	<u>x</u>		x	x	α(1→6)	Fig. 8d in Study I
4	2	701	WCBIM4	x			x	α(1→6)	Fig. 8a in Study I
4	3	701→503	WCBIM4	x		x	<u>x</u>	α(1→6)	Fig. 8b in Study I
<u>[M+Cl-X-HCl]<sup>-</sup></u>				605	587	575	545	Precursor	
4	2	701	LCBIM4	x			<u>x</u>	α(1→6)	Fig. 8c in Study I
4	2	701	WCBIM4	x		x	<u>x</u>	α(1→6)	Fig. 8a in Study I

## 5.2 ESI-MS<sup>n</sup> of trisaccharide acceptor products of *W. confusa* (II)

In study II, the acceptor reaction products of *W. confusa* VTT E-90392 dextransucrase were analysed. In these acceptor reactions, sucrose was used as the donor for the lactose and cellobiose acceptors. The major products in the reaction mixtures were identified as 2<sup>Glc</sup>-α-Glcp-lactose and 2<sup>1</sup>-α-Glcp-cellobiose by NMR and HPAEC analysis (study II, sections 3.2 and 3.3.) These branched reducing trisaccharides had glucosyl residue attached to the reducing end unit of lactose and cellobiose by the (1→2)-linkage. The lactose reaction mixture also contained non-reducing isomelezitose (6<sup>Fru</sup>-α-Glcp-sucrose).

For the quick identification of the trisaccharide products, the ESI-MS<sup>n</sup> method was implemented. The fragmentation patterns of isomeric products 2<sup>Glc</sup>-α-Glcp-lactose and 2<sup>1</sup>-α-Glcp-cellobiose were found to be similar in both [M+Li]<sup>+</sup> and [M+Cl]<sup>-</sup> MS/MS spectra (study II, supplementary Figures S6 and S8), indicating comparable structural features. However, the MS<sup>n</sup> spectra were difficult to interpret because the samples contained small amounts of isomeric impurities.

To characterise the fragment ions, the lactose acceptor reaction was prepared using  $^{13}\text{C}_6^{\text{glc}}$ -labelled sucrose based on Harrison et al. (2012). The negative ESI-ITMS spectrum of the reaction mixture is presented in Figure 14. The  $2^{\text{Glc}}$ - $\alpha$ -Glc-p-lactose (Product I) and isomelezitose ( $6^{\text{Fru}}$ - $\alpha$ -Glc-p-sucrose, Product II) were observed at  $m/z$  545 and  $m/z$  551, respectively. The former had one  $^{13}\text{C}$ -labelled glucose unit, and the latter had two  $^{13}\text{C}$ -labelled glucose units. The reaction mixture also contained tetrasaccharides, pentasaccharides and hexasaccharides, all of which had at least one unlabelled unit.

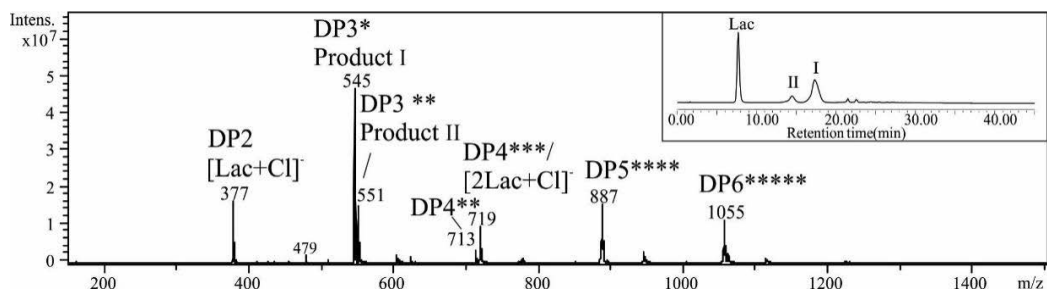


Figure 14. Negative ion ESI-ITMS spectrum of acceptor reaction mixture prepared from lactose and  $^{13}\text{C}_6^{\text{glc}}$ -labelled sucrose. Product I =  $2^{\text{Glc}}$ - $\alpha$ -Glc-p-lactose and Product II = isomelezitose,  $6^{\text{Fru}}$ - $\alpha$ -Glc-p-sucrose. \* =  $^{13}\text{C}_6$ -labelled glucose units (Supplementary Fig. S9 in study II)

The negative ion MS/MS in  $2^{\text{Glc}}$ - $\alpha$ -Glc-p-lactose (Figure 15) was dominated by the cross-ring fragment  $^{0,4}\text{X}_0\text{-H}_2\text{O}$  ion ( $m/z$  431) cleaved from the reducing end. Other ions were not abundant, so further  $\text{MS}^n$  stages were impossible. Contrary to the negative ionisation MS/MS, the  $^{0,4}\text{X}_0\text{-H}_2\text{O}$  ion was not observed in positive ionisation MS/MS (Figure 15b). The  $^{13}\text{C}_6^{\text{glc}}$ -labelled units enabled the separation and analysis of the positively charged Y-ions by  $\text{MS}^3$ . The  $\text{Y}_1$  ion produced  $^{0,2}\text{X}_0$  ( $m/z$  235, loss of 120 Da), which was found diagnostic for (1 $\rightarrow$ 2)-linkage in study I (Table 9).  $\text{Y}_{1a}$  were found to produce  $^{0,2}\text{A}_2$  and  $^{2,4}\text{A}_2$  cross-ring fragments (neutral loss 60 Da and 120 Da), which were diagnostic for the (1 $\rightarrow$ 4)-linkage (Table 9).

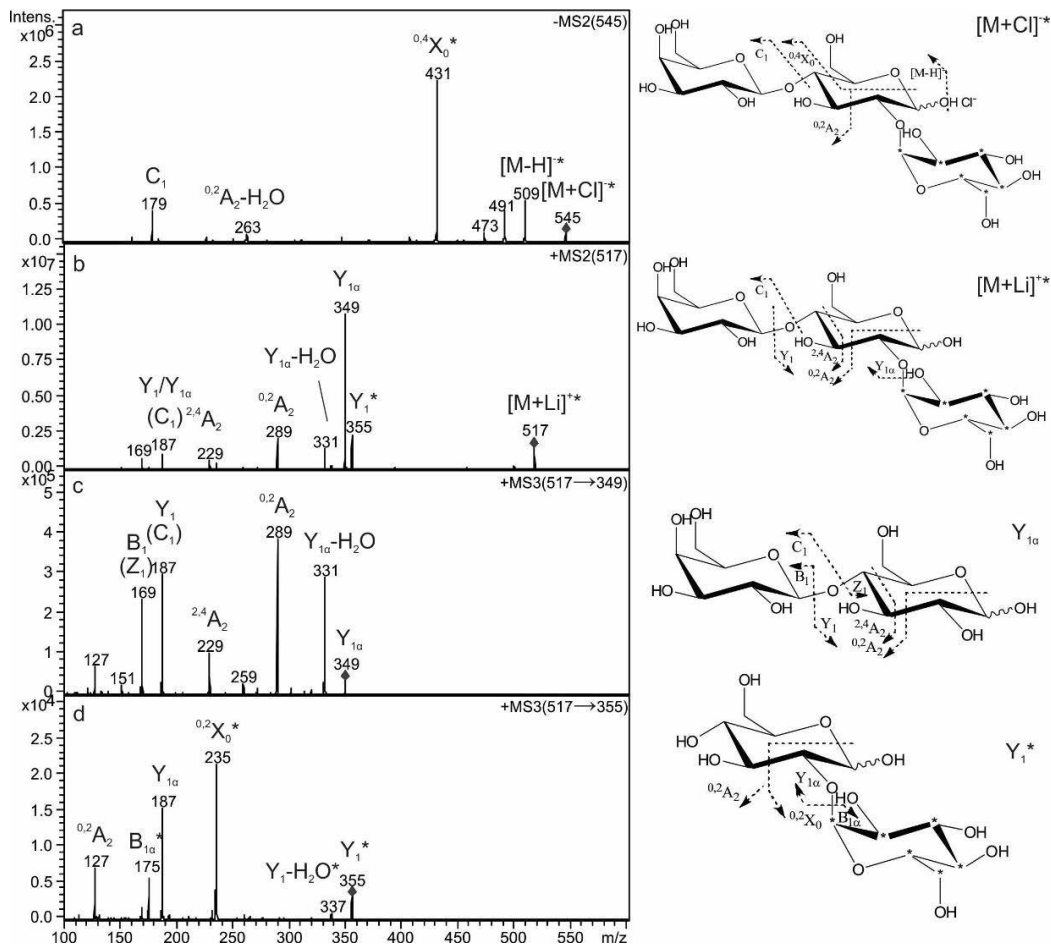


Figure 15. The ESI-ITMS/MS and ESI-ITMS<sup>3</sup> spectra of <sup>13</sup>C<sub>6</sub><sup>glc</sup>-labelled acceptor product 2<sup>Glc</sup>- $\alpha$ -Glc $p$ -lactose. \* (in the structural model) = the <sup>13</sup>C carbon, \* (in the spectra) = number of <sup>13</sup>C<sub>6</sub>-labelled glucose units. a) Negative MS/MS spectrum of [M+Cl]<sup>-</sup> ion,  $m/z$  545 b) positive MS/MS spectrum of [M+Li]<sup>+</sup> ion,  $m/z$  517, c) positive MS<sup>3</sup> spectrum of Y<sub>1 $\alpha$</sub> ,  $m/z$  349, d) positive MS<sup>3</sup> spectrum of Y<sub>1</sub>  $m/z$  355 (Fig. 4 in study II).

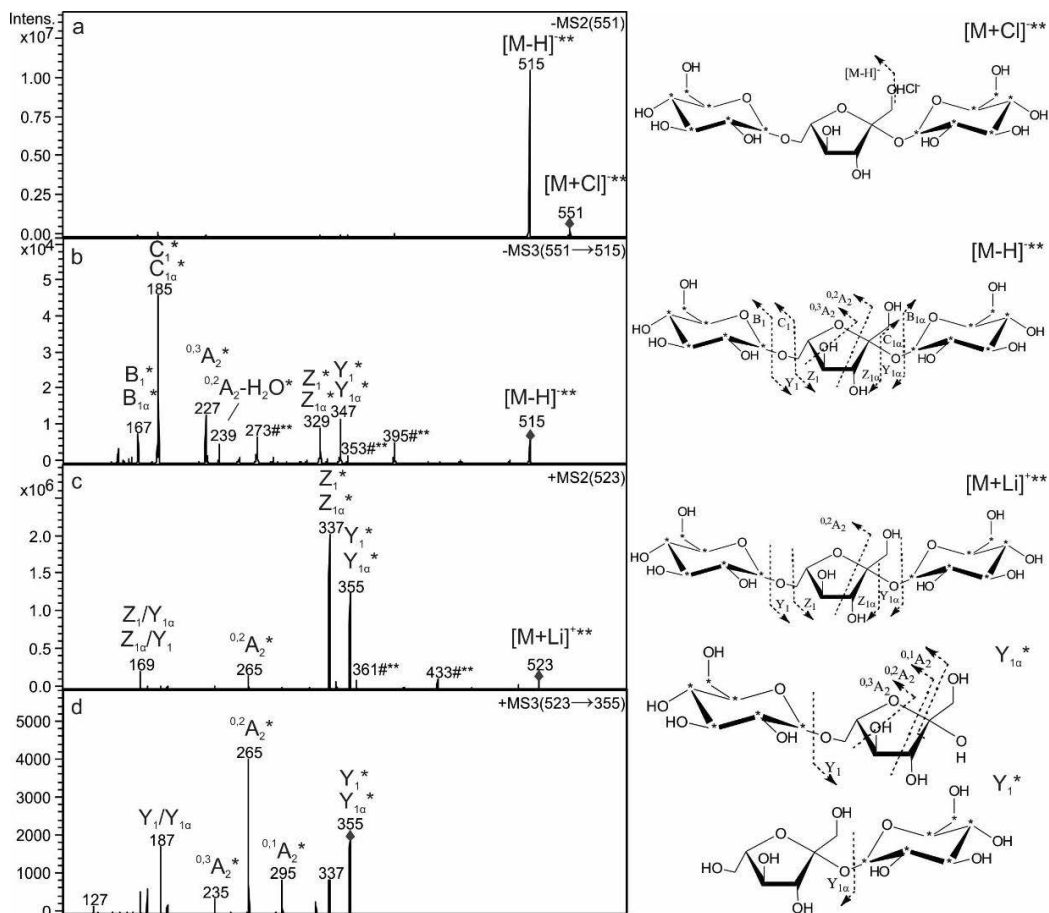


Figure 16. The ESI-MS/MS and ESI-MS<sup>3</sup> spectra of <sup>13</sup>C<sub>6</sub><sup>glc</sup>-labeled acceptor product isomelezitose (<sup>6</sup>Fru- $\alpha$ -Glc $\beta$ -sucrose), \* (in the structural model) = the <sup>13</sup>C carbon, # (in the spectra) = fragment ions of unknown trisaccharide, \* (in the spectra) = number of <sup>13</sup>C<sub>6</sub>-labelled glucose units. a) Negative MS/MS spectrum of [M+Cl]<sup>-</sup> ion, *m/z* 551, b) negative MS<sup>3</sup> spectrum of [M-H]<sup>-</sup>, c) positive MS/MS spectrum of [M+Li]<sup>+</sup> ion, *m/z* 523 d) positive MS<sup>3</sup> spectrum of Y<sub>1 $\alpha$</sub>  and Y<sub>1</sub> ions *m/z* 355. (Fig. 5 in study II).

The <sup>13</sup>C<sub>6</sub><sup>glc</sup>-labeled isomelezitose (<sup>6</sup>Fru- $\alpha$ -Glc $\beta$ -sucrose) was the minor trisaccharide product in the lactose reaction mixture. It fragmented only by the loss of hydrogen chloride (HCl) in negative ion MS/MS and produced a deprotonated molecular ion [M-H]<sup>-</sup> at *m/z* 515. The lack of any glycosidic bond or cross-ring cleavage fragments fits to the absence of reducing end. The fragmentation of [M-H]<sup>-</sup> in MS<sup>3</sup> showed an interesting cross-ring fragment ion at *m/z* 239, which was formed by the cross-ring cleavage of the middle

fructofuranosyl unit. Some fragments that were considered to originate in small amounts of impurity were observed at  $m/z$  395,  $m/z$  353 and  $m/z$  273.

The Z- and Y-ions ( $m/z$  337 and  $m/z$  355) were the most abundant ions in the positive MS/MS spectrum of isomelezitose. No cross-ring fragments were formed from the terminal units, which was assumed to be because isomelezitose is a non-reducing trisaccharide. In the MS<sup>3</sup> analysis, the Y<sub>1a</sub> were found to fragment to <sup>0,1</sup>A<sub>2</sub>, <sup>0,2</sup>A<sub>2</sub> and <sup>0,3</sup>A<sub>2</sub> cross-ring ions. The Y<sub>1</sub> ion had the structure of sucrose; as a non-reducing sugar, it did not produce cross-ring fragments. The peak at  $m/z$  433 (M-90 Da) was likely due to impurity because it was not present in the unlabelled and fractionated isomelezitose MS/MS.

### 5.3 Linkage analysis of linear (A)XOS by ESI-MS<sup>n</sup> (III)

In the first part of study III, the objective was to determine how the linkage positions in pentose oligosaccharides, XOS and AXOS influenced the MS<sup>n</sup> ion spectra, particularly cross-ring fragment ion distribution. The MS/MS of [M+Cl]<sup>-</sup> precursor ions were analysed first. Then the (assumed) C-ions were analysed in the MS<sup>3</sup> step.

Figure 17 presents the negative ion ESI-MS<sup>n</sup> spectra of linear (A)XOS. All the linear samples were found to produce [M-60 Da-H] and [M-78 Da-H] cross-ring fragment ions from their (1→4)-linked reducing ends in ESI-MS/MS ( $m/z$  485 and  $m/z$  467 in Figure 17a, Figure 17f, Figure 17i;  $m/z$  353 and  $m/z$  335 in Figure 17d). The C-ions were further fragmented in MS<sup>3</sup>. The middle units of (1→4)-linked (A)XOS also produced [C-60 Da-H]<sup>-</sup> and/or [C-78 Da-H]<sup>-</sup> cross-ring ions ( $m/z$  353 and  $m/z$  335 in Figure 17b and Figure 17g).

The  $m/z$  191 [C-90 Da-H]<sup>-</sup> and  $m/z$  233 [C-48Da-H]<sup>-</sup> cross-ring ions were found in (1→2)-linked units in A<sup>2</sup>XX and D<sup>2,3</sup>X MS<sup>3</sup> spectra (Figure 17g, Figure 17h, Figure 17j, Figure 17k). The MS<sup>3</sup> spectra of A<sup>2</sup>XX and D<sup>2,3</sup>X were almost identical (Figure 17h and Figure 17k); therefore, it was not possible to differentiate β-D-Xylp-(1→2)-α-L-Araf from α-L-Araf-(1→2)-β-D-Xylp. The A<sup>3</sup>X and D<sup>2,3</sup>X, which had (1→3)-linkages between their middle residues, did not form <sup>0,2</sup>A or any other kind of cross-ring fragments in O-3-position linked residues in MS/MS (Figure 17d and Figure 17j). However, in the MS<sup>3</sup> stage, A<sup>3</sup>X was found to form [C-60-H] cross-ring fragment ions (Figure 17e) similar to (1→4)-linked X<sub>4</sub> (Figure 17c).

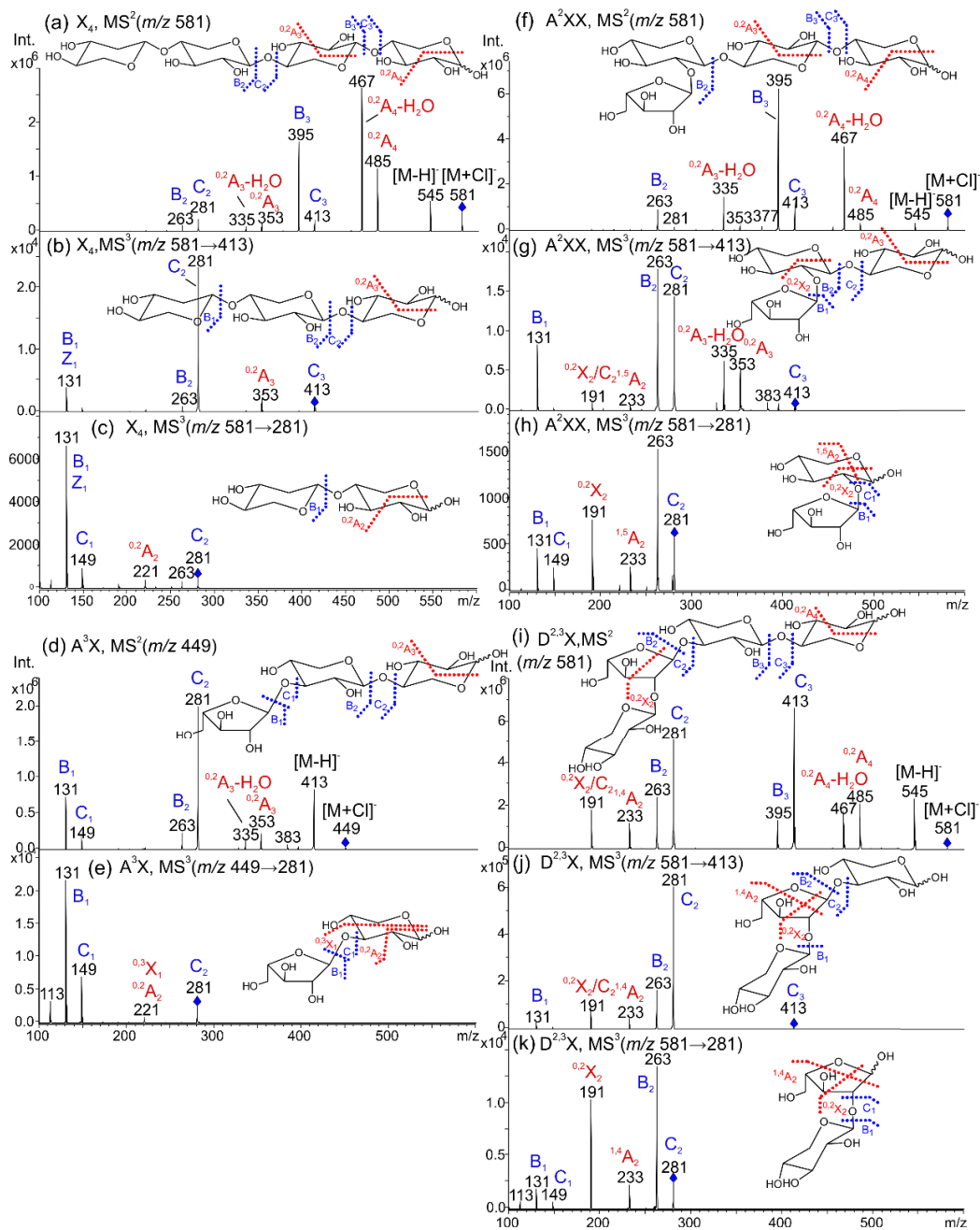


Figure 17. Negative ionization ESI-MS<sup>n</sup> spectra of linear (A)XOS. (Fig. 2 in study III). Precursor ions are [M + Cl]<sup>-</sup> and product ions are deprotonated. / = double cleavage. (a) X<sub>4</sub>, MS/MS m/z 581, (b) X<sub>4</sub>, MS<sup>3</sup> m/z 581→413, (c) X<sub>4</sub>, MS<sup>3</sup> m/z 449→281, (d) A<sup>3</sup>X, MS<sup>2</sup> m/z 449, (e) A<sup>3</sup>X, MS<sup>3</sup> m/z 449→281, (f) A<sup>2</sup>XX, MS<sup>2</sup> m/z 581, (g) A<sup>2</sup>XX, MS<sup>3</sup> m/z 581→413, (h) A<sup>2</sup>XX, MS<sup>3</sup> m/z 581→281, (i) D<sup>2,3</sup>X, MS<sup>2</sup> m/z 581, (j) D<sup>2,3</sup>X, MS<sup>3</sup> m/z 581→413, and (k) D<sup>2,3</sup>X, MS<sup>3</sup> m/z 581→281.



#### 5.4 Identification of branches from (A)XOS by ESI-MS<sup>3</sup> (III)

The negative ion ESI-IT-MS/MS spectra of branched (A)XOS is presented in Figure 18. The branched (A)XOS also formed typical fragments from the reducing ends of (1→4)-linked xylan backbone (i.e., <sup>0,2</sup>A ions and <sup>0,2</sup>A-H<sub>2</sub>O ions shown in Figure 18). It was expected that if fragmentation occurred mainly from reducing end, the branching unit could be observed in the spectrum as an area lacking cross-ring ions. However, the lack of cross-ring ions was found only in monosubstituted XA<sup>2</sup>XX and XA<sup>3</sup>XX spectra. All other samples had cross-ring ions in the assumed branching unit range, which means that the fragmentation occurred also from the non-reducing end, and double-cleaved A/Y-ions were formed.

Branched samples presented some characteristic fragmentation in MS/MS and MS<sup>3</sup>. The XA<sup>3</sup>XX produced abundant peak at *m/z* 299 both in the MS/MS and MS<sup>3</sup> spectra. This peak was not present in any other samples' spectra. In addition, the disubstituted samples were found to have stronger cross-ring fragment ion [M-90 Da]<sup>-</sup> and [M-pentose-90 Da]<sup>-</sup> (*m/z* 455, *m/z* 587, *m/z* 719) than the monosubstituted or the linear samples. Furthermore, Araf disubstituted A<sup>2+3</sup>X and A<sup>2+3</sup>XX were found to have peak at *m/z* 263 which was not present in other branched AXOS.

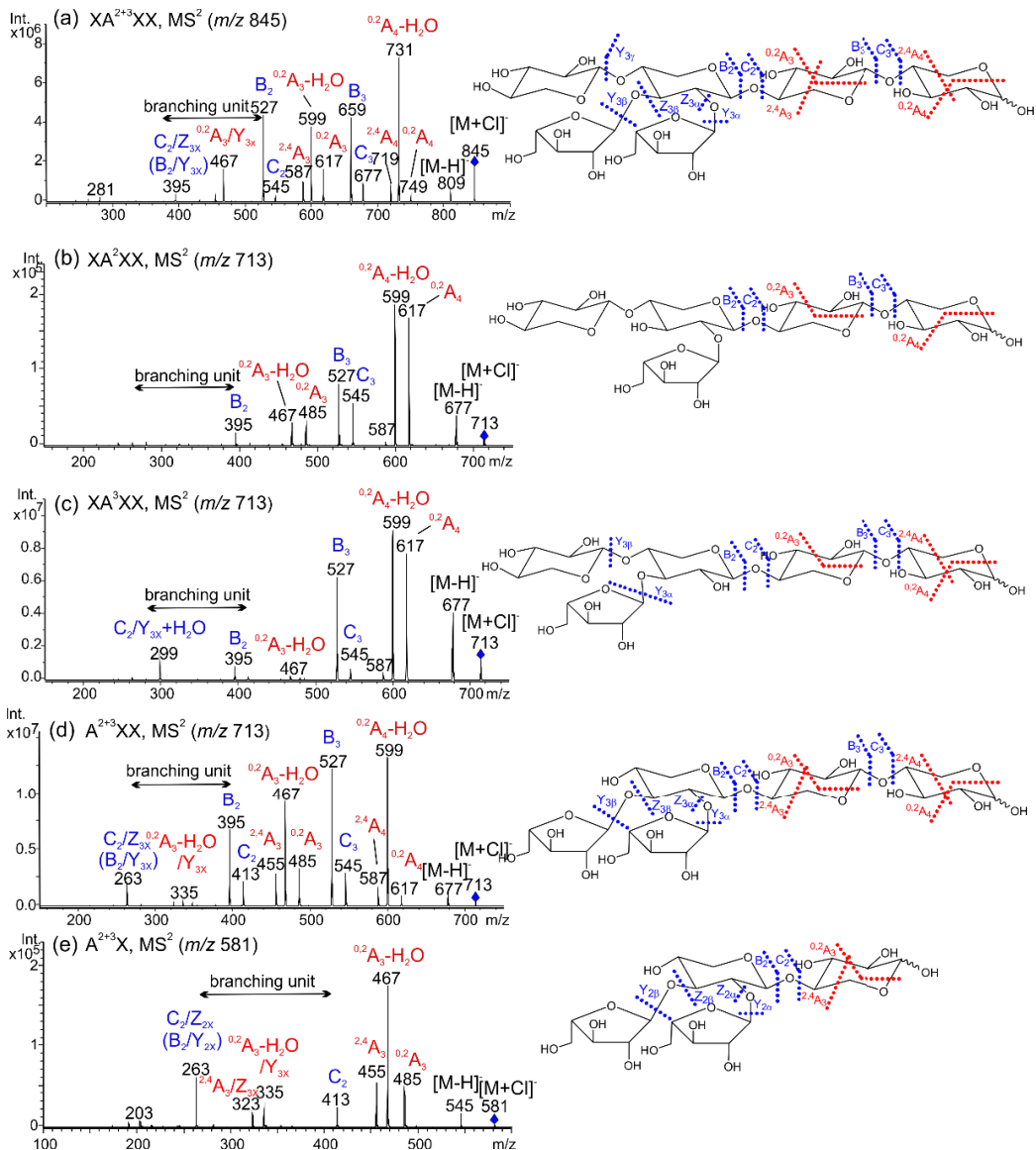


Figure 18. Branched AXOS analysed by negative ionisation ESI-MS/MS as  $[M+Cl]^-$  adducts (Fig 3. in study III). The expected branching unit MS/MS area marked for fragmentation reaction starting from the reducing end. / = double cleavage,  $x = \alpha, \beta,$  or  $\gamma$  fragment ion. a)  $XA^{2+3}XX$ , b)  $XA^2XX$  (+  $XA^3XX$ ), c)  $XA^3XX$ , d)  $A^{2+3}XX$  and e)  $A^{2+3}X$

The C-ions MS<sup>3</sup> spectra of (A)XOS showed specific fragmentation patterns in all isomeric (A)XOS samples (Fig. 4 in study III), which allowed the structures to be determined by the presence or absence of diagnostic ions. Table 13 shows a summary of the diagnostic ions and absent ions in (A)XOS C-ions in negative ESI-ITMS<sup>3</sup>.

Table 13. Negative ESI-ITMS<sup>3</sup> diagnostic and absent ions of (A)XOS. Deprotonated fragment ions produced from [M+Cl]<sup>-</sup> precursors. (summarised from Fig. 2 and Fig. 4 in study III).

Oligosaccharide	<i>m/z</i>	C-ion	C-ion, <i>m/z</i>	Diagnostic ions, <i>m/z</i>	Absent ions, <i>m/z</i>
A <sup>3</sup> X	449	A <sup>3</sup>	281	221	191,233
D <sup>2,3</sup> X	581	Xyl(1→2)Ara	281	191	221
A <sup>2</sup> XX	581	A <sup>2</sup>	281	191	221
X <sub>4</sub>	581	X <sub>2</sub>	281	221,263	191,233
D <sup>2,3</sup> X	581	D <sup>2,3</sup>	413	191,233	335,353,299
A <sup>2</sup> XX	581	A <sup>2</sup> X	413	191,233,335,353	221,299
X <sub>4</sub>	581	X <sub>3</sub>	413	(221),353	191,233,299
XA <sup>3</sup> XX	713	XA <sup>3</sup>	413	<u>263,299</u> ,353	191,245
A <sup>2+3</sup> XX	713	A <sup>2+3</sup>	413	245, <u>263</u> ,353	191,299
XA <sup>2+3</sup> XX	845	XA <sup>2+3</sup>	545	<u>395</u> ,431	299,467
XA <sup>2</sup> XX	713	XA <sup>2</sup> X	545	395, <u>467</u> <u>299</u> ,	299
XA <sup>3</sup> XX	713	XA <sup>3</sup> X	545	395,431,467,485	
A <sup>2+3</sup> XX	713	A <sup>2+3</sup> X	545	<u>413</u> , 455,467	299,395

Underline = base peak

### 5.5 Implementation of HILIC-MS/MS for identification of AXOS (III)

To analyse AXOS in mixtures, the negative ionisation HILIC-MS/MS method with the post-column addition of NH<sub>4</sub>Cl was implemented for Bruker Esquire IT. First, the IT parameters were optimized according to XOS standards. Because the HILIC-MS test showed that various anion adducts were formed, NH<sub>4</sub>Cl was added to obtain exclusively chloride adducts, which also raised the intensity levels of the ions (Fig. 5 in study II). The concentration and flow rate of the post-column addition of ammonium chloride were optimized to achieve the best peak abundance with the smallest amount of chloride. The post-column addition technique was chosen because it enabled the use of the same eluents in the positive mode.

Next, HILIC-MS/MS were optimized for every DP in the samples. EIC chromatograms of samples were presented in Figure 6 in study III. All the samples had different retention times (Table 14). The following elution order was observed in samples with same XOS backbone length: 1) unsubstituted; 2) O-3-Araf-substituted; 3) O-2-Araf-substituted; 4) disubstituted XOS. For example, xylo-tetraose backbone containing (A)XOS were eluted in the following order: X<sub>4</sub>, XA<sup>3</sup>XX, XA<sup>2</sup>XX and XA<sup>2+3</sup>XX. In addition, the lengthening of the xylan backbone increased the retention, and the Araf-substitution decreased the retention. For example, linear X<sub>3</sub> was slower than the Araf-substituted A<sup>3</sup>X, A<sup>2</sup>X, and A<sup>2+3</sup>X.

As observed earlier in ESI-MS<sup>n</sup>, negative ion HILIC-MS/MS also produced a specific spectrum in each studied (A)XOS. A summary of the retention times, the diagnostic ions and absent ions in all studied (A)XOS is presented in Table 14. The results showed that the HILIC-MS/MS identified and separate all the studied (A)XOS samples.

Table 14. Diagnostic and absent fragment ions of studied (A)XOS by negative ion HILIC-ITMS/MS. (Supplementary OR3 in study III)

Oligosaccharide	DP	Rt (min)	Diagnostic peaks (m/z)	Absent peaks (m/z)
A <sup>3</sup> X	3	10.3	<u>281</u> , 353	335
A <sup>2</sup> X	3	12.1	<u>335</u>	353
X <sub>3</sub>	3	15.3	<u>263</u>	
A <sup>2+3</sup> X	4	13.5	455, <u>467</u>	
D <sup>2,3</sup> X	4	15.9	191, 395, <u>413</u>	455
A <sup>2</sup> XX	4	17.6	335, <u>395</u>	413, 455
X <sub>4</sub>	4	20.7	<u>395</u>	413, 455
A <sup>2+3</sup> XX	5	18.5	263, 467, <u>599</u>	299
XA <sup>3</sup> XX	5	21.3	263, 299, 599, <u>617</u>	
XA <sup>2</sup> XX	5	22.4	467, <u>599</u> , 617	263, 299
X <sub>5</sub>	5	25.6	281, 467, <u>599</u> , 617	263, 299
XA <sup>2+3</sup> XX	6	24.3	-	-

Rt = retention time (min), DP = degree of polymerisation, underline = base peak.

## 5.6 Identifying AXOS isomers by IMS-MS/MS method (IV)

### 5.6.1 Separation of precursors by ESI-TWIMS-MS

First, the potential of TWIMS-MS to differentiate (A)XOS isomers was studied. Table 15 presents the drift times of each precursor measured in both negative and positive ionisation.

The drift time of X<sub>3</sub> was differentiated from the other trisaccharides (A<sup>2</sup>X and A<sup>3</sup>X) as [M+Na]<sup>+</sup> adducts, and the drift time of A<sup>3</sup>X was differentiated from the others as [M-H]<sup>-</sup> adducts. The best separation in tetrasaccharides was achieved as [M+Na]<sup>+</sup> adducts, but only X<sub>4</sub> was clearly differentiated from the others. All negatively charged tetrasaccharide precursors had very similar drift times. In contrast, the drift times of the positively charged pentasaccharide samples were differentiated from each other. The negatively charged precursors had closer drift times; hence linear X<sub>5</sub> was differentiated from the branched samples A<sup>2+3</sup>XX, XA<sup>2</sup>XX and XA<sup>3</sup>XX by a difference greater than 0.2 ms.

Table 15. Drift times of (A)XOS precursors in ESI-TWIMS-MS. (Table 1 in study IV)

Oligosaccharide	DP	[M+Na] <sup>+</sup>		[M-H] <sup>-</sup>		[M+Cl] <sup>-</sup>	
		m/z	dt (ms)	m/z	dt (ms)	m/z	dt (ms)
A <sup>2</sup> X	3	437	3.34	413	3.09	449	3.36
A <sup>3</sup> X	3	437	3.36	413	3.31	449	3.42
X <sub>3</sub>	3	437	3.69	413	3.42	449	3.47
A <sup>2</sup> XX	4	569	4.56	545	4.07	581	4.39
A <sup>2+3</sup> X	4	569	4.45	545	4.18	581	4.45
D <sup>2,3</sup> X	4	569	4.45	545	4.12	581	4.39
X <sub>4</sub>	4	569	4.94	545	4.12	581	4.39
A <sup>2+3</sup> XX	5	701	5.64	677	4.83	713	5.21
XA <sup>2</sup> XX(+XA <sup>3</sup> XX)	5	701	5.86,(5.32)	677	5.10	713	5.26
XA <sup>3</sup> XX	5	701	5.32	677	5.10	713	5.21
X <sub>5</sub>	5	701	5.26	677	4.99	713	4.99

DP = degree of polymerisation, dt = drift time

### 5.6.2 Separation of fragment ions ESI-CID-TWIMS-MS/MS

Next, the ability of TWIMS to differentiate the isomeric fragment ions of AXOS was studied. The samples were analysed by the ESI-CID-TWIMS-MS/MS method in both positive  $[M+Na]^+$  and negative  $[M+Cl]^-$  ionisation. ESI-CID-TWIMS-MS/MS indicated that the precursor ions were fragmented by CID prior to IM separation and  $m/z$  detection. The drift times of the glycosidic bond fragments and the most common cross-ring ions are presented in Table 16.

It was not possible to distinguish the disaccharide fragment ions from each other according to the drift time. All differences in the extracted ion mobilograms (EIM) were in  $< 0.1$ ms. Hence, the method could not differentiate Ara(1→3)Xyl, Ara(1→2)Xyl, Xyl(1→4)Xyl, or Xyl(1→2)Ara fragment ions. This result was observed in both positive and negative ionisation modes of the fragment ions at  $m/z$  305 (Y- and C-ions), at  $m/z$  287 (B- and Z-ions) and  $m/z$  263 (B- and Z-ions) (Tables 2 and 3 in study IV).

However, Ara-substituted trisaccharide fragment ions at  $m/z$  437 (drift times 4.67–4.75 ms) were clearly distinguishable from xylotriose (drift time 5.15–5.17 ms) in the positive mode (Table 2, in study IV). The Xyl-Ara-Xyl fragment also had a different drift time: 4.99 ms. Similar to the positive mode, in the negative mode, the  $m/z$  413 fragment ions divided in to two groups based on the drift times. The Ara-substituted fragment ions had drift times from 4.31–4.45 ms, and the xylotriose fragment ions had drift times from 4.68–4.75 ms. The Ara-disubstituted fragments were slightly slower (4.45 ms) than the monosubstituted fragments (4.31–4.32 ms).

In the positive mode, the linear xylo-tetraose fragment ( $m/z$  569) travelled much slower in TWIMS (7.2–7.24 ms) than the substituted or branched AXOS tetrasaccharide fragment ions did (6.10–6.69 ms). The xylo-tetraose fragment ion was found to be a minor peak in the EIM of  $XA^2XX$  ( $+XA^3XX$ ) and  $XA^3XX$  and a major peak in  $X_5$ . Furthermore, in all the pentasaccharide samples, the drift times of the main  $[M+Na]^+$  tetrasaccharide fragment ion were different.

Table 16 presents a summary of the drift times and the assumed structures of the fragment ions based on the TWIMS-MS/MS results.

Table 16. Drift times of (A)XOS precursor and fragment ions measured by CID-TWIMS-MS/MS. (Table 4 in study IV)

Structure	[M+Na] <sup>+</sup>		[M-H] <sup>-</sup>	
	<i>m/z</i>	dt (ms)	<i>m/z</i>	dt (ms)
A <sup>2</sup> X	437	4.7	413	4.3
A <sup>3</sup> X	437	4.7	413	4.5 <sup>a</sup>
D <sup>2,3</sup>	437	5.0	413	4.3
X <sub>3</sub>	437	5.2	413	4.7
A <sup>2</sup> XX	569	6.6	545	5.7
A <sup>3</sup> XX	569	6.1	545	
A <sup>2+3</sup> X	569	6.4	545	6.1
D <sup>2,3</sup> X	569	6.4	545	5.9
XA <sup>2</sup> X	569	6.7 <sup>b</sup>	545	6.5 <sup>b</sup>
XA <sup>3</sup> X	569	6.6	545	6.3
X <sub>4</sub>	569	(6.7-6.8),7.2	545	5.7-5.8
A <sup>2+3</sup> XX	701	8.5	677	6.9
XA <sup>2</sup> XX	701	8.9	677	7.4 <sup>b</sup>
XA <sup>3</sup> XX	701	7.5,7.9	677	7.7
X <sub>5</sub>	701	7.8	677	7.2

<sup>a</sup> = drift time from TWIMS-MS, <sup>b</sup> = drift time uncertain, sample is a mixture.

### 5.6.3 Base peak mobilogram (BPM) as a fingerprinting tool

The BPM in CID-TWIMS-MS/MS was studied as a tool for the identification of (A)XOS (study IV). The BPM was used as a fingerprint with MS/MS to identify the isomeric samples. Figure 19 shows the BPM of tetrasaccharide isomers  $D^{2,3}X$  and  $A^2XX$ . Even though their  $[M+Cl]^-$  precursors had the same drift times (6.29 ms), the BPM in the fragment ions were identified by entirely different profiles.

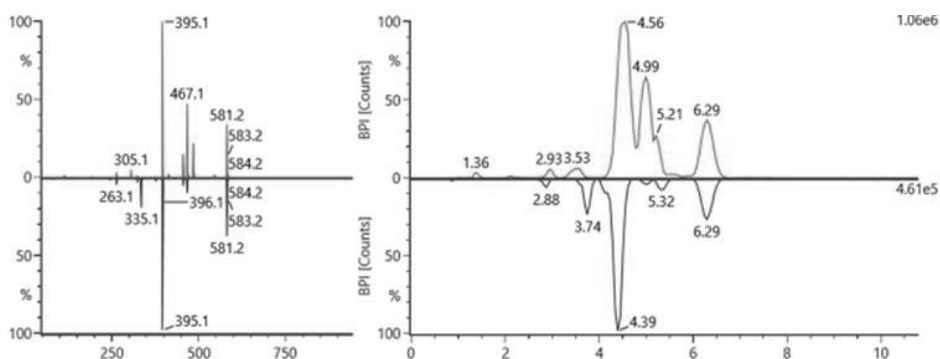


Figure 19. The MS/MS spectra (left) and BPMs (right) of  $D^{2,3}X$  (above) and  $A^2XX$  (below) from negative ionisation CID-TWIMS-MS/MS (Fig 2. in study IV)



## 6 DISCUSSION

### 6.1 Remarks on labelling the fragments according to a nomenclature (I–IV)

Throughout the study, the oligosaccharide fragment ions were labelled according to Domon and Costello's (1988) nomenclature. This nomenclature was originally created for the fragment ions of reducing oligosaccharides and aglycones. In study II, isomelezitose is a non-reducing trisaccharide that presented challenges in naming the fragment ions. The reducing-end containing ions usually would be named X, Y and Z fragment ions, but regarding non-reducing oligosaccharides, there are no instructions on how to proceed. It was decided that the structure would be named like a branched oligosaccharide; the palatinose unit was the core, and the glucose attached to it was deemed the branch. Similar naming to the branched trisaccharides allowed for the comparison of the spectra to the other two trisaccharides that had reducing ends. However, in retrospect, in study II the original nomenclature could have been retained if the fructose residue had been marked as the core unit and both glucose residues as antennae designated by the symbols  $\alpha$  and  $\beta$ . This procedure would have eased the markings in the spectra; instead of marking  $Y_1$  or  $Y_{1\alpha}$ , the mark would have been  $Y_{1x}$ . The same process could have been used to name the other two trisaccharides.

In studies I and II, another dilemma was encountered when the cross-ring ions were assigned. The original nomenclature divides the cross-ring ions into two categories: A- and X-labelled ions. The division is based on whether the charge is retained on carbohydrate (A-ions) or aglycone (X-ions). In study I, all the cross-ring fragments were named A-ions because the charge was retained at the non-reducing end. However, in study II, it was realised that the cross-ring ions marked as  $^{0,2}A$  ions in the (1→2)-linked structure should have been marked as  $^{0,2}X_i$  ions. The reason is that the name would always indicate the way in which the ring was cleaved and which side of the ring the charge retained. Moreover, it would help to differentiate both kinds of cross-ring ions, such as  $^{0,2}A$  and  $^{0,2}X$  from 2<sup>Glc</sup>- $\alpha$ -Glc-p-lactose in study II, (Figure 15d). The same approach was presented by Mischnik (2011).

Furthermore, naming the fragment ions in different steps in  $MS^n$  was not straightforward. The precursor ions were increasingly fragmented in every stage, but the question was whether the labelling of fragments should be

according to the original precursor or be changed to fit the current precursor. It was decided to use the original MS<sup>2</sup> stage labelling because it would be easier for the reader to follow.

## **6.2 Feasibility of MS in the structural analysis of neutral oligosaccharides**

### **6.2.1 Determination of glycosidic linkage positions by MS<sup>n</sup> (I, III)**

Several studies have demonstrated the determination of the positions of glycosidic linkages according to the cross-ring fragmentation patterns in di- and oligosaccharides in both negative and positive ionisation MS/MS (Table 2 and Table 3).

In this thesis, the cross-ring fragmentation patterns of the linear reducing oligosaccharides GLOS (study I) and AXOS (study III) were studied to determine the linkage positions. The model isomeric disaccharides and oligosaccharides (study I) and the GLOS and (A)XOS were found to produce diagnostic cross-ring fragment ions in ESI-MS<sup>n</sup>. Both positive and negative ionisation modes determined the positions of reducing end linkages in the studied di-, tri-, tetra- and pentasaccharide samples according to the presence or absence of diagnostic cross-ring ions. However, the negative ionisation mode was found to better determine the linkages in larger GLOS and (A)XOS. Because the fragmentation mechanisms in the negative mode favour C-ions over Y-ions (Chai et al. 2001), the negatively charged linear GLOS and (A)XOS fragmented mainly from the reducing end toward non-reducing end. This was beneficial in the linkage analysis because a new reducing end was formed in each step, and new linkage diagnostic cross-ring fragments were observed.

In the positive mode, the Y-type fragmentation predominated, which was probably due to the location of the cation adduct near the reducing end in neutral oligosaccharides. Furthermore, because both the AXOS and GLOS are built of only one mass monomer, the C- and Y-ions are isobaric and cannot be differentiated from each other. The domination of Y-type fragmentation indicated that at the MS<sup>3</sup> stage, the non-reducing end fragment ions were hidden under the dominant reducing end ions. However, the following strategies were used to analyse the non-reducing end linkages in the positive mode.

In study I, the linkage position of the non-reducing end was analysed by fragmenting the MS/MS  $[M+Li-H_2O]^+$  ions in MS<sup>3</sup>. Because the loss of water occurs in the carbonyl of the reducing end (Hofmeister et al. 1991), the  $[M+Li-H_2O]$  ion is always formed in the original non-reducing end. The linkage positions of the middle and non-reducing end could be determined according to the MS<sup>3</sup> spectrum of the  $[M+Li-H_2O]^+$  ion. This strategy was suitable in samples such as panose and glucotetraose, which had abundant  $[M+Li-H_2O]$ . The same procedure was recently further developed as a structural method by Hsu et al. (2018). In their method, the cross-ring ions from the reducing end are also further fragmented in MS<sup>3</sup>.

In the second strategy, the CID-TWIMS-MS method was used to separate the Y- and C-ions. In the third strategy, the product ions were separated by derivatising part of the molecule using isotope labelling. The usability of these two methods is discussed in section 6.2.3.

Some observations of the determination of (1→3)-linkages by ESI-MS<sup>n</sup> were made. First, the (1→3)-linkages were the most uncertain linkages to determine from GLOS and AXOS. The (1→3)-linked disaccharides are known to produce <sup>0,3</sup>X fragment ion by the loss of 90 Da neutral in positive ion CID and not to produce any cross-ring fragment ions in negative mode  $[M+Cl]^-$  ion (Asam & Glish 1997; Zhu & Cole 2001). These fragmentations were also observed in study I in GLOS and in study II in AXOS. However, deprotonated disaccharide ions were reported to fragment differently: the negatively charged deprotonated (1→3)-linked disaccharide fragments by <sup>0,3</sup>X ion (loss of 90 Da) similar to the positive mode (Garozzo et al. 1991). In study III, the cross-ring ions were formed by the loss of 60 Da from the (1→3)-linked A<sup>3</sup>X. It was realised that pentose oligosaccharides, such as AXOS, form isobaric <sup>0,3</sup>X and <sup>0,2</sup>A cross-ring ions because both are formed by the fragmentation of 60 Da neutrals. Hence, a similar fragmentation pattern was observed in the (1→4)-linked and (1→3)-linked disaccharide ions of deprotonated X<sub>4</sub> and A<sup>3</sup>X. It should be noted that Quemener et al. (2006) observed that deprotonated (1→3)-linked AXOS did not fragment via cross-ring cleavages in the negative mode, further complicating the identification of (1→3)-linkage. Overall, the identification of (1→3)-linkage in oligosaccharides is always uncertain by negative ESI-MS/MS because the identification is based on the absence of

cross-ring ions, which can be caused by other factors (e.g. branched residue, non-reducing sugar or the instrument's inability to measure small ions).

### 6.2.2 Influence of branch on fragmentation of oligosaccharides in MS/MS (II,III)

The influence of the branch on the fragmentation pattern was studied using ESI-MS<sup>n</sup>. The studied oligosaccharides had a branch at either the reducing end (study II) or the non-reducing end (studies III and IV).

#### *Branch in the reducing end*

The (*O*-2)- and (*O*-4)-branched trisaccharides, 2<sup>Glc</sup>- $\alpha$ -Glc<sub>p</sub>-lactose and 2<sup>1</sup>- $\alpha$ -Glc<sub>p</sub>-cellobiose, were found to fragment by the abundant loss of 78 Da cross-ring cleavage in negative ionisation ESI-MS<sup>n</sup>. The loss of 78 Da has been suggested as <sup>0,2</sup>A-type cross-ring fragmentation through retro-aldol reaction starting from the reducing end (Hofmeister et al. 1990; Garozzo et al. 1990). However, the (*O*-2)- and (*O*-4)-branched structures could fragment only from the reducing end unit by <sup>0,4</sup>X-type fragmentation with the loss of water. The loss of water is most likely due to the hydrolysis of the hydroxyl group from C-1 in the reducing sugar ring (Garozzo et al. 1990). Furthermore, surprisingly, it was observed that the cross-ring fragmentation at the reducing end happened only in negative mode and was lacking in the [M+Li]<sup>+</sup> MS/MS spectra. The knowledge that the fragmentation pathways in negative and positive ionisation modes are different will be useful in analysing oligosaccharides with similar *O*-2 and *O*-4 branching structures at the reducing end.

In study II, the MS/MS spectra (Fig.4, Supplementary Figures S6 and S8) were probably the first published MS/MS of 2<sup>Glc</sup>- $\alpha$ -Glc<sub>p</sub>-lactose and 2<sup>1</sup>- $\alpha$ -Glc<sub>p</sub>-cellobiose. Indeed, no MS/MS spectra of neutral *O*-2 and *O*-4 branched trisaccharide are mentioned in the relevant literature. The closest structure was found in a study on pectic oligosaccharides, in which galacturonic acid disaccharide had (1 $\rightarrow$ 2)-linked xylose substitute at the reducing end unit (Zandleven et al. 2005). In the negative mode, this acidic trisaccharide did not produce cross-ring fragments; instead, there was a strong loss of the water peak formed in the <sup>18</sup>O-isotope labelled reducing end. This result implies that in study II, the loss of the water ion observed from (1 $\rightarrow$ 2)-linked trisaccharides was also from C-1.

### *Branches at the non-reducing end*

Because the AXOS had a branch at the penultimate or at the non-reducing end unit, the C-ion fragmentation in MS<sup>3</sup> was found to be the best way to differentiate them in negative ionisation ESI-MS<sup>n</sup> (study III). All branches could be analysed based on the presence or absence of diagnostic ions in MS<sup>3</sup>. In addition, the diagnostic ions distinguished branched structures from linear structures. The negatively charged AXOS were found to fragment in MS/MS not only by C-type fragmentation but also by Y-type fragmentation in the branched unit. Because a stepwise analysis was performed of C-ions, the possible mixture of ions might have caused confusion. This risk was avoided in study IV because the Y- and C- product ions could be separated by ion mobility MS.

Branched XA<sup>3</sup>XX was observed to produce a diagnostic peak at  $m/z$  299 in all stages of negative ionisation ESI-MS<sup>n</sup>. The  $m/z$  299 ion was been found and reported by Quemener et al. (2006). They found it in similar *O*-3-branched and deprotonated AXOS, and they suggested that the ion was formed by double C- and Y-cleavages with the addition of water. In the current study, similar water addition ions were found also in the MS<sup>3</sup> spectra of XA<sup>2+3</sup>XX and XA<sup>3</sup>XX with  $m/z$  431, but they were one pentose unit larger than  $m/z$  299. Both ions ( $m/z$  299 and  $m/z$  431) were formed only in *O*-3- and *O*-4-branched structures. If the water molecule were covalently attached to the sugar ring, the ring must have opened and formed an aldehyde before the addition of water and the formation of a hydrate. Quemener et al. (2006) reported that the distribution of  $m/z$  263 and  $m/z$  299 ions could discriminate mono- or disubstituents at the penultimate unit in GH11 hydrolysed AXOS. In study III,  $m/z$  263 ions were found in disubstituted A<sup>2+3</sup>X and A<sup>2+3</sup>XX in ESI-MS/MS, but not in monosubstituted or XA<sup>2+3</sup>XX, which could differentiate them in MS/MS. The ions could have been formed by C- and Z-type double cleavage similar to D-ions (Chai et al. 2001). However, linear (A)XOS also formed isobaric B-ions at  $m/z$  263; therefore, the ion could not be diagnostic of disubstitution.

### 6.2.3 Differentiation of oligosaccharide isomers (I-IV)

Isomeric oligosaccharides can be challenging to analyse, which in MS means analysis of the same  $m/z$  precursor ions and the same  $m/z$  fragment ions. In this thesis, some methods of differentiating and analysing the isomeric structures were implemented.

The use of negative ionisation and the stepwise fragmentation of C-ions enabled the analysis of the linkage position isomers in the tri-, tetra- and pentasaccharide samples: GLOS in study I, and AXOS in study III. The results are discussed in detail in section 6.2.1.

In study III, it was found that HILIC-MS could separate all the isomeric DP3-DP5 (A)XOS precursors. In HILIC, retention is increased by the hydrophilicity of the analytes. The retention of (A)XOS was found to increase by DP. Moreover, the linear XOS were found have more retention than the Ara $\beta$ -substituted samples had. Because XOS have a linear molecular structure, more hydroxyl groups are available to interact with the amide phase compared with the compactly structured Ara $\beta$ -substituted AXOS. The ethylene bridge hybrid (BEH) amide was chosen as the HILIC stationary phase because of its recommendation in recent studies (Brokl et al. 2011; Hernández-Hernández et al. 2012). Brokl et al. (2011) reported that a graphitised carbon column gave the best chromatographic separation in the same molecular weights of isomeric oligosaccharides, but if the mixture contained oligosaccharides with different DPs, the HILIC provided better separation. In this study, the retention times of DP3-DP6 (A)XOS were found to vary widely between 10.3 min and 25.6 min. Moreover, the isomeric (A)XOS of every DP were separated. No split peaks occurred because ammonia was added to prevent anomeric separation, as suggested by Hernandez-Hernandez et al. (2012).

In study II,  $^{13}\text{C}$  isotope labelling enabled the study of isomeric trisaccharides by ESI-MS<sup>n</sup>. The labelling was performed using  $^{13}\text{C}_6$ -glucose-labelled sucrose in the acceptor reaction according to Harrison et al. (2012). The isomeric products, 2<sup>Glc</sup>- $\alpha$ -Glc-p-lactose and isomelezitose (6<sup>Fru</sup>- $\alpha$ -Glc-p-sucrose), had either one or two labelled glucose units and hence different molecular weights. The precursors were separated according to their different  $m/z$  and then analysed by ESI-MS<sup>n</sup>. Furthermore, the Y-ions fragmented in 2<sup>Glc</sup>- $\alpha$ -Glc-p-lactose had different  $m/z$ , and they could be isolated and further fragmented. The cross-ring fragmentation was found to be diagnostic for the (1 $\rightarrow$ 2) and

(1→4)-linked samples, as expected. In the MS<sup>3</sup> analysis, the Y<sub>1a</sub> ion of isomelezitose was found to fragment to <sup>0,1</sup>A<sub>2</sub>, <sup>0,2</sup>A<sub>2</sub> and <sup>0,3</sup>A<sub>2</sub> cross-ring ions, similar to isomaltulose (6-O- $\alpha$ -D-glucopyranosyl-D-fructose) (Lee et al. 2012). A benefit of derivatisation by isotope labelling is that the ion is not chemically modified. However, the addition of whole labelled monosaccharide units can be used only when the carbohydrates are synthesised. In hydrolysed polysaccharides or oligosaccharides, the hydroxyl groups can be labelled, such as <sup>18</sup>O labelling of the reducing end or deuteration of the hydroxyl carbons (Hofmeister et al. 1991; Quemener et al. 2010).

It was reported that IM could “provide a high-resolution dimension” to ordinary MS analysis (Clowers et al. 2005). In study IV, the CID-TWIMS-MS/MS analysis was conducted to separate the isomeric fragment ions of linear and branched (A)XOS. The findings showed that CID-TWIMS-MS/MS could separate Ara-substituted fragment ions from linear XOS fragments in both positive and negative ionisation.  $\beta$ -D-Xylp-(1→2)- $\alpha$ -L-Araf-(1→3) substituted ions were also differentiated from the monosubstituted ions. However, the method could not distinguish smaller disaccharide fragment ions.

So far, only a few studies have used IM to analyse MS/MS fragment ions. Both et al. (2014) differentiated monosaccharide fragment ions from epimeric disaccharides by TWIMS. They also demonstrated that the same technique could be used to sequence glycan oligosaccharides. In Both et al. (2014), the instrument and IM conditions were the same as in this study. However, unlike the present study, in Both et al. (2014), the disaccharide fragment ions could be separated. The reason for the different results must be structural differences in the samples: N-linked glycan disaccharides are built of two different mass monomers, and (A)XOS are built of the same mass pentoses. However, they reported very close drift times distinguishable (e.g. Gal $\beta$ 1-4GalNAc 6.62 ms and Gal $\beta$ 1-3GalNAc 6.68 ms). This result suggests that the B-ions of A<sup>2</sup>X and A<sup>3</sup>X, which had 0.2 ms drift time difference, could be differentiated by optimization of parameters. However, further research is needed.

Gabryelski and Froese (2002) reported that the separation of anomeric, linkage isomeric and position isomeric disaccharide precursors was achieved by ESI-FAIMS-MS combined with the reducing end derivatisation in the samples. They found that the best separation in the studied linkage isomers was achieved by proton, sodium and chloride adducts, but anomers were better separated

using adducts such as rubidium and caesium. Based on these findings, sodium and chloride adducts were chosen for use in the study IV. However, it could be beneficial to test other adducts. Moreover, the derivatisation of the reducing end would help in differentiating the reducing and non-reducing end fragments.

#### **6.2.4 Advantages and limitations of MS methods in structural analysis of oligosaccharides**

In the past the NMR has been the superior analytical technique in the structural analysis of oligosaccharides. By NMR it is possible to analyse whole structure of oligosaccharide in very detailed level, such as the stereochemistry of monomers (Duus et al. 2000). Compared to the NMR, the advantages in structural analysis by MS are a high sensitivity, a small sample amount requirement and a compatibility to other analytical methods, such as LC or IM. This research showed that, even though the MS cannot characterise the structures in so detailed manner as NMR, it provides a lot of information about the structures. The MS methods could differentiate the studied oligosaccharides and the isomers within the same DP, and furthermore give structural information of their molecular sizes, monosaccharide sequences and monosaccharide compositions. Combining the MS to LC or IM enabled the separation of isomeric oligosaccharides, with some exceptions, and these methods could be further developed for analysis of oligosaccharide mixtures. Advantage of the TWIMS-MS was also fast analysis acquisition time; the analysis took only milliseconds compared to minutes in LC-MS.

To characterize oligosaccharides, MS and MS/MS analyses require standards/model compounds for the comparison. The MS/MS spectra can be collected to spectral library and be used as a reference in the forthcoming studies. However, the use of MS/MS spectral libraries is often limited to “in-house” use, because the spectra from mass spectrometers used with soft ionisation techniques are equipment specific and depend on fragmentation techniques, adducts and used amount of fragmentation energy. National Institute of Standards and Technology (NIST) has been developing the tandem mass spectra library which includes spectra from both positive and negative modes from IT and ‘beam-type’ collision cells (qTOF, higher-energy collision dissociation (HCD), and triple quadrupole (QQQ) (NIST 2020). However, currently the library is mainly focused on human and plant metabolites and



drugs and only the minor part of the data is from glycans. The oligosaccharides libraries are established only for human and mammalian milk (NIST 2020).

Recently, a new type of library has been established in oligosaccharide analysis: CCS value library. The CCS values have already been collected from hundreds of oligosaccharides (Fenn & McLean 2011, Gaye et al. 2015). The TWIMS does not provide CCS values, but drift times can be converted to CCS values by analysing calibrants with known CCS values and same chemical properties as analytes (Gabelica & Marklund 2018, Pagel & Harvey 2013). In this thesis, the conversion of drift times to CCS was not performed, because the IM calibrant used, polyalanine mixture, was not a carbohydrate. However, it is likely that the CCS library will be important reference source for oligosaccharides in the future, like the GC-EI-MS spectral library for monosaccharides.

## 7 CONCLUSIONS

In this thesis, MS methods were developed for use in the analysis of the oligosaccharides present in cereal matrices. In cereal matrices, such as sourdough, the oligosaccharides can be natural grain oligosaccharides, or they can be produced by LAB or cereal grain endogenous enzymes, such as glucansucrase synthesised acceptor products and endoxylanase hydrolysed plant cell walls (A)XOS.

The ESI-MS<sup>n</sup> method provided structural information about the linear oligosaccharides linkages, molecular weights and sequences of both GLOS and (A)XOS. The negative ionisation ESI-MS<sup>n</sup> was found to be more informative than the positive ionisation mode. The stepwise C-ion fragmentation from the reducing end toward the non-reducing end allowed the study of the linkage diagnostic fragment ions from the middle and the non-reducing end.

The influence of the branch to the fragmentation of oligosaccharides was also studied to determine whether the linkage(s) of the branch could be determined. The negative ionisation ESI-ITMS<sup>3</sup> could distinguish all branches in the studied AXOS. Furthermore, the CID-TWIMS-MS/MS could separate most of the isomeric glycosidic bond fragments and differentiate the Araf-substituted fragment ions from the XOS backbone fragments. In future studies, the combination of both methods, MS<sup>3</sup> and CID-TWIMS-MS/MS (CID-TWIMS-

CID-MS/MS), should be tested. This analytical tool would contribute one more step in differentiating the isomeric structures of oligosaccharides. CID-TWIMS-MS/MS was found to separate positively and negatively charged ions differently. The best identification of the ions was achieved using both ionisation modes.

Overall, ESI-ITMS<sup>n</sup> was demonstrated to be a very useful tool in exploring the structures of neutral oligosaccharides. However, the method's ability to determine the isomeric structures in underivatized samples was limited. Therefore, some strategies for separating and analysing the isomers were implemented. In one strategy, MS was combined with LC. The negative ionisation HILIC-MS/MS could separate all the studied (A)XOS by the retention times and MS/MS spectra. In future research, this method could be applied to obtain the quick profiling of isomers containing oligosaccharide mixtures, such as arabinoxylan hydrolysates and glucansucrase acceptor reaction products.

The use of <sup>13</sup>C<sub>6</sub>-labelled sucrose as glucose donor was found feasible for differentiation of the two isomeric trisaccharide acceptor products by ESI-ITMS/MS. Furthermore, the isotope labelling enabled the separation of the formed glycosidic bond ions and further confirmed the linkage position in ESI-MS<sup>3</sup>. In addition, the use of both positive and negative ionisation modes was found to be beneficial in the analyses of these branched trisaccharides.

In summary, the results showed that the developed MS methods could differentiate the studied (A)XOS and GLOS as well as determine their structural differences. The linkage positions in linear and branched tri-, tetra- and pentasaccharides were analysed by the negative ionisation ESI-ITMS<sup>n</sup>. The CID-TWIMS-MS/MS was found to be a promising solution for the separation of isomeric fragment ions. In addition, the negative ionisation HILIC-MS/MS was successfully developed for the quick profiling of (A)XOS mixtures.

The HILIC-MS/MS analysis could be performed also by reasonable cost LC-MS instrument and therefore be suitable for a routine laboratory work. The HILIC-MS/MS could be utilised, for example, for determining the known oligosaccharides in mixtures by comparing their retention times and MS/MS spectra to standards. Because MS is very sensitive and the analysis can be

performed from small amount of sample, also the oligosaccharides with lower concentration could be determined from the mixtures.

The TWIMS-MS method showed its power on isomeric differentiation and that opened the door for the structural studies of unknown oligosaccharides. However, due to high cost of IM mass spectrometers, it is unlikely that TWIMS-MS will be used in routine work in small laboratories soon. Nevertheless, TWIMS-MS is definitely a potential competitor for NMR and GC-MS methylation methods in the structural analysis of oligosaccharides.

## 8 REFERENCES

Alpert AJ. 1990. Hydrophilic-interaction chromatography for the separation of peptides, nucleic acids and other polar compounds. *Journal of Chromatography A* 499:177-196:

Asam MR, Glish GL. 1997. Tandem mass spectrometry of alkali cationized polysaccharides in a quadrupole ion trap. *J. Am. Soc. Mass Spectrom.* 8:987-995.

Ashline D, Singh S, Hanneman A, Reinhold V. 2005. Congruent strategies for carbohydrate sequencing. 1. Mining structural details by MS<sup>n</sup>. *Anal. Chem.* 77:6250-6262.

Barron C, Surget A, Rouau X. 2007. Relative amounts of tissues in mature wheat (*Triticum aestivum* L.) grain and their carbohydrate and phenolic acid composition. *J. Cereal Sci.* 45:88-96.

Biliaderis C, Izydorczyk M. 2007. Arabinoxylans: technologically and nutritionally functional plant polysaccharides. *In: Functional Food Carbohydrates*. Biliaderis C, Izydorczyk M. (Eds.), CRC Press, USA, pp. 249-290.

Biliaderis CG, Izydorczyk MS, Rattan O. 1995. Effect of arabinoxylans on bread-making quality of wheat flours. *Food Chem.* 53:165-171.

Björndal H, Lindberg B, Svensson S. 1967. Gas-liquid chromatography of partially methylated alditols as their acetates. *Acta Chemica Scandinavica* 21:1801-1804.

Black BA, Lee VS, Zhao YY, Hu Y, Curtis JM, Ganzle MG. 2012. Structural identification of novel oligosaccharides produced by *Lactobacillus bulgaricus* and *Lactobacillus plantarum*. *J. Agric. Food Chem.* 60:4886-4894.

Both P, Green AP, Gray CJ, Sardzik R, Voglmeir J, Fontana C, Austeri M, Rejzek M, Richardson D, Field RA, Widmalm G, Flitsch SL, Evers CE. 2014. Discrimination of epimeric glycans and glycopeptides using IM-MS and its potential for carbohydrate sequencing. *Nature Chemistry* 6:65-74.

Boulos S, Nyström L. 2016. UPLC-MS/MS investigation of  $\beta$ -glucan oligosaccharide oxidation. *Analyst* 141:6533-6548.

Bowman MJ, Dien BS, Hector RE, Sarath G, Cotta MA. 2012a. Liquid chromatography–mass spectrometry investigation of enzyme-resistant xylooligosaccharide structures of switchgrass associated with ammonia pretreatment, enzymatic saccharification, and fermentation. *Bioresource Technology* 110:437-447:

Bowman MJ, Dien BS, O'Bryan P,J., Sarath G, Cotta MA. 2012b. Comparative analysis of end point enzymatic digests of arabino-xylan isolated from switchgrass (*panicum virgatum* l) of varying maturities using LC-MS<sup>n</sup>. *Metabolites* 2:959-982.

Broekaert WF, Courtin CM, Verbeke K, Van dW, Verstraete W, Delcour JA. 2011. Prebiotic and other health-related effects of cereal-derived arabinoxylans, arabinoxylan-oligosaccharides, and xylooligosaccharides. *Crit. Rev. Food Sci. Nutr.* 51:178-194.

Brokl M, Hernández-Hernández O, Soria AC, Sanz ML. 2011. Evaluation of different operation modes of high performance liquid chromatography for the analysis of complex mixtures of neutral oligosaccharides. *J Chromatogr A* 1218:7697-7703.

Carroll JA, Willard MD, Lebrilla CB. 1995. Energetics of cross-ring cleavages and their relevance to the linkage determination of oligosaccharides. *Anal. Chim. Acta* 307:431-447.

Chai W, Piskarev V, Lawson AM. 2001. Negative-ion electrospray mass spectrometry of neutral underivatized oligosaccharides. *Anal. Chem.* 73:651-657.

Chai W, Lawson AM, Piskarev V. 2002. Branching pattern and sequence analysis of underivatized oligosaccharides by combined MS/MS of singly and doubly charged molecular ions in negative-ion electrospray mass spectrometry. *J. Am. Soc. Mass Spectrom.* 13:670-679.

Chong S, Nissila T, Ketola RA, Koutaniemi S, Derba-Maceluch M, Mellerowicz EJ, Tenkanen M, Tuomainen P. 2011. Feasibility of using atmospheric pressure matrix-assisted laser desorption/ionisation with ion trap mass spectrometry in the analysis of acetylated xylooligosaccharides derived from hardwoods and *Arabidopsis thaliana*. *Anal. Bioanal. Chem.* 401:2995-3009.

Ciucanu I, Kerek F. 1984. A simple and rapid method for the permethylation of carbohydrates. *Carbohydr. Res.* 131:209-217.

Ciucanu I. 2006. Per-O-methylation reaction for structural analysis of carbohydrates by mass spectrometry. *Anal. Chim. Acta* 576:147-155.

Clowers BH, Dwivedi P, Steiner WE, Hill HH, Bendiak B. 2005. Separation of sodiated isobaric disaccharides and trisaccharides using electrospray ionisation-atmospheric pressure ion mobility-time of flight mass spectrometry. *Journal of the American Society for Mass Spectrometry* 16:660-669:

Čmelík R, Štikarovská M, Chmelík J. 2004. Different behavior of dextrans in positive-ion and negative-ion mass spectrometry. *J. Mass Spectrom.* 39:1467-1473.

Čmelík, R., & Chmelík, J. (2010). Structural analysis and differentiation of reducing and nonreducing neutral model starch oligosaccharides by negative-ion electrospray ionization ion-trap mass spectrometry. *International Journal of Mass Spectrometry*, 291(1), 33-40.,

Courtin CM and Delcour JA. 2002. Arabinoxylans and endoxylanases in wheat flour bread-making. *Journal of Cereal Science* 35:225-243:

Creaser CS, Reynolds JC, Harvey DJ. 2002. Structural analysis of oligosaccharides by atmospheric pressure matrix-assisted laser desorption/ionisation quadrupole ion trap mass spectrometry. *Rapid Commun. Mass Spectrom.* 16:176-184.

Dallinga JW, Heerma W. 1991. Reaction mechanism and fragment ion structure determination of deprotonated small oligosaccharides, studied by negative ion fast atom bombardment (tandem) mass spectrometry. *Biol. Mass Spectrom.* 20:215-231.

Damen B, Verspreet J, Pollet A, Broekaert WF, Delcour JA, Courtin CM. 2011. Prebiotic effects and intestinal fermentation of cereal arabinoxylans and arabinoxylan oligosaccharides in rats depend strongly on their structural properties and joint presence. *Mol. Nutr. Food Res.* 55:1862-1874.

Davies GJ, Wilson KS, Henrissat B. 1997. Nomenclature for sugar-binding subsites in glycosyl hydrolases. *Biochem. J.* 321:557-559.

Domon B, Costello CE. 1988. A systematic nomenclature for carbohydrate fragmentations in FAB-MS/MS spectra of glycoconjugates. *Glycoconj. J.* 5:397-409.

Dwivedi P, Bendiak B, Clowers BH, Hill HH. 2007. Rapid resolution of carbohydrate isomers by electrospray ionisation ambient pressure ion mobility spectrometry-time-of-flight mass spectrometry (ESI-APIMS-TOFMS). *Journal of the American Society for Mass Spectrometry* 18:1163-1175.

Duus JO, Gotfredsen CH, Bock K. 2000. Carbohydrate structural determination by NMR spectroscopy: modern methods and limitations. *Chem. Rev.* 100:4589-4614.

El-Aneed A, Cohen A, Banoub J. 2009. Mass Spectrometry, review of the basics: electrospray, MALDI, and commonly used mass analyzers. *Applied Spectroscopy Reviews* 44:210-230.

Everest-Dass A, Kolarich D, Campbell M, Packer N. 2013. Tandem mass spectra of glycan substructures enable the multistage mass spectrometric identification of determinants on oligosaccharides. *Rapid Communications in Mass Spectrometry* 27:931-939.

FAO. 1998. Carbohydrates in human nutrition, Report of a Joint FAO/WHO Expert Consultation, Rome, Italy, 14-18 April 1997.

FAO. 2018. FAOSTAT. Food and Agriculture data. Crop statistics 2018. <http://www.fao.org/faostat/en/#data/QC>.

Fauré R, Courtin CM, Delcour JA, Dumon C, Faulds CB, Fincher GB, Fort S, Fry SC, Halila S, Kabel MA, Pouvreau L, Quemener B, Rivet A, Saulnier L, Schols HA, Driguez H, O'Donohue MJ. 2009. A Brief and informationally rich naming system for oligosaccharide motifs of heteroxylans found in plant cell walls. *Aust. J. Chem.* 62:533-537.

Fenn LS, McLean JA. 2011. Structural resolution of carbohydrate positional and structural isomers based on gas-phase ion mobility-mass spectrometry. *Phys. Chem. Chem. Phys.* 13:2196-2205.

Fincher GB. 2016. Cereals: chemistry and physicochemistry of non-starchy polysaccharides. 208-223. Oxford.

Gabelica V and Marklund E. 2018. Fundamentals of ion mobility spectrometry. *Current Opinion in Chemical Biology* 42:51-59

Gabelica V, Shvartsburg AA, Afonso C, Barran P, Benesch JLP, Bleiholder C, Bowers MT, Bilbao A, Bush MF, Campbell JL, Campuzano IDG, Causon T, Clowers BH, Creaser CS, De Pauw E, Far J, Fernandez-Lima F, Fjeldsted JC, Giles K, Groessl M, Hogan Jr CJ, Hann S, Kim HI, Kurulugama RT, May JC, McLean JA, Pagel K, Richardson K, Ridgeway ME, Rosu F, Sobott F, Thalassinos K, Valentine SJ, Wytenbach T. 2019. Recommendations for reporting ion mobility mass spectrometry measurements. *Mass Spec Rev* 38:291-320.

Gabryelski W, Froese KL. 2003. Rapid and sensitive differentiation of anomers, linkage, and position isomers of disaccharides using High-Field Asymmetric Waveform Ion Mobility Spectrometry (FAIMS). *J. Am. Soc. Mass Spectrom.* 14:265-277.

García-Cayuela T, Díez-Municio M, Herrero M, Martínez-Cuesta MC, Peláez C, Requena T, Moreno FJ. 2014. Selective fermentation of potential prebiotic lactose-derived oligosaccharides by probiotic bacteria. *International Dairy Journal* 38:11-15:

Garozzo D, Giuffrida M, Impallomeni G, Ballistreri A, Mon taudo G. 1990. Determination of linkage position and identification of the reducing end in linear oligosaccharides by negative ion fast atom bombardment mass spectrometry. *Anal. Chem.* 62:279-286.

Garozzo D, Impallomeni G, Spina E, Sturiale L, Zanetti F. 1995. Matrix-assisted laser desorption/ionisation mass spectrometry of polysaccharides. *Rapid Commun. Mass Spectrom.* 9:937-941.

Gaye MM, Kurulugama R, Clemmer DE. 2015. Investigating carbohydrate isomers by IMS-CID-IMS-MS: precursor and fragment ion cross-sections. *Analyst* 140:6922-6932.

Guan B, Cole RB. 2008. MALDI Linear-field reflectron TOF post-source decay analysis of underivatized oligosaccharides: determination of glycosidic linkages and anomeric configurations using anion attachment. *J. Am. Soc. Mass Spectrom.* 19:1119-1131.



Guignard C, Jouve L, Bogéat-Triboulot MB, Dreyer E, Hausman J, Hoffmann L. 2005. Analysis of carbohydrates in plants by high-performance anion-exchange chromatography coupled with electrospray mass spectrometry. *Journal of Chromatography A* 1085:137-142.

Gänzle MG. 2014. Enzymatic and bacterial conversions during sourdough fermentation. *Food Microbiology* 37:2-10.

Harrison S, Xue H, Lane G, Villas-Boas S, Rasmussen S. 2012. Linear ion trap MS<sup>n</sup> of enzymatically synthesized <sup>13</sup>C-labeled fructans revealing differentiating fragmentation patterns of beta (1-2) and beta (1-6) fructans and providing a tool for oligosaccharide identification in complex mixtures. *Anal. Chem.* 84:1540-1548.

Harvey DJ. 2005. Fragmentation of negative ions from carbohydrates: Part 1. Use of nitrate and other anionic adducts for the production of negative ion electrospray spectra from N-linked carbohydrates. *J. Am. Soc. Mass Spectrom.* 16:622-630.

Harvey DJ. 2005b. Fragmentation of negative ions from carbohydrates: Part 2. Fragmentation of high-mannose N-linked glycans. *J. Am. Soc. Mass Spectrom.* 16:631-646.

Harvey DJ, Scarff CA, Edgeworth M, Crispin M, Scanlan CN, Sobott F, Allman S, Baruah K, Pritchard L, Scrivens JH. 2013. Travelling wave ion mobility and negative ion fragmentation for the structural determination of N-linked glycans. *Electrophoresis* 34:2368-2378.

Hernandez-Hernandez O, Calvillo I, Lebron-Aguilar R, Moreno FJ, Sanz ML. 2012. Hydrophilic interaction liquid chromatography coupled to mass spectrometry for the characterization of prebiotic galactooligosaccharides. *J. Chromatogr. A* 1220:57-67.

Hofmann J, Struwe WB, Scarff CA, Scrivens JH, Harvey DJ, Pagel K. 2014. Estimating collision cross sections of negatively charged n-glycans using traveling wave ion mobility-mass spectrometry. *Anal. Chem.* 86:10789-10795.

Hofmann J, Hahm HS, Seeberger PH, Pagel K. 2015. Identification of carbohydrate anomers using ion mobility-mass spectrometry. *Nature* 526:241-244.

Hofmann J, Stuckmann A, Crispin M, Harvey DJ, Pagel K, Struwe WB. 2017. Identification of Lewis and blood group carbohydrate epitopes by ion mobility-tandem-mass spectrometry fingerprinting. *Anal. Chem.* 89:2318-2325.

Hofmeister GE, Zhou Z, Leary JA. 1991. Linkage position determination in lithium-cationized disaccharides- tandem mass-spectrometry and semiempirical calculations. *J. Am. Chem. Soc.* 113:5964-5970.

Höije A, Sandström C, Roubroeks JP, Andersson R, Gohil S, Gatenholm P. 2006. Evidence of the presence of 2-O- $\beta$ -D-xylopyranosyl- $\alpha$ -L-arabinofuranose side chains in barley husk arabinoxylan. *Carbohydrate Research* 341:2959-2966.

Hsu HC, Liew CY, Huang S, Tsai S, Ni C. 2018. Simple method for de novo structural determination of underivatized glucose oligosaccharides. *Scientific Reports* 8:5562.

Jiang Y, Cole RB. 2005. Oligosaccharide analysis using anion attachment in negative mode electrospray mass spectrometry. *J. Am. Soc. Mass Spectrom.* 16:60-70.

Jonathan MC, DeMartini J, Van Stigt Thans S, Hommes R, Kabel MA. 2017. Characterisation of non-degraded oligosaccharides in enzymatically hydrolysed and fermented, dilute ammonia-pretreated corn stover for ethanol production. *Biotechnology for Biofuels* 10:112.

Karlsson NG, Schulz BL, Packer NH. 2004. Structural determination of neutral O-linked oligosaccharide alditols by negative ion LC-electrospray-MSn. *J. Am. Soc. Mass Spectrom.* 15:659-672.

Katina K, Maina NH, Juvonen R, Flander L, Johansson L, Virkki L, Tenkanen M, Laitila A. 2009. In situ production and analysis of *Weissella confusa* dextran in wheat sourdough. *Food Microbiol.* 26:734-743.

Knudsen KEB. 1997. Carbohydrate and lignin contents of plant materials used in animal feeding. *Animal Feed Science and Technology* 67:319-338:

König S, Leary JA. 1998. Evidence for linkage position determination in cobalt coordinated pentasaccharides using ion trap mass spectrometry. *J. Am. Soc. Mass Spectrom.* 9:1125-1134.

Korakli M, Rossmann A, Ganzle MG, Vogel RF. 2001. Sucrose metabolism and exopolysaccharide production in wheat and rye sourdoughs by *Lactobacillus sanfranciscensis*. J. Agric. Food Chem. 49:5194-5200.

Lee S, Valentine SJ, Reilly JP, Clemmer DE. 2012. Analyzing a mixture of disaccharides by IMS-VUVPD-MS. International Journal of Mass Spectrometry 161-167.

Leemhuis H, Pijning T, Dobruchowska JM, van Leeuwen SS, Kralj S, Dijkstra BW, Dijkhuizen L. 2013. Glucansucrases: Three-dimensional structures, reactions, mechanism,  $\alpha$ -glucan analysis and their implications in biotechnology and food applications. Journal of Biotechnology 163:250-272:

Leijdekkers AGM, Sanders MG, Schols HA, Gruppen H. 2011. Characterizing plant cell wall derived oligosaccharides using hydrophilic interaction chromatography with mass spectrometry detection. J. Chromatogr. A 1218:9227-9235.

Leijdekkers AGM, Huang J, Bakx EJ, Gruppen H, Schols HA. 2015. Identification of novel isomeric pectic oligosaccharides using hydrophilic interaction chromatography coupled to traveling-wave ion mobility mass spectrometry. Carbohydrate Research 404:1-8:

Lemoine J, Fournet B, Despeyroux D, Jennings KR, Rosenberg R, de Hoffmann E. 1993. Collision-induced dissociation of alkali metal cationized and permethylated oligosaccharides: Influence of the collision energy and of the collision gas for the assignment of linkage position. J. Am. Soc. Mass Spectrom. 4:197-203.

Li H, Bendiak B, Siems WF, Gang DR, Hill HH. 2013. Carbohydrate structure characterization by tandem ion mobility mass spectrometry (IMMS)<sup>2</sup>. Anal. Chem. 85:2760-2769.

Liu J, Kisonen V, Willför S, Xu C, Vilaplana F. 2016. Profiling the substitution pattern of xyloglucan derivatives by integrated enzymatic hydrolysis, hydrophilic-interaction liquid chromatography and mass spectrometry. J. Chromatogr. A 1463:110-120.

Liu Z, Rochfort S. 2015. Identification and quantitative analysis of oligosaccharides in wheat flour using LC-MS. J. Cereal Sci. 63:128-133.

MacEvilly C. 2003. CEREALS | Contribution to the Diet. In: Encyclopedia of food sciences and nutrition (Second edition). Caballero B. (Eds.), Academic Press, Oxford, pp. 1008-1014.

Maina NH, Virkki L, Pynnönen H, Maaheimo H, Tenkanen M. 2011. Structural analysis of enzyme-resistant isomaltooligosaccharides reveals the elongation of  $\alpha(1-3)$ -linked branches in *Weissella confusa* dextran. *Biomacromolecules* 12:409-418.

Maslen SL, Goubet F, Adam A, Dupree P, Stephens E. 2007. Structure elucidation of arabinoxylan isomers by normal phase HPLC-MALDI-TOF/TOF-MS/MS. *Carbohydr. Res.* 342:724-735.

Matamoros Fernández LE, Obel N, Scheller HV, Roepstorff P. 2003. Characterization of plant oligosaccharides by matrix-assisted laser desorption/ionisation and electrospray mass spectrometry. *Journal of Mass Spectrometry* 38:427-437.

Matamoros Fernández LE, Obel N, Scheller HV, Roepstorff P. 2004. Differentiation of isomeric oligosaccharide structures by ESI tandem MS and GC-MS. *Carbohydr. Res.* 339:655-664.

Mathew S, Abraham TE. 2004. Ferulic acid: an antioxidant found naturally in plant cell walls and feruloyl esterases involved in its release and their applications. *Crit. Rev. Biotechnol.* 24:59-83.

Mazumder K, York WS. 2010. Structural analysis of arabinoxylans isolated from ball-milled switchgrass biomass. *Carbohydr. Res.* 345:2183-2193.

Mendis M, Simsek S. 2014. Arabinoxylans and human health. *Food Hydrocoll.* 42, Part 2:239-243.

Mischnick P. 2011. Mass spectrometric characterization of oligo- and polysaccharides and their derivatives. In: *Mass spectrometry of polymers – new techniques. Advances in Polymer Science, vol 248*. Hakkarainen M. (Eds.), Springer, Berlin, Heidelberg, pp. 105-174.

Morelle W, Faid V, Michalski J. 2004. Structural analysis of permethylated oligosaccharides using electrospray ionization quadrupole time-of-flight tandem mass spectrometry and deuterio-reduction. *Rapid Commun. Mass Spectrom.* 18:2451-2464.

NIST. 2020. NIST 17 Tandem mass spectral libraries and search program. <https://chemdata.nist.gov/dokuwiki/doku.php?id=chemdata:msms>.

Pagel K, Harvey DJ. 2013. Ion mobility-mass spectrometry of complex carbohydrates: collision cross sections of sodiated N-linked glycans. *Anal. Chem.* 85:5138-5145.

Pasanen S, Jänis J, Vainiotalo P. 2007. Cello-, malto- and xylooligosaccharide fragmentation by collision-induced dissociation using QIT and FT-ICR mass spectrometry: A systematic study. *International Journal of Mass Spectrometry* 263:22-29.

Pastell H, Tuomainen P, Virkki L, Tenkanen M. 2008. Step-wise enzymatic preparation and structural characterization of singly and doubly substituted arabinoxylo-oligosaccharides with non-reducing end terminal branches. *Carbohydr Res* 343:3049-3057.

Pastell H, Virkki L, Harju E, Tuomainen P, Tenkanen M. 2009. Presence of 1→3-linked 2-O-β-D-xylopyranosyl-α-L-arabinofuranosyl side chains in cereal arabinoxylans. *Carbohydr. Res.* 344:2480-2488.

Pfenninger A, Karas M, Finke B, Stahl B. 2002a. Structural analysis of underivatized neutral human milk oligosaccharides in the negative ion mode by nano-electrospray MS<sup>n</sup> (Part 1: Methodology). *J. Am. Soc. Mass Spectrom.* 13:1331-1340.

Pfenninger A, Karas M, Finke B, Stahl B. 2002b. Structural analysis of underivatized neutral human milk oligosaccharides in the negative ion mode by nano-electrospray MS<sup>n</sup> (part 2: application to isomeric mixtures). *J. Am. Soc. Mass Spectrom.* 13:1341-1348.

Plancot B, Vanier G, Maire F, Bardor M, Lerouge P, Farrant JM, Moore J, Driouich A, Vitré-Gibouin M, Afonso C, Loutelier-Bourhis C. 2014. Structural characterization of arabinoxylans from two African plant species *Eragrostis nindensis* and *Eragrostis tef* using various mass spectrometric methods. *Rapid Commun. Mass Spectrom.* 28:908-916.

Pollet A, Delcour JA, Courtin CM. 2010. Structural determinants of the substrate specificities of xylanases from different glycoside hydrolase families. *Crit. Rev. Biotechnol.* 30:176-191.

Poutanen K. 1997. Enzymes: An important tool in the improvement of the quality of cereal foods. *Trends in Food Science & Technology* 8:300-306:

Pu J, Zhao X, Wang Q, Wang Y, Zhou H. 2016. Development and validation of a HPLC method for determination of degree of polymerization of xylo-oligosaccharides. *Food Chemistry* 213:654-659.

Pu J, Zhao X, Xiao L, Zhao H. 2017. Development and validation of a HILIC-ELSD method for simultaneous analysis of non-substituted and acetylated xylo-oligosaccharides. *Journal of Pharmaceutical and Biomedical Analysis* 139:232-237.

Quemener B, Ordaz-Ortiz JJ, Saulnier L. 2006. Structural characterization of underivatized arabino-xylo-oligosaccharides by negative-ion electrospray mass spectrometry. *Carbohydr. Res.* 341:1834-1847.

Rantanen H, Virkki L, Tuomainen P, Kabel M, Schols H, Tenkanen M. 2007. Preparation of arabinoxylobiose from rye xylan using family 10 *Aspergillus aculeatus* endo-1,4- $\beta$ -D-xylanase. *Carbohydr. Polym.* 68:350-359.

Reis A, Coimbra MA, Domingues P, Ferrer-Correia AJ, Domingues MRM. 2004. Fragmentation pattern of underivatized xylo-oligosaccharides and their alditol derivatives by electrospray tandem mass spectrometry. *Carbohydrate Polymers* 55:401-409:

Reis A, Pinto P, Coimbra MA, Evtuguin DV, Neto CP, Ferrer Correia AJ, Domingues MRM. 2004. Structural differentiation of uronosyl substitution patterns in acidic heteroxylans by electrospray tandem mass spectrometry. *J. Am. Soc. Mass Spectrom.* 15:43-47.

Reis A, Pinto P, Evtuguin DV, Neto CP, Domingues P, Ferrer-Correia AJ, Domingues MRM. 2005. Electrospray tandem mass spectrometry of underivatized acetylated xylo-oligosaccharides. *Rapid Commun. Mass Spectrom.* 19:3589-3599.

Remaud-Simeon 2015. Glycoside hydrolase family 70 in CAZypedia, [url:www.cazypedia.org/index.php](http://www.cazypedia.org/index.php).

Ruhaak LR, Zauner G, Huhn C, Bruggink C, Deelder AM, Wührer M. 2010. Glycan labeling strategies and their use in identification and quantification. *Analytical and Bioanalytical Chemistry* 397:3457-3481.

Ruiz-Matute A, Brokl M, Sanz ML, Soria AC, Côté GL, Collins ME, Rastall RA. 2011. Effect of dextransucrase cellobiose acceptor products on the growth of human gut bacteria. *J. Agric. Food Chem.* 59:3693-3700.

Saulnier L, Sado P, Branlard G, Charmet G, Guillon F. 2007. Wheat arabinoxylans: Exploiting variation in amount and composition to develop enhanced varieties. *J. Cereal Sci.* 46:261-281.

Schwarz PB, Han J. 1995. Arabinoxylan Content of Commercial Beers. *Journal of the American Society of Brewing Chemists* 53:157-159.

Simpson DJ, Fincher GB, Huang AHC, Cameron-Mills V. 2003/3. Structure and function of cereal and related higher plant (1→4)-β-xylan endohydrolases. *Journal of Cereal Science* 37:111-127.

Spengler B, Dolce JW, Cotter RJ. 1990. Infrared laser desorption mass spectrometry of oligosaccharides: Fragmentation mechanisms and isomer analysis. *Anal. Chem.* 62:1731-1737.

Spina E, Sturiale L, Romeo D, Impallomeni G, Garozzo D, Waidelich D, Glueckmann M. 2004. New fragmentation mechanisms in matrix-assisted laser desorption/ionisation time-of-flight/time-of-flight tandem mass spectrometry of carbohydrates. *Rapid Commun. Mass Spectrom.* 18:392-398.

Struwe, W. B., Baldauf, C., Hofmann, J., Rudd, P. M., & Pagel, K. 2016. Ion mobility separation of deprotonated oligosaccharide isomers – evidence for gas-phase charge migration. *Chem. Commun.* 52:12353-12356.

Tieking M, Korakli M, Ehrmann MA, Gänzle MG, Vogel RF. 2003. In situ production of exopolysaccharides during sourdough fermentation by cereal and intestinal isolates of lactic acid bacteria. *Appl. Environ. Microbiol.* 69:945-952.

Tieking M, Ganzle MG. 2005. Exopolysaccharides from cereal-associated lactobacilli. *Trends in Food Science & Technology* 16:79-84.

Tryfona T, Sorieul M, Feijao C, Stott K, Rubtsov DV, Anders N, Dupree P. 2019. Development of an oligosaccharide library to characterise the structural variation in glucuronoarabinoxylan in the cell walls of vegetative tissues in grasses. *Biotechnology for Biofuels* 12:109.

Usui T, Ogata M, Murata T, Ichikawa K, Sakano Y, Nakamura Y. 2009. Sequential analysis of  $\alpha$ -glucooligosaccharides with  $\alpha$ -(1 $\rightarrow$ 4) and  $\alpha$ -(1 $\rightarrow$ 6) linkages by negative Ion Q-TOF MS/MS spectrometry. *J. Carbohydr. Chem.* 28:421-430.

Vandamme, E.J., Renard, C.E.F., Arnaut, F.R.J., Vekemans, N.M.F. and Tossut, P.P.A. Process for obtaining improved structure build-up of baked products, EP 0 790 003A1. European Patent.

Verspreet J. 2015. LC-MS analysis reveals the presence of graminan- and neo-type fructans in wheat grains. *J. Cereal Sci.*133-138.

Vinueza NR, Gallardo VA, Klimek JF, Carpita NC, Kenttämäa HI. 2013. Analysis of xyloglucans by ambient chloride attachment ionisation tandem mass spectrometry. *Carbohydr. Polym.* 98:1203-1213.

Wang J, Yuan X, Sun B, Cao Y, Tian Y, Wang C. 2009. On-line separation and structural characterisation of feruloylated oligosaccharides from wheat bran using HPLC-ESI-MS n. *Food Chem.* 115:1529-1541.

Welman AD. 2009. Exploitation of exopolysaccharides from lactic acid bacteria: Nutritional and functional benefits. *In: Bacterial polysaccharides: Current innovations and future trends.* Ullrich M. (Eds.), Caister Academic Press, Norfolk, UK, pp. 331-344.

Wende G and Fry SC. 1997. 2-O- $\beta$ -d-xylopyranosyl-(5-O-feruloyl)-l-arabinose, a widespread component of grass cell walls. *Phytochemistry* 44:1019-1030:

Yamagaki T, Sato A. 2009. Isomeric oligosaccharides analyses using negative-ion electrospray ionisation ion mobility spectrometry combined with collision-induced dissociation MS/MS. *Anal. Sci.* 25:985-988.

Zhang H, Brokman SM, Fang N, Pohl NL, Yeung ES. 2008. Linkage position and residue identification of disaccharides by tandem mass spectrometry and linear discriminant analysis. *Rapid Communications in Mass Spectrometry* 22:1579-1586.

Zhu JH, Cole R. 2001. Ranking of gas-phase acidities and chloride affinities of monosaccharides and linkage specificity in collision-induced



decompositions of negative ion electrospray-generated chloride adducts of oligosaccharides. *J. Am. Soc. Mass Spectrom.* 12:1193-1204.

Zhu M, Bendiak B, Clowers B, Hill HH. 2009. Ion mobility-mass spectrometry analysis of isomeric carbohydrate precursor ions. *Analytical and Bioanalytical Chemistry* 394:1853-1867.